

Long Term Monitoring of Moisture under Pavements

*Dr. William Wolfe
Dr. Tarunjit Butalia
James Howdyshell*

for the
Ohio Department of Transportation
Office of Research and Development

State Job Number 134170

January 2010



1. Report No. FHWA/OH-2010/1	2. Government Accession No.	3. Recipient's Catalog No.	
4. Title and subtitle Long Term Monitoring of Moisture Under Pavements		5. Report Date January 2010	
		6. Performing Organization Code	
7. Author(s) William Wolfe, Tarunjit Butalia, James Howdysell		8. Performing Organization Report No.	
		10. Work Unit No. (TRAIIS)	
9. Performing Organization Name and Address The Ohio State University Department of Civil and Environmental Engineering & Geodetic Science 470 Hitchcock Hall 2070 Neil Ave. Columbus, Ohio 43210		11. Contract or Grant No. 134170	
		13. Type of Report and Period Covered Final Report	
12. Sponsoring Agency Name and Address Ohio Department of Transportation 1980 West Broad Street Columbus, OH 43223		14. Sponsoring Agency Code	
15. Supplementary Notes			
16. Abstract <p>Monitoring of the environmental instrumentation installed under select pavement sections constructed by the Ohio Department of Transportation (ODOT) in 1995 on US 23 in Delaware County, Ohio was continued. The measurements made consisted of soil moisture, temperature and frost depth profiles.</p> <p>OSU constructed and installed tensiometers to directly measure the porewater pressures in the subsurface soils at seven locations at the DEL23 SHRP test road (four during original road construction and three more in 2002). Tensiometers were also installed and monitored at seven additional locations within the state. Those devices were monitored throughout the duration of the current project.</p> <p>A laboratory testing program was conducted to identify relationships between static soil properties and the design resilient modulus for compacted cohesive subgrade soils. Resilient modulus as well as classification and strength tests were performed on cohesive soil samples. The program to establish the relationships between dynamic soil behavior and static properties is described and a predictive tool developed through the use of artificial neural networks is presented.</p>			
17. Key Words Resilient Modulus, SPS Studies, tensiometers		18. Distribution Statement No restrictions. This document is available to the public through the National Technical Information Service, Springfield, Virginia 22161	
19. Security Classif. (of this report) Unclassified	20. Security Classif. (of this page) Unclassified	21. No. of Pages 98	22. Price
Form DOT F 1700.7 (8-72)		Reproduction of completed pages authorized	

Long Term Monitoring of Moisture under Pavements

William E. Wolfe, Ph.D.

Professor, Dept. of Civil and Environmental Engineering and Geodetic Science,
The Ohio State University, Columbus, OH 43210

Tarunjit S. Butalia, Ph.D.

Research Scientist, Dept. of Civil and Environmental Engineering and Geodetic Science,
The Ohio State University, Columbus, OH 43210

James R. Howdyshell

Graduate Student, Dept. of Civil and Environmental Engineering and Geodetic Science,
The Ohio State University, Columbus, OH 43210

January 2010

A Report to Sponsors:
The Ohio Department of Transportation,
and
The U.S. Department of Transportation,
Federal Highway Administration

State Job No. 134170

Prepared in Cooperation with the Ohio Department of Transportation and the U.S.
Department of Transportation, Federal Highway Administration

The contents of this report reflect the views of the authors, who are responsible for the facts and accuracy of the data presented herein. The contents do not necessarily reflect the official views or policies of the Ohio Department of Transportation or the Federal Highway Administration. This report does not constitute a standard, specification or regulation.

ACKNOWLEDGEMENTS

The Ohio Department of Transportation (ODOT) and the Federal Highway Administration (FHWA) supported this research.

The work presented in this report was part of a project to install and monitor seasonal instrumentation at five SHRP pavement sections. That effort was in turn part of a larger effort to install and monitor seasonal and structural performance instrumentation at 33 pavement test sections on US 23 in Delaware, Ohio. Many individuals participated in this research. Help with instrumentation installation, scheduling and sample collection from R. Green. Direction and insight into modulus testing and usage from R. Green and A. Morse of ODOT are greatly appreciated. R. Green, A. Morse and W. Christensen graciously agreed to test early versions of the resilient modulus program. Their suggestions greatly improved the utility of the program. The efforts of several students collecting and presenting field data and performing laboratory tests should be cited. Of particular note were the efforts of G. Rodgers, B. Zand, W. Tu , and W. Hannitinan.

TABLE OF CONTENTS

1. INTRODUCTION	1
2. RESEARCH OBJECTIVES	2
3. DESCRIPTION OF THE RESEARCH	3
3.1 Literature Review	3
3.1.1 Resilient Modulus	3
3.1.1.1 Factors Affecting Resilient Modulus	3
3.1.1.2 Prediction of M_R - Current Popular Models	4
3.1.1.3 Data from Published Reports	5
3.1.1.3.1 Purdue University Study	6
3.1.1.3.2 University of Mississippi Study	7
3.1.2 Neural Network Algorithms to Predict Resilient Modulus	7
3.1.2.1 Background	8
3.1.2.2 Back-Propagation Modeling Algorithms	12
3.1.2.3 Application to the Resilient Modulus Study	15
3.1.2.4 Experimental data usage in model development	16
3.1.2.5 Estimating Resilient Modulus from Incomplete Data Sets	16
3.1.2.5.1 q_u prediction ANNs	17
3.1.2.5.2 M_R prediction ANNs	17
3.2 Summary	18
4. FIELD INSTRUMENTATION SITE DETAILS	19
4.1 DEL 23	19
4.2 WAY 30	22
4.3 MAD 70	25
4.4 ROS 207	27
4.5 I -71/I -270 Interchange	28
4.6 OSU FDR Sites	30
4.7 Summary	35
5. FIELD MEASUREMENTS	36
5.1 DEL 23	36
5.1.1 SHRP Instrumentation	36
5.1.1.1 Moisture Content	36
5.1.1.2 Soil Temperature	37
5.1.1.3 Resistivity	37
5.1.2 Tensiometers	37
5.2 WAY 30	38
5.3 MAD 70	38
5.4 ROS 207	39
5.5 I-71/I-270 Interchange	39
5.6 OSU FDR Sites	39
5.7 Summary	39
6. ADDITIONAL LABORATORY RESILIENT MODULUS TESTING	60
6.1 Classification Tests	60
6.2 Unconfined Compression Tests	61
6.3 Resilient Modulus Tests	62

6.4 Summary	68
7. RESILIENT MODULUS NEURAL NETWORK MODELS	69
8. RESILIENT MODULUS PREDICTION MODEL	73
8.1 Introduction	73
8.2 Input Command Controls for Data Entry	73
8.3 Additional Features and Functions	73
8.4 Summary	80
9. IMPLEMENTATION	81
10. REFERENCES	82
11. APPENDICES	94
11.1 APPENDIX A: RESILIENT MODULUS USERS GUIDE	94

LIST OF FIGURES

Figure 3.1 A simplified biological neuron network system	9
Figure 3.2 A simplified engineering structure of feed forward and back-propagation neural networks	10
Figure 3.3 A simplified engineering neuron (node)	11
Figure 3.4 Flow forward procedures in a two layer back-propagation neural network (after Hanittinan)	12
Figure 3.5 Flow backward procedures in a two layer back-propagation neural network (after Hannitinan)	13
Figure 3.6 A simplified engineering diagram of a neural network	15
Figure 4.1 Locations of OSU Instrumentation Sites	20
Figure 4.2 Locations of OSU Field Instrumentation at DEL23	21
Figure 4.3 OSU WAY 30 Site Station Layout	23
Figure 4.4 Damaged Sensors at WAY 30 Station Three	24
Figure 4.5 Instrumentation Damaged at MAD 70 Eastbound after Installation	25
Figure 4.6 OSU MAD 70 Site Location Layout	26
Figure 4.7 OSU MAD 70 Site Station Layout – Aerial View	26
Figure 4.8 OSU ROS 207 Site Station Layout	27
Figure 4.9 ROS 207 Site Instrumentation Location	28
Figure 4.10 OSU I-71/I-270 Site Station Layout	29
Figure 4.11 OSU I-71/I-270 Site Station Layout – Aerial View	29
Figure 4.12 Plan View of OSU FDR Pavement Site at Delaware County, Ohio	31
Figure 4.13 OSU S. Section Line Rd. Site Station Layout	32
Figure 4.14 OSU S. Section Line Rd. Site Station Layout – Aerial View	32
Figure 4.15 OSU Warren County Site Station Layout	33
Figure 4.16 OSU Warren County Site Station Layout – Aerial View	33
Figure 4.17 OSU Muskingum County Site Station Layout	34
Figure 4.18 OSU Muskingum County Site Station Layout – Aerial View	34
Figure 5.1 Instrumentation Configurations (390263 from 2004 report)	40
Figure 5.2 Seasonal Moisture Content for 2007 (390904)	42
Figure 5.3 Seasonal Moisture Content in 2006 (390904)	42
Figure 5.4 Seasonal Moisture Content for 2005 (390904)	43
Figure 5.5 Seasonal Moisture Content in 2004 (390904)	43
Figure 5.6 Seasonal Moisture Content for 2003 (390904)	44
Figure 5.7 Moisture Content (390904) Topmost TDR 1996-2007	45
Figure 5.8 Moisture Content (390904) Top of Subgrade 1996-2007	45
Figure 5.9 Moisture Content Middle of Subgrade 1996-2007 (390904)	46
Figure 5.10 Moisture Content Bottom of Subgrade 1996-2007 (390904)	47
Figure 5.11 Moisture Content at TDR in Base 1996-2006 (390263)	47
Figure 5.12 Moisture Content at Top of Subgrade 1996-2006 (390263)	48
Figure 5.13 Moisture Content Middle of Subgrade 1996-2006 (390263)	48
Figure 5.14 Moisture Content Bottom of Subgrade 1996-2006 (390263)	49
Figure 5.15 Pore Water Pressure at Section 390904	49
Figure 5.16 Pore Water Pressure at Section 390211	50
Figure 5.17 Pore Water Pressure at Section 390160	51

Figure 5.18 Pore Water Pressure at Section 390901	51
Figure 5.19 Pore Water Pressure at Section 390106	52
Figure 5.20 Pore Water Pressure at Instrumented Weather Station	52
Figure 5.21 Pore Water Pressure at WAY 30 Station 1	53
Figure 5.22 Dynamic Pore Pressure Response at WAY 30 Station 1 (April 06)	53
Figure 5.23 Dynamic Pore Pressure Response at WAY 30 Station 2 (April 06)	54
Figure 5.24 Dynamic Pore Pressure Response at WAY 30 Station 4 (April 06)	54
Figure 5.25 Dynamic Pore Pressure Response at WAY 30 Station 1 (October 06)	55
Figure 5.26 Pore Water Pressure at MAD 70 Station 1	56
Figure 5.27 Pore Water Pressure at MAD 70 Station 2	57
Figure 5.28 Pore Water Pressure at ROS 207	58
Figure 5.29 Dynamic Pore Water Pressure at Section Line Rd Station 6	59
Figure 6.1 M_R test results for W30ST10MCS2	62
Figure 6.2 M_R test results for WAY 30 Station 1 at 41 kPa Confining Stress	63
Figure 6.3 M_R test results for WAY 30 Station 1 at 21 kPa Confining Stress	63
Figure 6.4 M_R test results for WAY 30 Station 1 at 0 kPa Confining Stress	64
Figure 6.5 M_R test results for MAD 70 at 41 kPa Confining Stress	64
Figure 6.6 M_R test results for MAD 70 at 21 kPa Confining Stress	65
Figure 6.7 M_R test results for MAD 70 at 0 kPa Confining Stress	65
Figure 6.8 M_R test results for WAY 30 Station 2 at 41 kPa Confining Stress	66
Figure 6.9 M_R test results for WAY 30 Station 2 at 21 kPa Confining Stress	66
Figure 6.10 M_R test results for WAY 30 Station 2 at 0 kPa Confining Stress	67
Figure 7.1 M_R vs. Deviator Stress, A-6 Soil	69
Figure 7.2 M_R vs. Deviator Stress, A-4 Soil	70
Figure 7.3 M_R vs. Deviator Stress, A-7-6 Soil	70
Figure 7.4 Predicted vs. Measured M_R University of Mississippi Test Soils	71
Figure 7.5 Predicted vs. Measured M_R Purdue Test Soils	72
Figure 8.1 The main window screen for M_R prediction	74
Figure 8.2 Window screen for CBR and M_R prediction according to the ME-PDG model	75
Figure 8.3 Window screen for CBR and M_R prediction according to ODOT [ODOT, 1999]	75
Figure 8.4 Charts to determine Group Index for Ohio soils from a CBR	76
Figure 8.5 Ohio Typical Soil Moisture vs. Density Family Curves [ODOT, 2002]	77
Figure 8.6 Optimum moisture content using one point proctor testing	78
Figure 8.7 The main window screen with a predicted M_R range	79

LIST OF TABLES

Table 3.1 Current Popular Models (After Table 3.2 in 2004 Final Report to ODOT)	1
Table 3.2 Examples of Published Reports Reviewed	2
Table 3.3 Information on Sampling Sites for Indiana Soils	3
Table 3.4 Engineering Properties of Indiana Soils	4
Table 3.5 Information on Sampling Sites for Mississippi Soils	5
Table 3.6 Engineering Properties of Mississippi Soils	6
Table 3.7 Options for estimating q_u using ANN simulations (3 soil types for each option)	17
Table 3.8 Available options for M_R ANN simulations (3 soil types for each option)	18
Table 5.1 Ohio State University DEL 23 Test Sections	41
Table 6.1 Sample Description and Location	60
Table 6.2 Classification and Engineering Properties	60
Table 6.3 Optimum Moisture Content and Maximum Dry Density	61
Table 6.4 Unconfined Compressive Strength Test Results	61
Table 6.5 Design and Actual Soil Sample Moisture Contents and Dry Densities	68

1. INTRODUCTION

The research program discussed in this report consisted of three parallel activities. The first activity was a continuation of the monitoring of environmental instrumentation under select pavement sections originally constructed by the Ohio Department of Transportation (ODOT) in 1995 on US 23 in Delaware County, Ohio. The measurements made by the OSU team at that site consisted of soil moisture, temperature and frost depth profiles. The installation procedures along with the data collected over an eight year period were described in two previous reports (“Seasonal Instrumentation of SHRP Pavements – The Ohio State University State Job No. 14586(0); Contract No. 8011,” dated September, 1998, and “Seasonal Instrumentation Of SHRP Pavements, Final Report – The Ohio State University State Job No. 14586(0); Contract No. 8011,” dated June 2004). In the second activity, OSU constructed and installed tensiometers to directly measure the pore water pressures in the subsurface soils at seven locations at the DEL23 SHRP test road (four during original road construction and three more in 2002). Those devices were monitored throughout the duration of the current project.

As part of the existing research program, tensiometers were installed between 2003 and 2005 at four locations identified by ODOT engineers. The data from tensiometers installed at three additional sites in 2006-07, while not part of the actual scope work of the project, are included in this report to increase the range of conditions under which pore pressure readings have been recorded. The data from all the readings are presented and discussed in subsequent sections.

In the third activity, begun during the previous contract, a testing program was conducted to identify relationships between static soil properties that can be routinely measured in the laboratory, and the design resilient modulus for compacted cohesive subgrade soils. Approximately 800 laboratory resilient modulus tests were performed on cohesive soil samples collected by OSU and ODOT personnel. The laboratory program to establish the relationships between dynamic soil behavior and static properties was described in detail in the 2004 report, as was the regression model developed from the experimental data to predict the resilient modulus. In this report the laboratory testing performed on the additional soil samples is presented and the predictive tool is substantially modified and improved through the use of artificial neural networks.

2. RESEARCH OBJECTIVES

The present program is a continuation of the field study begun with the 1995-1997 long term pavement performance program and the laboratory investigation of subgrade performance that started in 2000. This additional laboratory effort was included because the numerical models being used in the design of pavements are becoming increasingly more capable of incorporating direct measurements of the response of subsurface materials to changing states of stresses into the description of the behavior of subgrade materials. Therefore, it should be possible for engineers/researchers, when evaluating long term pavement performance at the DEL23 pavement sections, to relate the observed and/or measured performance to subsurface soil conditions.

In modern pavement system designs, an essential input is the dynamic elastic stiffness of the supporting soil layers. In this project, we developed a rational method to predict the elastic response of the supporting soil using data readily obtained in ODOT laboratories.

The regression model developed as part of the previous project (The Ohio State University State Job No. 14586(0); Contract No. 8011) and described in our 2004 report requires inputting nine different soil parameters (q_u , w , $P_{\#200}$, PI , LL , γ_{opt} , w_{opt} , w_c , and S_r), and two boundary conditions (σ_c and σ_d). However, in the early (planning) stages of a project, not all these parameters may be known, and yet accurate estimates of soil properties are needed to develop reasonable preliminary designs of pavement system cross-sections. In addition, even when laboratory data are available, past testing programs may not have included all the laboratory testing required to thoroughly characterize the soil layers.

One of the more powerful applications of the neural networks employed in the current resilient modulus study is the use of the algorithms to generate estimates of missing input data points. In fact, the artificial neural networks developed were used as data mining tools to extract implicit information from existing data pools.

The final version of the program delivered to ODOT upon completion of the research program has the ability to estimate missing input values as described in the following section.

3. DESCRIPTION OF THE RESEARCH

3.1 Literature Review

A review of the literature on the behavior of the saturated and unsaturated soil was presented in the 1998 and 2004 reports of the pavement monitoring projects. While a discussion of earlier research is summarized in this document, the reader is referred to our previous reports for more complete reviews of resilient modulus testing and modeling efforts as well as discussions on the uses of tensiometers in estimating the in-situ stresses and water content.

Because the mathematical model we developed is based on an application of artificial neural networks (ANNs), a topic that has not been covered in our earlier reports, we include a discussion of this methodology in this report. It is not a comprehensive review however, and the reader is directed to any of the several thorough presentations of ANNs available from both print and electronic sources (e.g. Schmidt, [1996], Haykin [1994]).

3.1.1 Resilient Modulus

Seed, et al. (1962) suggested that the most important subsurface response parameter in the characterization of pavement system response is the ratio of applied cyclic stress (σ_d) to the resulting elastic strain (ϵ_r). The Resilient Modulus (M_R), which Seed proposed as the measure of the dynamic stiffness, is obtained in the controlled environment of a laboratory cyclic triaxial test at loads typical of those found when pavement subgrades are loaded. In methods developed since Seed's proposal, M_R has been used either directly to design flexible pavements, or converted to a modulus of subgrade reaction (k-value) typically used in the design of rigid (concrete) pavements.

Although simple in concept, a direct measure of the resilient modulus requires a time consuming testing program, specialized equipment and specifically trained personnel. Even with these three components in place, current standards for resilient modulus testing don't always produce consistent and/or reproducible results, probably due to differences in test equipment, instrumentation, sample preparation, or sample end conditions. To minimize the effects of these difficulties with the resilient modulus test procedure, researchers have invested considerable effort in the development of methods to estimate appropriate design values for the resilient moduli using basic, usually static, engineering properties.

3.1.1.1 Factors Affecting Resilient Modulus

A review of the literature and our own earlier test results have shown that the measured resilient modulus is affected by a number of factors, including: stress state

(deviator and confining stress), moisture content, soil type and density. Decreases in M_R with increasing deviator stress have been observed (Seed, et al. (1962), Fredlund, et al. (1977), Drumm, et al. (1990), Li and Selig (1994), Pezo and Hudson (1994), Lee et al. (1995), Mohammad, et al. (1999), and Kim (1999), Lee (2002). M_R was shown to increase with increasing confining stress (Kim (1999), Li and Qubain (2003)). Subgrade resilient modulus has been shown to be highly dependent on the soil water content, with small increases in water content resulting in large decreases in M_R ((Seed, et al. (1962), Fredlund, et al. (1977), Li and Selig (1994), Pezo and Hudson (1994), Burczyk et al (1994) Lee, et al. (1995), Drumm, et al. (1997), Kim (1999), Masada and Sargand (2002), Lee (2002), Butalia, et al. (2003), and Li and Qubain (2003)).

3.1.1.2 Prediction of M_R - Current Popular Models

As mentioned above, the cost, time, difficulty, and lack of repeatability of results in resilient modulus tests have forced a search for alternative methods for predicting the resilient modulus. Several different models have been developed using simple laboratory tests and correlation equations. The existing models can be divided into two broad categories: 1) linear models, such as the United States Department of Agriculture (USDA) Model, Texas Department of Transportation (TxDOT) model and the Ohio Department of Transportation (ODOT) model, and 2) non linear models which include the Hyperbolic Model, Georgia Department of Transportation (GDOT) model and the OSU Model.

A description of the models commonly used by federal and state highway agencies was presented in our earlier (2006) report. Table 3.1, which presents the most important aspects of several common models in use, is an update of the table presented in our 2006 report.

Existing Model	Author(s)	Input Parameters	Advantages	Limitations
LINEAR MODELS				
USDA Model	Carmichael and Stuart, 1986	USCS soil type, PI, w , %- No. 200 sieve, σ_3 , σ_d	Includes effect of: w , σ_3 , PI	Soil type
TxDOT Model	Pezo & Hudson, 1994	w , γ_d , $\gamma_{d,max}$, PI, Sample age, σ_3 , σ_d	Includes effect of: w , - σ_3 - PI, Sample age	Narrow range for input parameters
ODOT Model	ODOT, 1999	GI (LL, PI, %-No. 200 sieve), CBR	Simplicity of model	σ_3 and σ_d not considered
NON LINEAR MODELS				
Hyperbolic Model	Drumm, et al., 1990	q_u , % clay, PI, γ , S, %-200 sieve, a , LL, σ_d	Includes effect of PI, q_u , S	σ_3 not considered
GDOT Model	Santha, 1994	w , w_{opt} , γ_d , σ_d , P_a , $\gamma_{d,max}$, %silt, %clay, % swell, LL, PI, %-No. 40 sieve, S, % shrinkage,	Includes effect of - w and w_{opt} S, LL and PI P_a	σ_3 not considered Complex model, many tests required
OSU Model	Kim, 2004	w , w_{opt} , γ_d , % passing No. 200 sieve, S, LL, PI, σ_d , σ_3	Includes effect of w and w_{opt} S, LL and PI σ_d and σ_3	Difficult to incorporate new data

Table 3.1 Current Popular Models (After Table 3.2 in 2004 Final Report to ODOT)

3.1.1.3 Data from Published Reports

Published resilient modulus test results from four recent studies were collected and analyzed (Table 3.2). The results of the studies conducted at Purdue University and the University of Mississippi were added to the experimental data generated at OSU and are included in our analyses. These two studies were selected to help validate the present M_R model because they included sufficient soil property information, plus directly measured resilient modulus laboratory test results allowing predicted and measured moduli to be properly compared.

Title	Conducted by	Year
Subgrade Resilient Modulus for Pavement Design and Evaluation	Purdue University, Indiana DOT (IDOT) and FHWA	1993
Resilient Modulus for New Hampshire Subgrade Soils for use in Mechanistic AASHTO Design	U.S Army Cold Region Research and Engineering Laboratory (CRREL)	1999
Prediction of Resilient Modulus from Soil Index Properties	University of Mississippi for Mississippi DOT and FHWA	2004
Laboratory Characterization of Cohesive Subgrade Materials	University of Akron	2005

Table 3.2 Examples of Published Reports Reviewed

3.1.1.3.1 Purdue University Study

Resilient modulus tests were performed on five cohesive soils and one granular soil in accordance with the AASHTO specification current at the time (AASHTO T 274-82). Both laboratory and field compacted samples were tested. The effects of freeze-thaw cycles were studied as well. Resilient response was correlated with the fabric parameters, clay content, and pore water content.

Resilient modulus test results from laboratory compacted soil samples from two sites were included into the database used in the present study (Tables 3.3, Information on Sampling Sites, and 3.4, Engineering Properties).

Site	ID	Location	Station	Soil Classification	Date Compacted	Date Sampled
South Bend	SB	US20 Bypass	140 - 141	A-4 / A-6 (CL)	Aug 89	Jan; May; July 90
Washington	WA	US50 Bypass	290	A-6/ A-4 (CL)	June 89	Jan 91

Table 3.3 Information on Sampling Sites for Indiana Soils

Site	ρ_{max} (pcf)	w_{OMC} (%)	GS	LL	LP	PI
South Bend	129.5	9.4	2.76	21	14	7
Washington	114	14.9	2.74	30	21	9

Table 3.4 Engineering Properties of Indiana Soils

3.1.1.3.2 University of Mississippi Study

Samples of soils from subgrade sections representing different districts in Mississippi were tested to determine the physical properties of the selected soils. Laboratory tests to measure M_R were performed according to the TP46 Protocol (AASHTO T294-94). The study concluded that the most important index properties influencing M_R were moisture content, degree of saturation, percentage of material passing No. 200 sieve, plasticity index and density. Input data are presented in Tables 3.5 and 3.6.

Resilient modulus laboratory results, as well as static soil properties from the Mississippi tests were used in the present OSU study to assess the performance of the neural network approach in general and in the proposed model in particular for predicting M_R for soils originating outside Ohio.

County/ Road Designation	Unified Soil Classification	AASHTO Classification
Montgomery/US 82 W	CL	A-4
Hinds / Norrel W	CL	A-6

Table 3.5 Information on Sampling Sites for Mississippi Soils

County/ Road	ρ_{max} (pcf)	w_{OMC} (%)	G_s	LL	LP	PI	UCS (psi)
Montgomery/US 82 W	115.20	13.80	2.72 (assumed)	22	16.20	6.10	15.4
Hinds / Norrel W	105.60	17.80	2.67 (assumed)	37.20	24.10	13.10	26.9

Table 3.6 Engineering Properties of Mississippi Soils

3.1.2 Neural Network Algorithms to Predict Resilient Modulus

Artificial Neural Networks are designed to mimic the response of the human nervous system. McCulloch and Pitts (1943) published an algorithm to imitate neurobiological activity and Rosenblatt (1962) developed a simple neural network. Werbos (1974) introduced the back propagating algorithm for neural network systems. The back-propagation algorithm has since become the most popular learning algorithm.

In pavement design and in the geotechnical field, neural network algorithms have been used to solve a variety of design problems. Meier & Rix (1994, 1995) and Brendenhan and van de Ven (2004) used back-propagation neural networks to estimate stiffness of a flexible pavement layer. Bayrak et al. (2005) used ANNs to evaluate the resilient moduli of flexible pavement materials. Hashash et al. (2006) developed an ANN to predict soil stress-strain behavior.

3.1.2.1 Background

The biological nervous system that an artificial neural network is designed to simulate is composed of a large number of simple elements operating in parallel. The four key elements in every biological neuron; the cell bodies, dendrites, axons and synapses, are illustrated in Figure 3.1. In the figure, axons and dendrites are the cell filaments extending from the cell bodies. The synapse is the gap between an axon of one neuron and the dendrite of another. Information contained in a cell body is sent through the system in the form of an electric impulse (signal). When a dendrite detects a signal, it forwards it to the cell body to which it is connected. The cell body sums up the signals received from its dendrites until the sum of incoming signals exceeds a specified limit. When this limit is exceeded, the cell body then transmits a signal to its axon. As the dendrites of other nearby neurons detect the incoming signals, the signal is processed through the system. Learning is the process by which the effectiveness of the signals sent from axons through the synapses is adjusted so that the influence of one neuron on another changes to achieve the conditions where predicted responses match (within acceptable limits) the observed outcomes. However, unlike their natural counterparts, artificial neural networks have a specified number of neurons and the firing rules are clear and fixed. The standard structure of an ANN consists of input receptors, at least one output layer and a number of hidden layers (Figure 3.2). Each ANN layer contains a number of artificial neurons, called nodes. Nodes are connected to adjacent nodes by networking lines to represent dendrites, axons, and synapses.

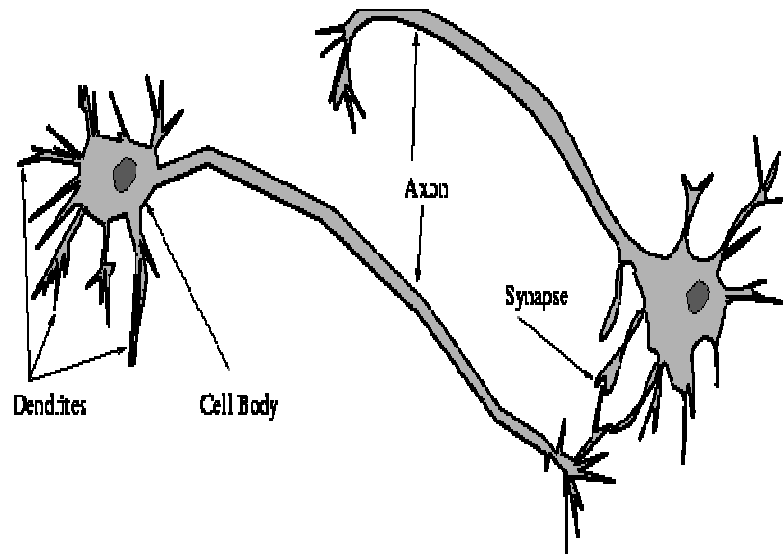


Figure 3.1 A simplified biological neuron network system

(source from: <http://www.teco.edu/~albrecht/neuro/html/node7.html> by Schmidt, 1996)

A weighting function, representing the information used by the net to solve the problem, is assigned to each link. This weight is used to modify the transmitted signals. The net uses the input data and a combination of weights to predict the corresponding outputs or targets. Inside the network, the net randomly assigns a weight to each link, this weight is updated in an iterative manner until the predicted output data are as close as possible to the actual data corresponding to the input data. A node connected to a second node by a line with a large weight has a great potential to impact output of the second node. Each node also inherits a transfer or activation function which is the firing/inhibitory rule. The strength of the output signal from each node depends on its input value, its activation function, and the specified weighting function. The engineering structure of each node is as characterized in Figure 3.3.

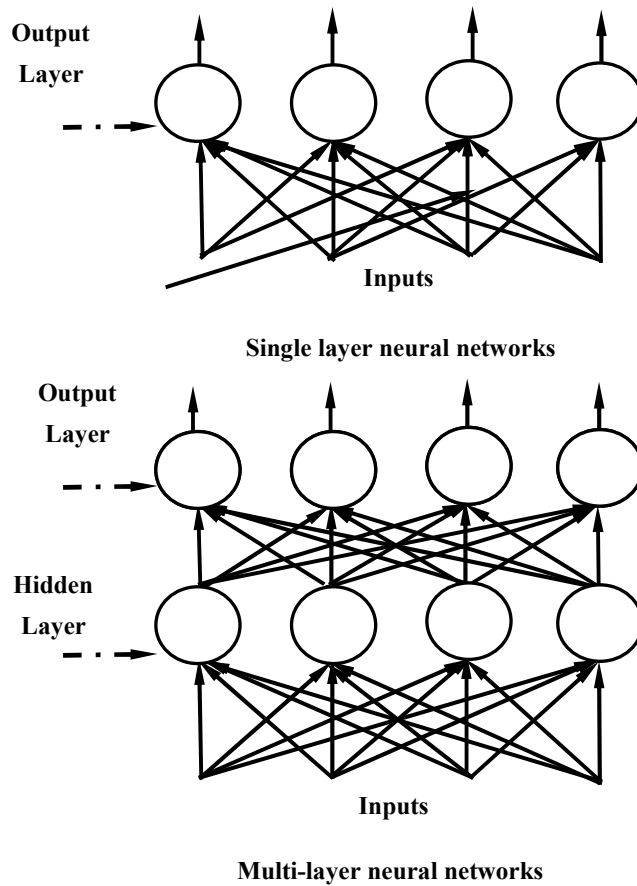


Figure 3.2 A simplified engineering structure of feed forward and back-propagation neural networks

During a training session, the weight associated with each line is adjusted to improve the final output. A learning rate, which is simply a control parameter to determine the step size for any weight adjustments, is also assigned to each node. The learning rate can be a fixed value or a function designed to vary during the training session. Each artificial node is connected to, and integrated into a networking structure. Data are submitted to each node, manipulated then sent to the next node in a different layer. Data can be transported back and forth to many nodes through different layers according to an established set of rules.

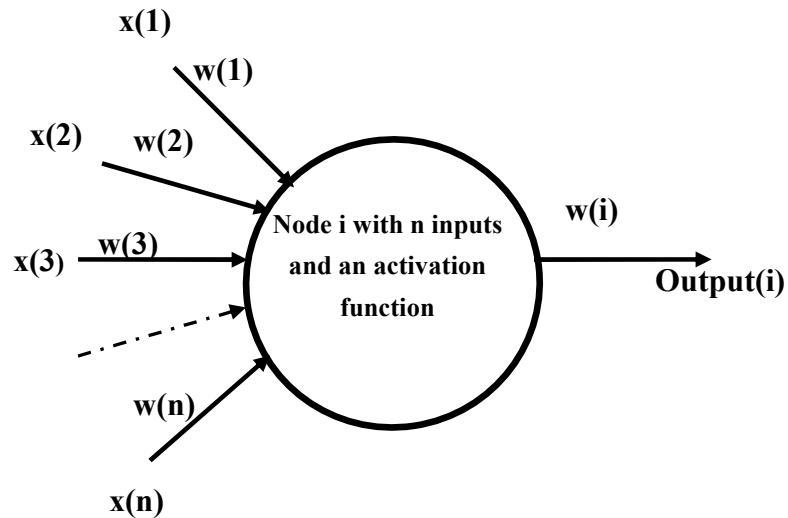


Figure 3.3 A simplified engineering neuron (node)

An input data set contains a recorded value for each defined input parameter. When the data set is input into the neural networks, information is gathered from each recorded data set. The final output signal for each node in the output layer is the response to all input data provided. The sum of the responses from all output-layer nodes is the system solution for each input data set. As with the biological nervous system, complex problems require a number of nodes and a complex neural structure to process realistic outputs. However, unlike their biological counterparts, two neural layers generally suffice to solve a typical non-linear problem.

There are a number of types of ANNs that have been introduced to solve specific problems. Supervised learning mechanisms behave similarly to a teacher with knowledge and ability to provide correct responses. Differences between an ANN's predicted response and the measured response can be detected and adjustments made iteratively so that the calculated response mimics the targeted response. ANNs with unsupervised learning algorithms do not have a teaching mechanism to oversee the learning process and there is no targeted response to compare to. Each node competes with the others to be active and influential. Responses are gradually improved as the networks organize themselves.

3.1.2.2 Back-Propagation Modeling Algorithms

The network structure of back-propagation is laid out in layers as shown in Figure 3.2. There may be several hidden layers but only one output layer. There is no direct connection between the nodes in the same layer, but each node is connected to all the nodes in any adjacent layer. As shown in Figures 3.4 and 3.5, back-propagation can be separated into feed-forward propagation and backward propagation phases depending on the direction of the flow of information through the neural network layers.

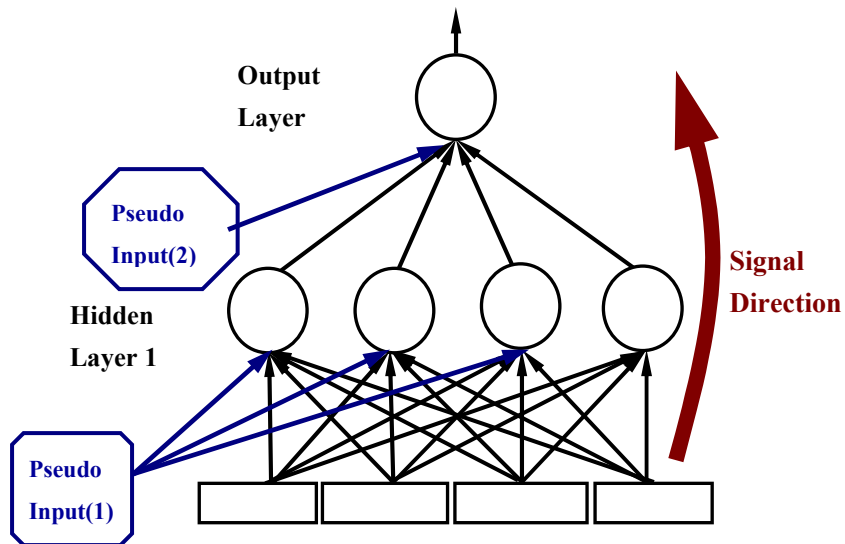


Figure 3.4 Flow forward procedures in a two layer back-propagation neural network (after Hanittinan)

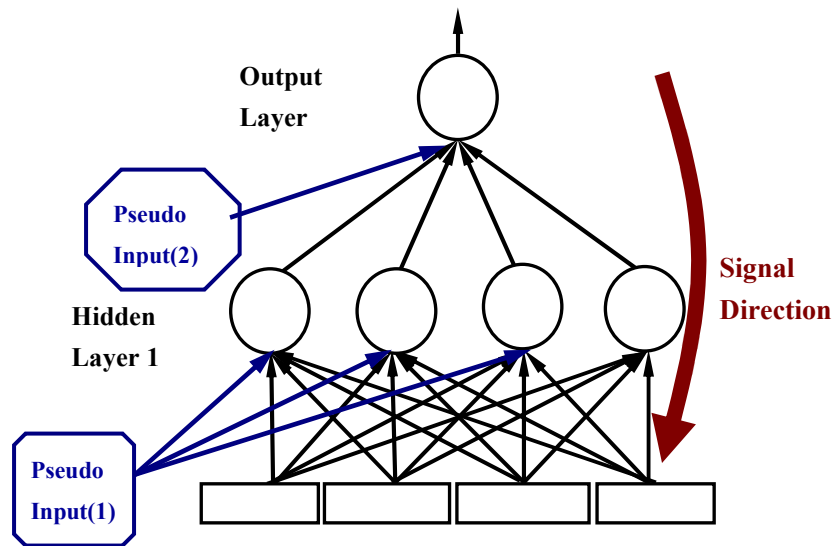


Figure 3.5 Flow backward procedures in a two layer back-propagation neural network (after Hannitinan)

In the feed forward phase, the information flow starts at the inputs to each node in the first hidden layer and from there to the nodes in the output layers (Figure 3.4). An incoming signal to each node can be calculated by summing the product of an input value and a corresponding weight transmitted along each directly connected line (Eq. 3.1 or Eq. 3.2).

$$\text{Input}(i) = x(1) \times w(1) + x(2) \times w(2) + x(3) \times w(3) + \dots + x(n) \times w(n) \quad \text{Eq.3. 1}$$

$$\text{Input}(i) = \sum_{j=1}^n [x(j) \times w(j)] \quad \text{Eq.3. 2}$$

- $w(1), w(2), w(3), \dots, w(n)$ = weights assigned to lines 1,2,3 connected to node i ,
- $x(1), x(2), x(3), \dots, x(n)$ = signal transmitted along lines 1, 2, 3 ...to node i ,
- n = the total number of incoming signals to node i
- Input (i) = sum of incoming signals or inputs to node i ,
- Output(i) = the output signal or response for node i ,
- = $x(1), x(2), x(3), \dots$ for node in the next layer
- $w(i)$ = a weight assigned to the line i between two nodes

Commonly, the initial weights are picked randomly within specified ranges. During training sessions the weights may change as the network is adjusted. The output of one node becomes an incoming signal for a node in the next connected layer and this process continues through to the nodes in the output layer. The signals of the output layer nodes are the predicted responses for that training round. At that point, the first forward propagation cycle is completed. An error at each output layer node is determined by comparing calculated with measured responses. A backward flow is called for when the difference between the design responses and the calculated responses exceeds prescribed allowable error levels. In such an occurrence, the output layer responses are modified by iterating and adjusting all the weights in the neural network. In order to calculate the adjustment needed for each weight, a local gradient at each node needs to be defined. For any node in the output layer, the local gradient can be estimated as:

$$\text{Delta}(i) = \text{Output}(i) \times [1 - \text{Output}(i)] \times [\text{Target}(i) - \text{Output}(i)] \quad \text{Eq. 3.3}$$

Delta(i) = a local gradient for node i, the node of interest
 Target(i) = the targeted response for node i, in the output layer

A local gradient for any node in a hidden layer can be determined, once the local gradient of its immediately connected node in the next layer closer to the output layer is defined.

$$\text{Delta}(i) = \text{Output}(i) \times [1 - \text{Output}(i)] \times \text{Weight}(i + 1) \times \text{Delta}(i + 1) \quad \text{Eq.3.4}$$

Delta(i+1) = a local gradient for a node in the layer closest to the output layer immediately connected to node i
 Weight(i+1) = a weight for the line from a node in the layer closest to the output layer immediately connected to node i

Adjusted weights for each line connected to the node of interest are each the product of the old weight and the amount of change needed. The adjusted weight can be expressed as:

$$\text{Weight}(i_{\text{new}}) = \text{Weight}(i_{\text{old}}) + \Delta\text{Weight}(i) \quad \text{Eq. 3.5}$$

$$\Delta\text{Weight}(i) = \text{Learningrate} \times \text{Delta}(i) \times \text{Input}(i) \quad \text{Eq.3.6}$$

Learning rate = rate assigned during each iteration (taken to be constant in this study)
 Weight(i_{new}) = new weight for the line from the layer away from the output layer immediately connected to node i

$Weight(i_{old})$ = old weight for the line from the layer away from the output layer immediately connected to node i
 $\Delta Weight(i)$ = adjusted amount given to a weight for the line from the layer away from the output layer immediately connected to node i

Figure 3.6 illustrates a simple neural network and its processing procedures. A full forward and backward propagation is counted as one iteration. Once the desired response is obtained, all weights are fixed. During a runtime session, the estimated response obtained in the output layers is the ANN prediction.

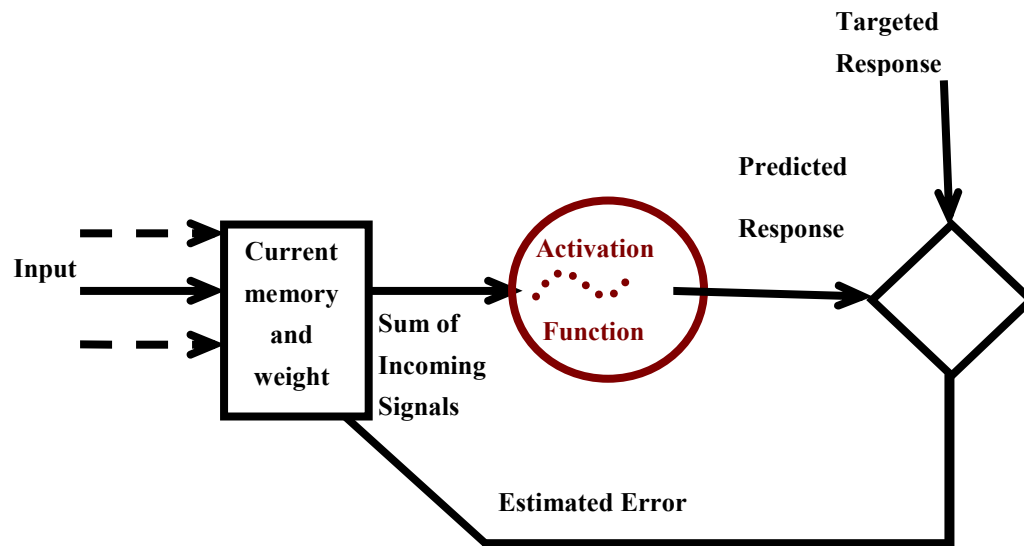


Figure 3.6 A simplified engineering diagram of a neural network

3.1.2.3 Application to the Resilient Modulus Study

In the developed network, one hidden layer and the output layer were set to handle the modulus estimation. Data were divided into three main groups based upon soil types (A-4, A-6, and A-7-6) with one neural network established for each soil type. The number of nodes in the first hidden layer was set to be the same as the number of input parameters. Only one node in the output layer, corresponding to the single valued estimate of modulus, was specified.

An appropriate number of nodes in the hidden layer is typically determined by trial and error. For the current study a ratio 1.5 hidden nodes to one input yielded the most reasonable results.

An ANN with a small learning rate learns slowly because only a small adjustment can be made to each weighting function during an iteration. However, too large a learning rate may cause weights to fluctuate and outputs to become unstable. Therefore a small learning rate was specified for the resilient modulus study.

3.1.2.4 Experimental data usage in model development

Recorded data for each soil type group were randomly divided into three categories for training, validating and testing purposes. The training data sets contained about 60% of the recorded data, with the remaining 40% being divided equally between model validation and testing.

3.1.2.5 Estimating Resilient Modulus from Incomplete Data Sets

The Neural Networks developed were designed to and can be used to estimate missing data in input data sets. The following sections briefly explain the required input parameters for the neural networks developed in this study including the ANNs created from the existing data sets to estimate unconfined compressive strength (q_u).

Eight q_u prediction neural networks were proposed for the three soil types studied. Six q_u prediction neural networks, ANN_{a/A-4}; ANN_{a/A-6}; ANN_{a/A-7-6}; ANN_{b/A-4}; ANN_{b/A-6}; ANN_{b/A-7-6}, were identified for each soil type and specific input parameter combinations. Separate training sessions were conducted for each of the three soil types. A combined characterization of the unconfined compressive strength (ANN_{a/All} and ANN_{b/All}) was also made for all fine grained soil data. These neural networks are described in Table 3.7 which provides the input combinations that were used to develop the q_u prediction neural networks.

Although potentially less precise than the model that uses all the recommended inputs, it is useful to provide algorithms to derive M_R when only limited information is available. The neural networks: ANN_{1/A-4}; ANN_{1/A-6}; ANN_{1/A-7-6}; ANN_{2/A-4}; ANN_{2/A-6}; ANN_{2/A-7-6}; ANN_{3/A-4}; ANN_{3/A-6}; and ANN_{3/A-7-6}, were developed for different combinations of known parameters for each specific soil type. In addition, three ANNs (ANN_{1/All}; ANN_{2/All}; and ANN_{3/All}) were constructed to determine M_R using as the database all the fine grained material data collected in this study without segregating the test results into categories based on the AASHTO classification. The input combinations for these M_R prediction ANNs are shown in Table 3.8.

3.1.2.5.1 q_u prediction ANNs

As shown in the Row a of Table 3.7, the ANNs: ANN_{a/A-4}; ANN_{a/A-6}; ANN_{a/A-7-6}; and ANN_{a/All}, require as input parameters $P_{\#200}$, PI, and LL, w_{opt} , w_c , and S_r in the estimation of q_u . Instead of $P_{\#200}$, PI, and LL input parameters (Row b, Table 3.7), soil type is used as the critical input parameter in q_u estimation for ANN_{b/A-4}; ANN_{b/A-6}; and ANN_{b/A-7-6}.

3.1.2.5.2 M_R prediction ANNs

The key input parameters typically used to estimate CBR are $P_{\#200}$, PI, and LL. The CBR value is, in turn, commonly used to estimate M_R . The neural networks developed in this activity were designed to require only $P_{\#200}$, PI, and LL as input parameters for an M_R prediction (Row 1, Table 3.8). If desired, these ANNs: (ANN_{1/A-4}; ANN_{1/A-6}; ANN_{1/A-7-6}; and ANN_{1/All}) can be used to compare the M_R results predicted directly from CBR values. However, if the model is used this way, a broad range in predicted values of M_R should be expected, since many soils may share similar $P_{\#200}$, PI, and LL combinations.

The neural networks ANN_{2/A-4}; ANN_{2/A-6}; ANN_{2/A-7-6}; and ANN_{2/All} required all numerical input parameters to calculate M_R . These required input parameters are $P_{\#200}$, PI, and LL, w_{opt} , w_c , S_r , q_u , σ_3 , and σ_d (Row 2, Table 3.8). Because all relevant numerical inputs are used in developing ANNs, these ANNs are able to respond with a precise estimate of M_R to a wide range of input data.

When a soil type can be assumed but its measured $P_{\#200}$, PI, and LL data are not available, it is convenient to use the soil type as the representative input parameters in M_R prediction. ANN_{3/A-4}; ANN_{3/A-6}; ANN_{3/A-7-6}, and ANN_{3/All} accept soil type, w_{opt} , w_c , S_r , q_u , σ_3 , and σ_d as inputs and generate an estimate of M_R as the response (Row 3, Table 3.8)

ANN	$P_{\#200}$	LL	PI	Soil Type	w_{opt}	w_c	S_r
A	Yes	Yes	Yes	N/A	Yes	Yes	Yes
b	N/A	N/A	N/A	Yes	Yes	Yes	Yes

Table 3.7 Options for estimating q_u using ANN simulations (3 soil types for each option)

ANN	P_{#200}	LL	PI	Soil Type	w_{opt}	w_c	S_r	q_u	σ₃	σ_d
1	Yes	Yes	Yes	N/A	N/A	N/A	N/A	N/A	N/A	N/A
2	Yes	Yes	Yes	N/A	Yes	Yes	Yes	Yes	Yes	Yes
3	N/A	N/A	N/A	Yes	Yes	Yes	Yes	Yes	Yes	Yes

Table 3.8 Available options for M_R ANN simulations (3 soil types for each option)

Note: N/A = not applicable

3.2 Summary

The artificial neural network is trained (the learning process) with the objective of recognizing interactions between inputs and the resulting response patterns. The ANN learns by example, it will associate a set of input values with the corresponding set of output values, and will remember the associated patterns for future comparisons. A network can be trained using the process of back propagation, in which the difference between the predicted and target M_R values are minimized and the error is redistributed to all neurons in the previous layer. A feed forward, back propagation network was used in the present study to estimate M_R. This type of network is the most common of ANN used to solve problems where the exact mathematical functions are unknown. The network needs to be trained all available information, but once trained, it can be used to make projections given new input data.

Training and validating activities have been completed for the large data set (>800 resilient modulus tests) introduced in our earlier (2004) report and supplemented with the data presented in Section 6 of this final report. The numerical program provided includes artificial neural networks suitable for M_R evaluation on a personal computer operating in the Windows environment (XP or higher). The program selects which of the ANNs is appropriate to the task of determining a design M_R based on the information provided on the input screen. All the ANNs have been trained and verified using the data generated in the experimental program conducted in the soil mechanics laboratory at OSU.

4. FIELD INSTRUMENTATION SITE DETAILS

Monitoring the subsurface conditions at the SPS experimental sites of US23 in Delaware, Ohio continued throughout the duration of the project. In addition to the DEL23 locations, tensiometers were installed at seven more sites with a variety of subgrade conditions. The locations of all the instrumented and monitored sites are shown on Figure 4.1. A typical tensiometer installation consisted of three measurement points separated vertically by 12 inches so that the shallow pore pressure could be recorded. Each is discussed in the following.

4.1 DEL 23

Monitoring the responses of the instrumentation embedded in the test sections assigned to OSU at the DEL 23 SHRP test road continued throughout the project duration. Actual locations of the original test sections as well as the added tensiometer locations have been described in the earlier referenced reports. For reference, the schematic locating the test sections which was given in those reports is presented here as Figure 4.2. Instruments at stations 390109, 390263, and 390212 were damaged or destroyed at different times during the project.

Ohio's Macro-Corridor Highway System

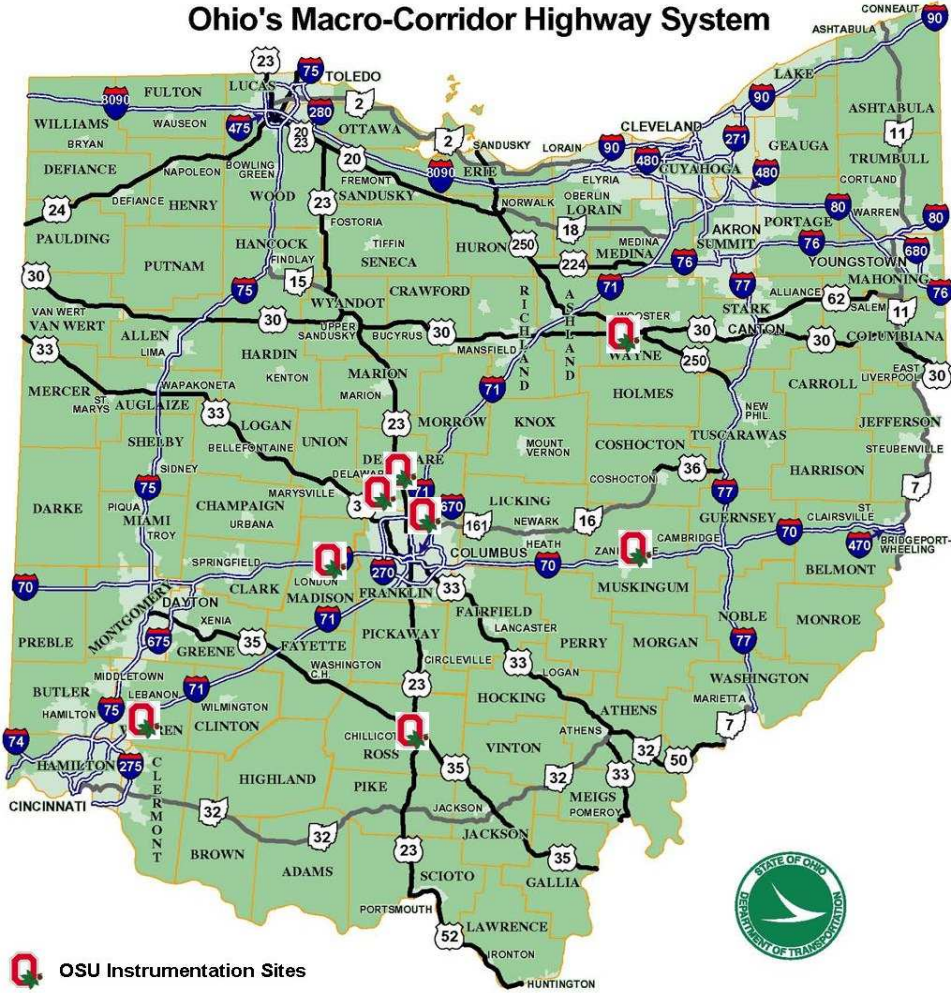


Figure 4.1 Locations of OSU Instrumentation Sites

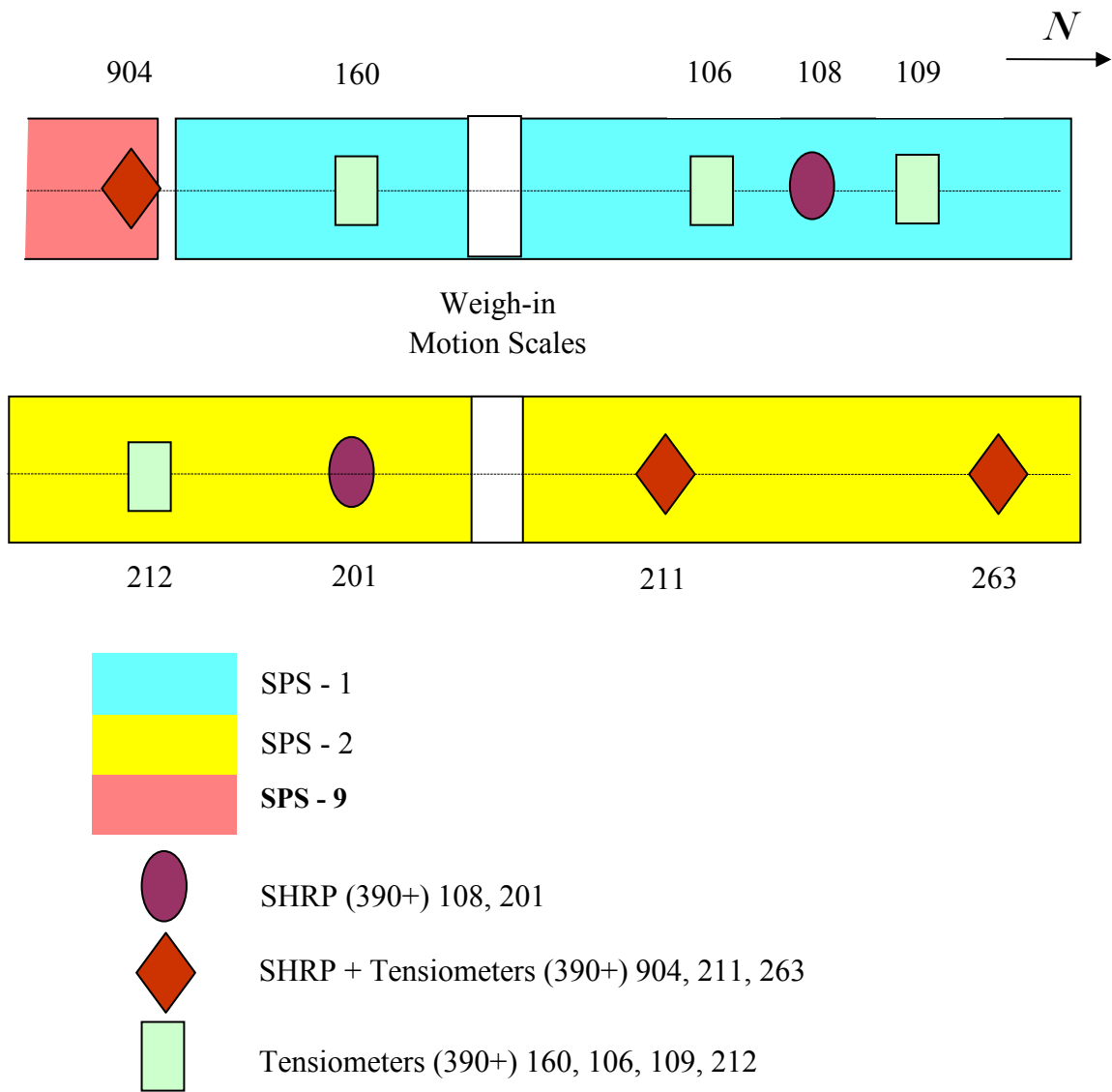


Figure 4.2 Locations of OSU Field Instrumentation at DEL23

4.2 WAY 30

The WAY 30 test pavement is a four-lane highway relocation of US 30 in Wayne County, Ohio. The test pavement begins just east of the city of Wooster, OH at an interchange with State Route 83 and extends east to Kansas Rd. near State Route 57. A perpetual asphalt pavement and a long lasting Portland cement pavement were designed and constructed. Pavement instrumentation was installed during construction to monitor the load and environmental conditions. Tensiometers were installed by OSU to monitor the pore water pressure profile in the subgrade at four stations (Figure 4.3). At station three, the sensors were damaged when the concrete pull box was moved by the contractor after installation (Figure 4.4).

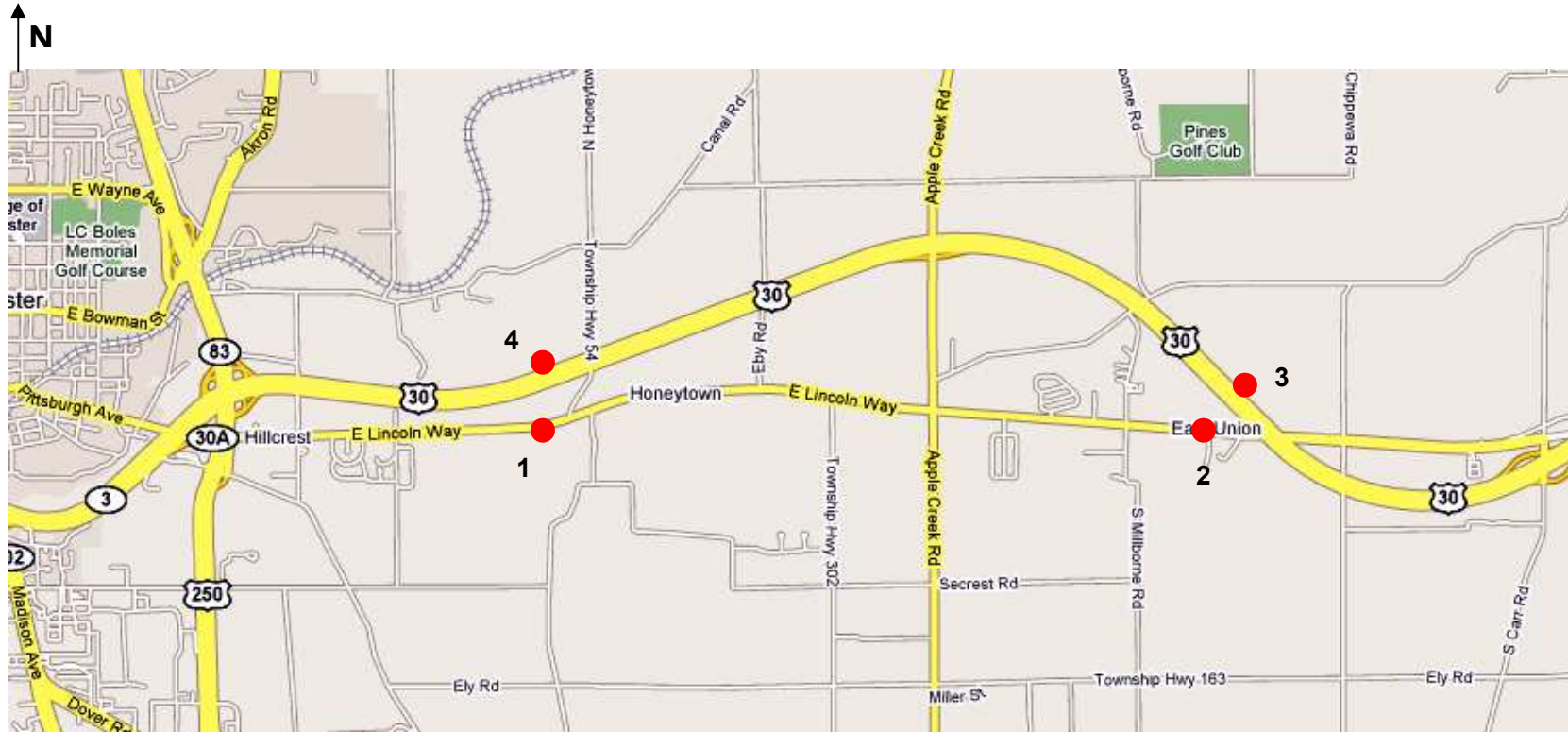


Figure 4.3 OSU WAY 30 Site Station Layout

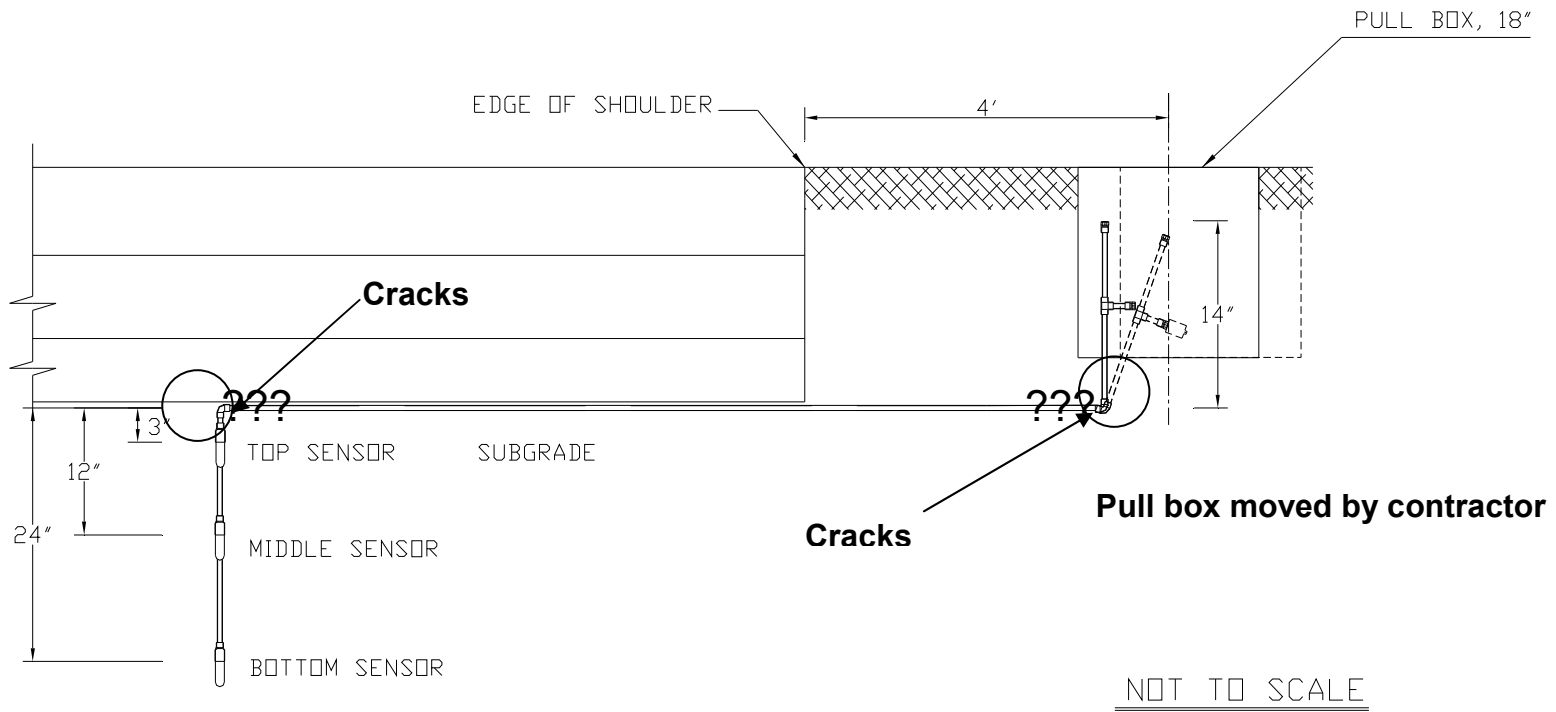


Figure 4.4 Damaged Sensors at WAY 30 Station Three

4.3 MAD 70

The MAD 70 site is located on the Madison/Clark County I-70 reconstruction project. The overall project was 14 miles long, extending from US 42 in Madison County to State Route 54 in Clark County. It involved resurfacing or full-depth reconstruction of the existing lanes and the addition of a third lane in each direction, deck repair, repair or repaving nine ramps and replacement or widening of 13 bridges. One tensiometer station was initially installed in September 2005 in the eastbound lanes of I-70 near the intersection of US 42. However, the sensors were damaged by construction crews shortly after the installation (Figure 4.5). Two replacement stations were installed under the MAD 70 westbound lanes in 2006 west of the US 42 overpass (Figure 4.6).



Figure 4.5 Instrumentation Damaged at MAD 70 Eastbound after Installation



Figure 4.6 OSU MAD 70 Site Location Layout

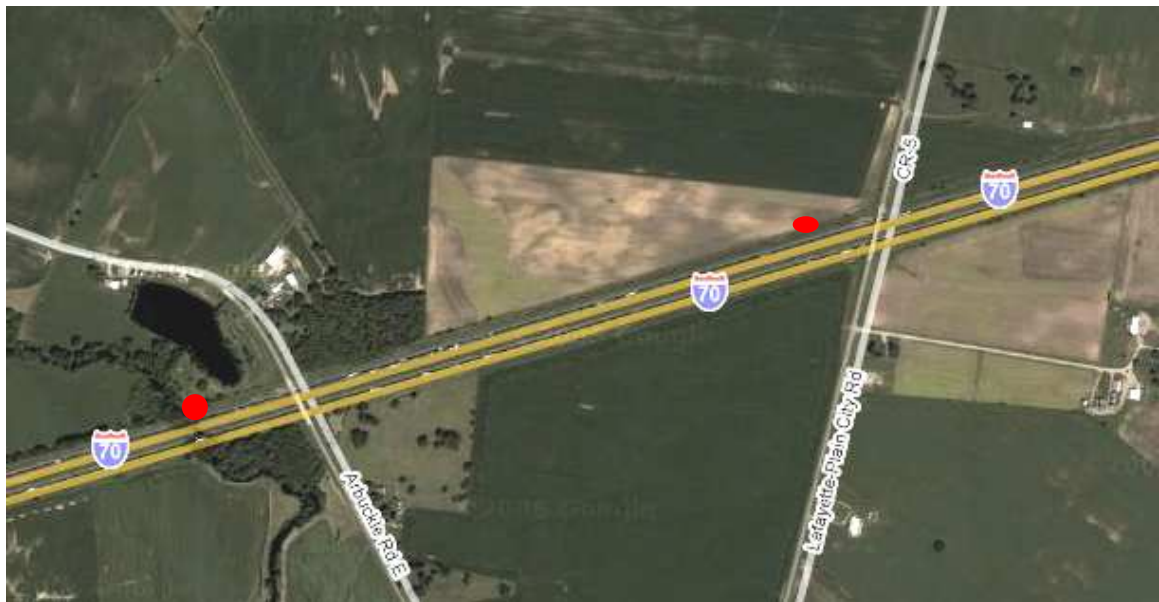


Figure 4.7 OSU MAD 70 Site Station Layout – Aerial View

4.4 ROS 207

The ROS 207 connector project involved the construction of a 2.67-mile, two-lane highway from State Route 104 at the Ross County Fairgrounds to U.S. Route 23 near Delano Road (Figure 4.8). The site for the tensiometer instrumentation was selected to be the culvert on the northeast bound lane of the connector near the intersection of State Route 104. The subgrade consisted of sandy soils from a nearby borrow pit.



Figure 4.8 OSU ROS 207 Site Station Layout



Figure 4.9 ROS 207 Site Instrumentation Location

4.5 I -71/I -270 Interchange

Three tensiometers were installed on ramp M at the interchange of I -270 and I- 71 in northern Franklin County (Figure 4.10). Following convention established in our earlier tensiometer installations, three sensors were arranged vertically with the uppermost sensor at the top of the subbase, with the second and third tensiometers 12 and 24 inches beneath the top sensor. However, heavy equipment damaged the topmost tensiometer during roadway construction shortly after installation.

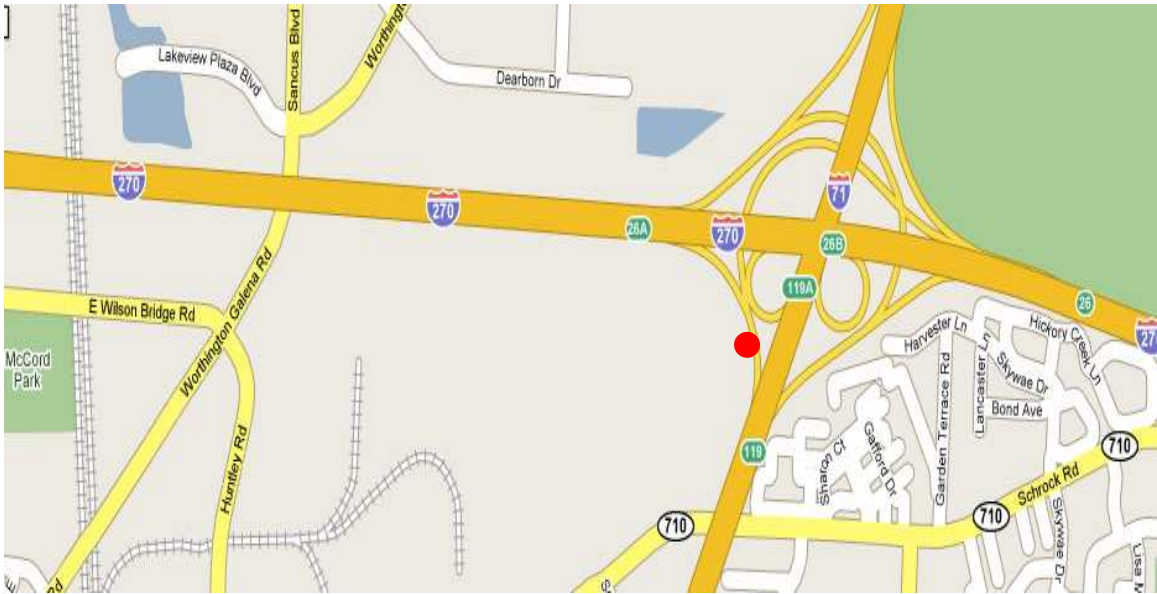


Figure 4.10 OSU I-71/I-270 Site Station Layout



Figure 4.11 OSU I-71/I-270 Site Station Layout – Aerial View

4.6 OSU FDR Sites

Tensiometers were also installed at the OSU Full Depth Reclamation (FDR) test pavement sites in Delaware, Warren and Muskingum counties. In this on-going study, three severely deteriorated Ohio county roads were rehabilitated using the FDR technology with different stabilizing agents including fly ash, lime-kiln dust, cement, and bituminous emulsions. The construction of the first two sites (in Delaware and Warren Counties), was completed in September 2006. During construction, tensiometers were installed along with load response (pressure cells, LVDTs, and strain gauges) and environmental sensors (lysimeters) to monitor pavement response and subsurface water quality. Standard FWD tests and pavement response data were collected and monitored regularly after the completion of construction. Figure 4.12 shows the plan view of the FDR test pavement sections in Delaware County. Tensiometers were also installed at the third FDR site located in Zanesville, Ohio in August 2007.

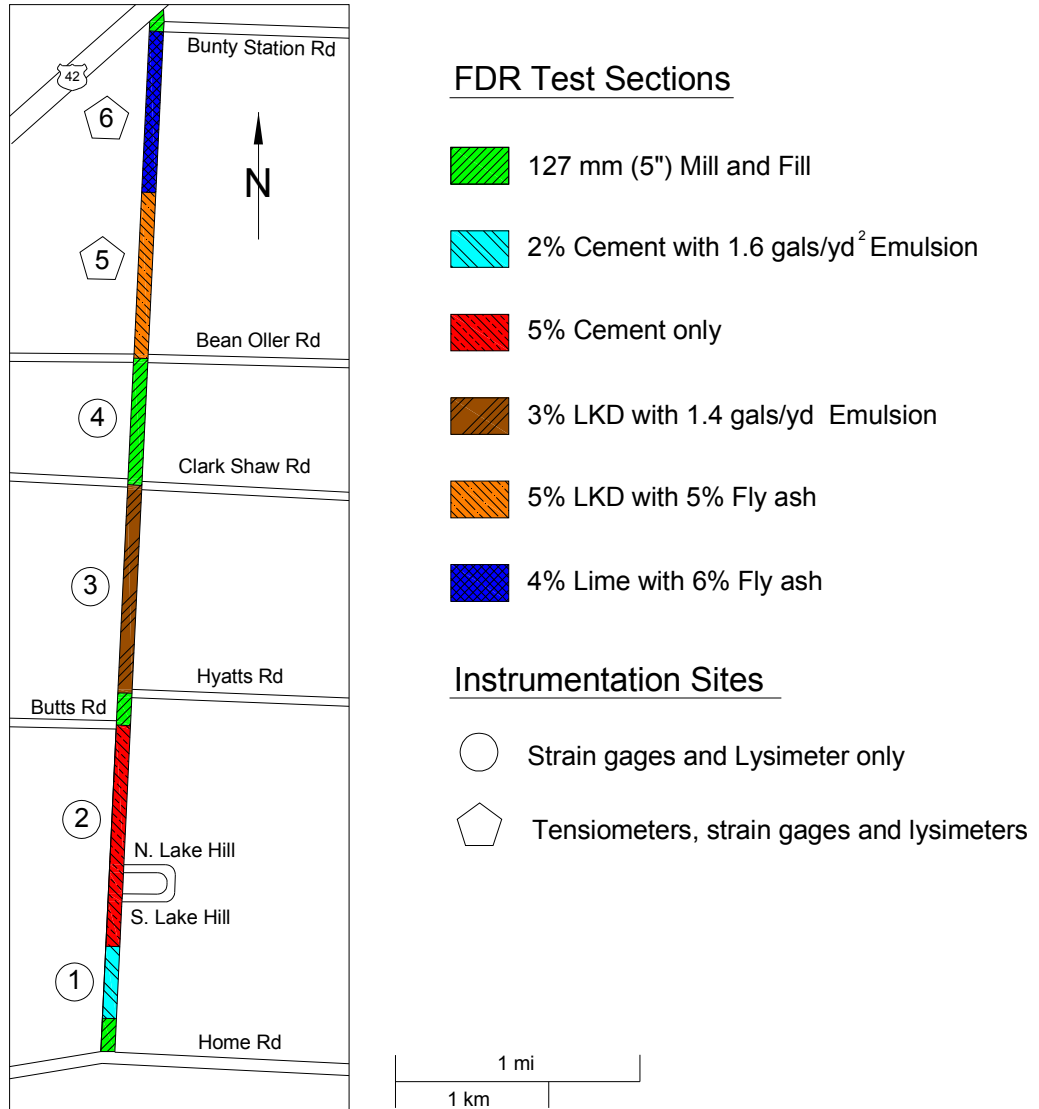


Figure 4.12 Plan View of OSU FDR Pavement Site at Delaware County, Ohio



Figure 4.13 OSU S. Section Line Rd. Site Station Layout

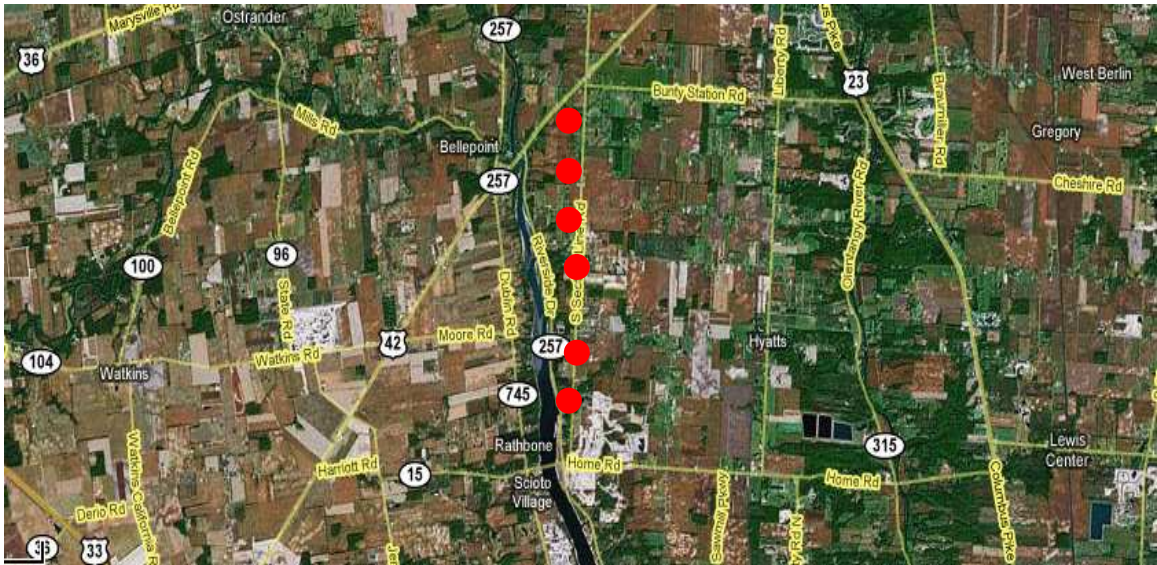


Figure 4.14 OSU S. Section Line Rd. Site Station Layout – Aerial View



Figure 4.15 OSU Warren County Site Station Layout



Figure 4.16 OSU Warren County Site Station Layout – Aerial View



Figure 4.17 OSU Muskingum County Site Station Layout

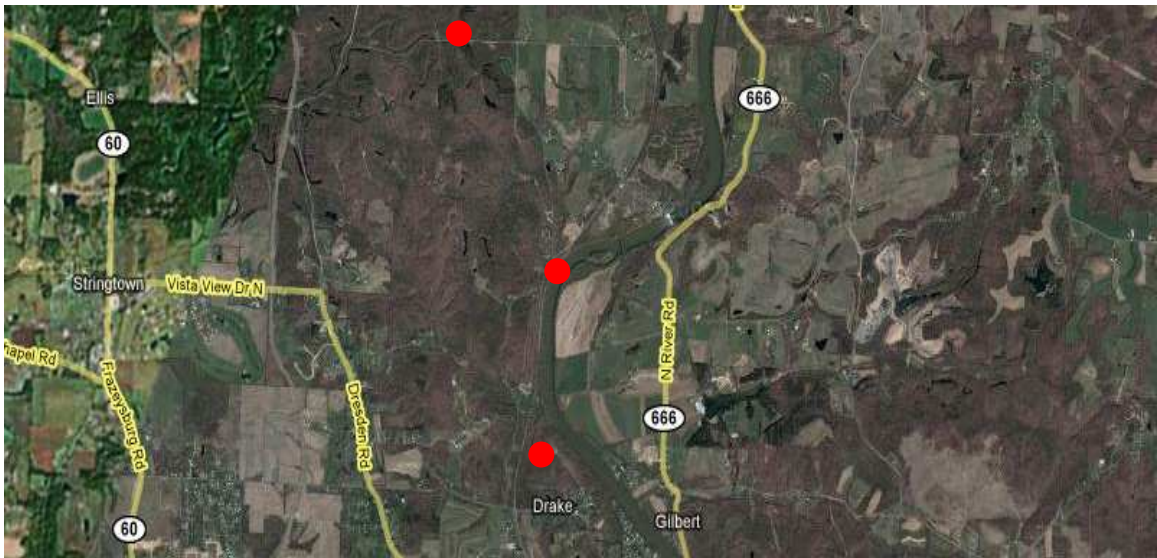


Figure 4.18 OSU Muskingum County Site Station Layout – Aerial View

4.7 Summary

Several sites were selected to represent a variety of subsurface conditions. These sites were monitored for periods of up to ten years. At the DEL23 site, LTPP instrumentation continued to be monitored for the life of the instruments. Many of those instruments reached the end of their useful lives during this phase of the project. Tensiometers capable of measuring either positive or negative pore water pressures and thereby giving a record of water effects on the soils supporting the overlying pavement systems, were installed at all the sites studied. The tensiometers require some care in manufacture, during and shortly after installation as evidenced by the number of instruments damaged or destroyed by highway construction crews within days of installation. However, once installed, the tensiometers have been shown to be rugged devices with a very high survival rate even after extended test periods. The data collected from all the installed instrumentation are presented in the following section.

5. FIELD MEASUREMENTS

At the DEL23 site, SHRP prescribed instrumentation was installed at the locations as shown in Figure 4.2. The several instruments were monitored during the initial construction period. Installation procedures and post-construction values were presented in our reports dated September 1998 and June 2004. Instrumentation hardware, recording procedures, as well as problems with reliability and longevity were discussed in detail in those two reports. Data collected, including tensiometer data, up to the date of the respective reports was also presented. Presented in this section is a summary of the data collected during the period 2004 to 2007.

5.1 DEL 23

5.1.1 SHRP Instrumentation

Table 5.1 lists the design parameters for each section at the DEL 23 site sampled by the OSU team, including the sections added after the original construction period. Figure 5.1 presents an example of a typical SHRP configuration of the installed instrumentation (here represented by test section 390263). Our previous reports have provided descriptions of the data collected and methods for reporting and storing responses. Since the methods of data collection and storage and preservation were unchanged, the reader is referred to those two reports for details.

5.1.1.1 Moisture Content

Using Section 390904 as an illustration of the data collected, moisture content (from TDRs) data can be plotted as shown in Figure 5.2 for the year 2007. The data are presented as seasonal averages (SU = Summer, AU = Autumn, WI = Winter, SP = Spring). They clearly show seasonal fluctuations in the moisture with the highest moisture contents occurring in the summer. Figures 5.3 through 5.6 show the same variations during the preceding years. The moisture content data over the full duration of the project (three reports) as a function of instrument location in the subsurface profile (Figures 5.7 through 5.10) highlight the seasonal variations in subgrade moisture content. It is apparent that, in the last four years of data collection, the average annual moisture content in the subgrade has remained at approximately 25%. Our earlier reports observed continuing increases in moisture content for several years after construction. However, our later data show that once full saturation was reached, increases in water content appear to have been limited to seasonal fluctuations. This observation is supported by the tensiometer data presented in Section 5.1.2 where predominantly positive pore pressures have been measured for several years.

Moisture content data are presented for section 390263 for comparison purposes. The same seasonal variations are observed at all depths, but despite considerable data scatter, it is apparent that the annual mean moisture content has remained approximately constant since 2003-04 (Figures 5.11 through 5.14).

5.1.1.2 Soil Temperature

The sections for which temperature data were collected during the period 2004 through 2007 are given in Table 5.1. Temperatures recorded for most of the thermistors indicated faults in either the sensor or the data logger during much of the study period. Temperature readings collected were uploaded to the project data base but were insufficient to show trends so were not included herein.

5.1.1.3 Resistivity

The soil resistivity profiles collected were of questionable quality for much of the project study period due either to electrical problems with the collection system or sensor failure. The stations at which resistivity gages were installed are given in Table 5.1.

5.1.2 Tensiometers

Tensiometers were installed under seven pavement sections plus the weather station. The locations are shown in Figure 4.2. The tensiometers at sections 390211, 390263 and 390904 and the weather station were all installed in 1996 when the original SHRP instrumentation was placed. The tensiometers at sections 390160, 390106, 390121 and 390109 were installed in 2002 and 2003. With the exception of the weather station location which had only two tensiometers installed, pore pressures were recorded at three depths at each location, typically at the interface between the base and subgrade and at depths of 12 and 24 inches (30, and 60 cm) below the base into the subgrade.

The time history of the water pressures for the DEL 23 sections are presented in Figures 5.15 through 5.19. By the spring of 2004, the tensiometers recorded positive pore water pressures (except at the weather station) and although there were seasonal fluctuations in the value of the water pressure at each location, the data were typically positive, meaning the static water table had risen to and stayed between the surface of the roadway and the sensor. At the time of installation, the pore pressure values recorded by the tensiometers installed in 2002 and 2003 were all negative (less than atmospheric pressure) at the interface with the base, but at 12 and 24 inches into the subgrade, positive pore pressures existed by the time the first readings were taken. In general, the pore pressures continued to increase through the following months. At the end of the recording period, the pore water pressures recorded were typically positive at all three elevations. It is interesting to note that the observation made in our earlier reports concerning the pore pressure measurements at the weather station were observed during this final phase of the project as well. The pore pressure measurements taken at the weather station

fluctuated more widely at the 12 inch depth than at any location under any pavement section. The effect of sealing the surface and thereby eliminating surface infiltration and evapo-transpiration as moisture regulating mechanisms was to reduce the seasonal variability in ground water levels while increasing the mean groundwater elevation as well as the average water content. A review of the pore pressures recorded at the weather station from the time the tensiometers were installed is presented in Figure 5.20. As stated in our 2004 report, these tensiometer data strongly suggest that water is being drawn up into the profile from depth. The continued high water levels over the most recent four year period support the observation made in 2004 that the base and subbase should not be considered as free draining.

5.2 WAY 30

As discussed in Section 4.2, the tensiometers installed under the WAY30 test pavements at locations 2 and 3 were field modified. Further, the tensiometers placed at location 3 were damaged beyond repair when the pull box was displaced by the contractor shortly after installation was completed. The change in pore pressure over an eight month period beginning in the spring after installation the previous summer is shown for location 1 in Figure 5.21. The pore pressures remained consistently negative, meaning the water table was below the sensor level, throughout this period. However, during a load test in the spring following installation, dynamic pore pressure response was recorded under the test pavements. As can be seen in Figures 5.22, 5.23, and 5.24, the effect on the pore water of the loaded trucks passing over the sensor was clearly recorded as a rapid increase in the static pore pressure indicating saturated conditions at all sensor locations at all three stations. The dynamic pore pressures were recorded in October when a truck passed over the tensiometers at Station 1 during a scheduled monthly reading. Figure 5.25 presents the results of those dynamic pore water pressure readings. As was the case the previous spring, the passing of the loaded truck was recorded as an instantaneous increase on pore water pressure. Although the pore water pressure returned to the preload conditions immediately after the truck passed the sensors, the fact that the sensors recorded the passing truck in real time means that the subsurface is saturated.

5.3 MAD 70

Tensiometers were installed in the westbound lanes of Interstate 70 west of the US 42 overpass in summer 2006. The pore pressure history over a 15 month period is shown for Station 1 in Figure 5.26 and for location 2 in Figure 5.27. Although pore pressures were negative shortly after installation, positive pore pressures were the norm in less than one year, indicating a high water table strongly indicating saturated conditions existed in the supporting soil beneath the pavement.

5.4 ROS 207

Pore pressure distribution recorded at the Ross County site is shown in Figure 5.28 for a 16 month period. It is interesting to note that at this location pore water pressure in the spring following the tensiometer installation was positive at the two lower sensors. At all other times and for the topmost tensiometer, the pressures were negative indicating a shallow but seasonally fluctuating groundwater table.

5.5 I-71/I-270 Interchange

The tensiometers installed in the ramp from I-270 to I-71 were damaged during installation. No reliable readings were retrieved at this location.

5.6 OSU FDR Sites

An example of the data collected at the instrumented full depth pavement reclamation sites discussed in Section 4 is presented in Figure 5.29. Pore water pressure response was recorded as heavy trucks passed over the Station 6 instrumentation. As has been seen at other instrumented locations, the pore water response was coincident with the applied load indicating the likelihood that saturated conditions prevailed under the reclaimed pavement sections.

5.7 Summary

By the end of the project, the temperature and resistivity gauges installed at the five locations at the DEL23 test pavement assigned to the OSU researchers had failed. Almost all the moisture content sensors (TDRs) were still functioning satisfactorily and data were collected up to the conclusion of the current work effort. The tensiometers installed as an extra source of data on the condition of the subsurface soils are still monitoring pore pressures. What has been determined from the TDRs is the moisture content under the paved sections varied seasonally but the mean value continued to rise for several years. In the latter years of the investigation the mean water content was essentially constant. The tensiometers that were installed to record the pore pressures also measured a response that varied seasonally but trended to higher and higher pore pressures with time. At most of the sites studied, the pore pressures became positive within one or at most two years after installation and remained positive for most of the year. This information combined with the TDR data strongly indicates that saturated soils were encountered at all sites studied and similar conditions should be expected to exist under other Ohio highways.

390263

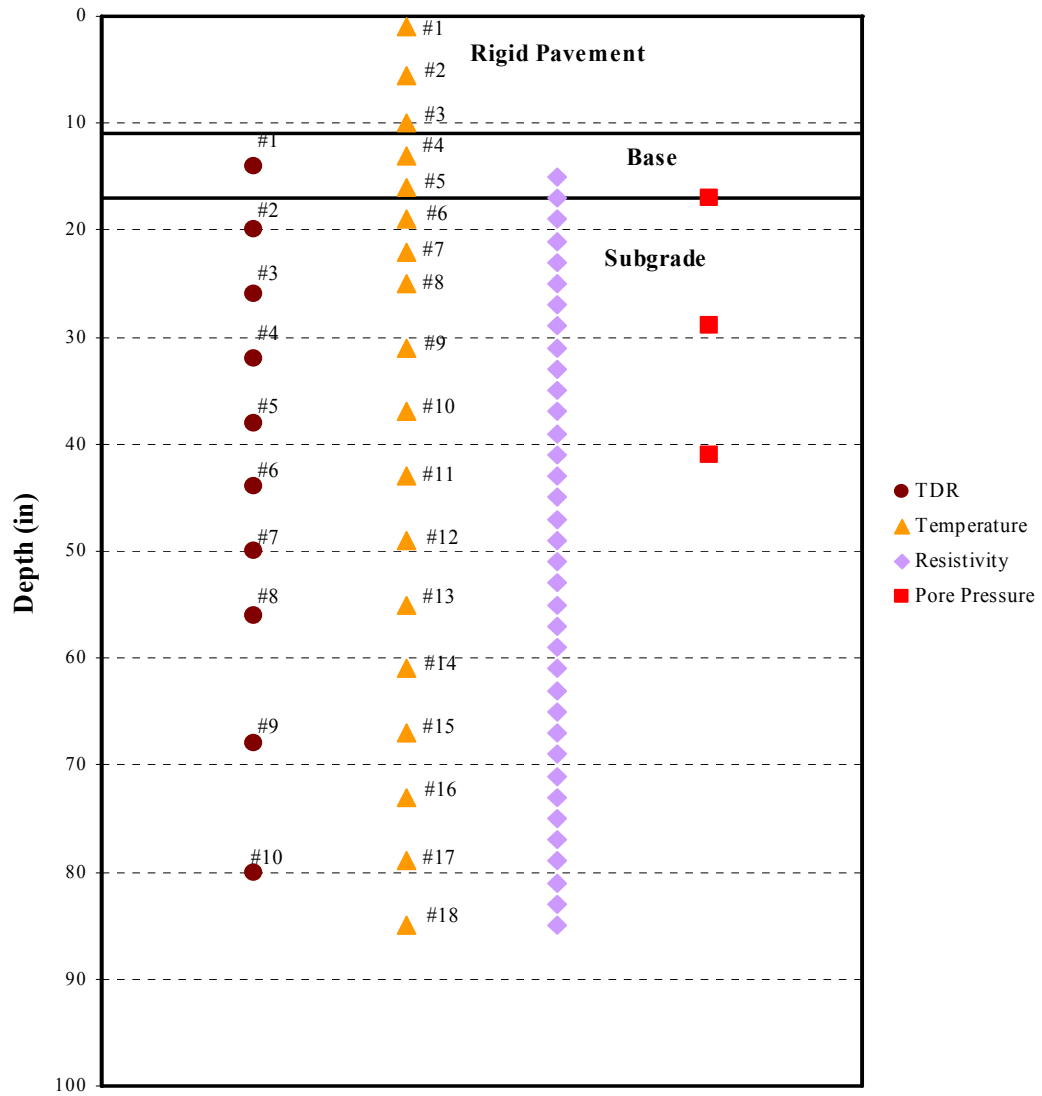


Figure 5.1 Instrumentation Configurations (390263 from 2004 report)

ID	Section	Designation	Thickness (in)			Base	Drain	Environment Instrument
			AC	PC	Base	Type		
390108	J8	SPS-1	7		12	4" PATB/ 8" DGAB	Yes	Temperature Moisture Frost Depth
390160	S7	SPS-1	4		15	11" ATB/ 4" DGAB	Yes	Soil Suction
390106	J6	SPS-1	7		12	8" ATB/ 4" DGAB	No	Soil Suction
390904	SHRP	Experimental SHRP Mix SPS-9	4		22	12" ATB/ 4" PATB/ 6" DGAB	Yes	Temperature Moisture Frost Depth Soil Suction
390201	J1	SPS-2		8	6	DGAB	No	Temperature Moisture Frost Depth
390211	J11	SPS-2		11	8	4" PATB/ 4" DGAB	Yes	Temperature Moisture Frost Depth Soil Suction
390212	J12	SPS-2		11	8	4" PATB/ 4" DGAB	Yes	Soil Suction
390263	S4	SPS-2		11	6	DGAB	Yes	Temperature Moisture Frost Depth Soil Suction

SPS-1: Strategic study of structural factors for flexible pavement

AC: Asphalt Concrete

SPS-2: Strategic study of structural factors for rigid pavement

PCC: Portland Cement Concrete

SPS-9: Asphalt program field verification studies.

DGAB: Dense Graded Aggregate Base

ATB: Asphalt Treated Base

PATB: Permeable Asphalt Treated Base

Table 5.1 Ohio State University DEL 23 Test Sections

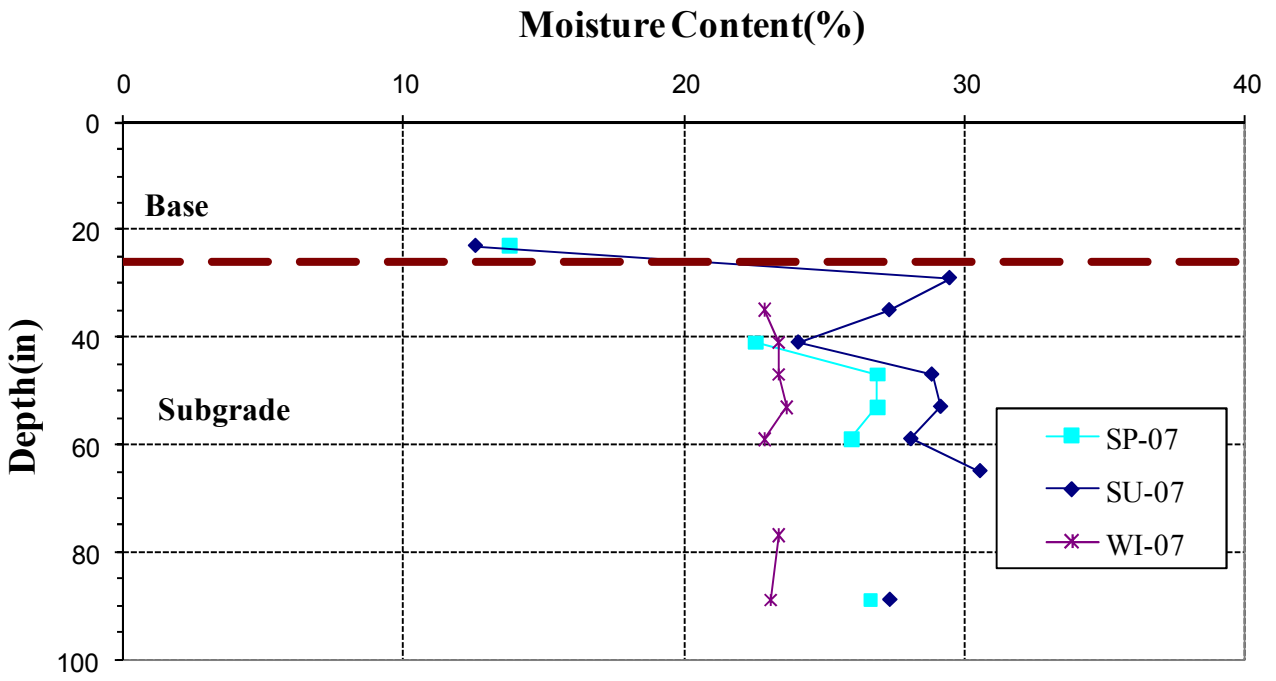


Figure 5.2 Seasonal Moisture Content for 2007 (390904)

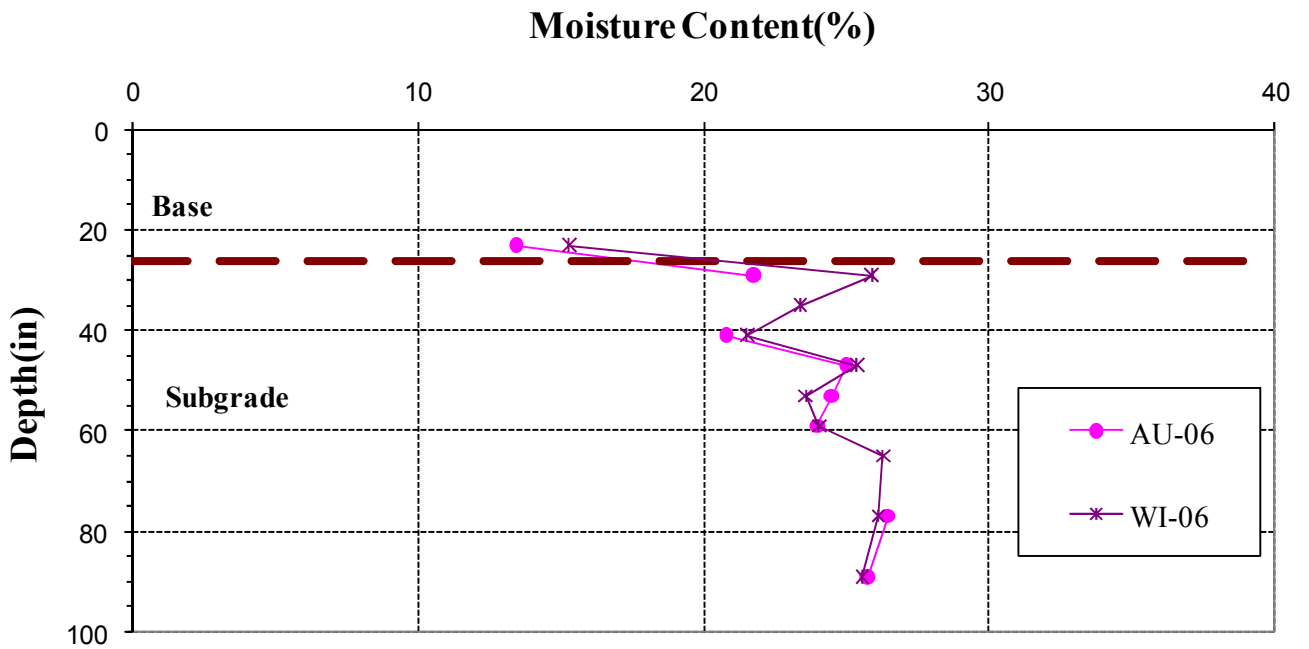


Figure 5.3 Seasonal Moisture Content for 2006 (390904)

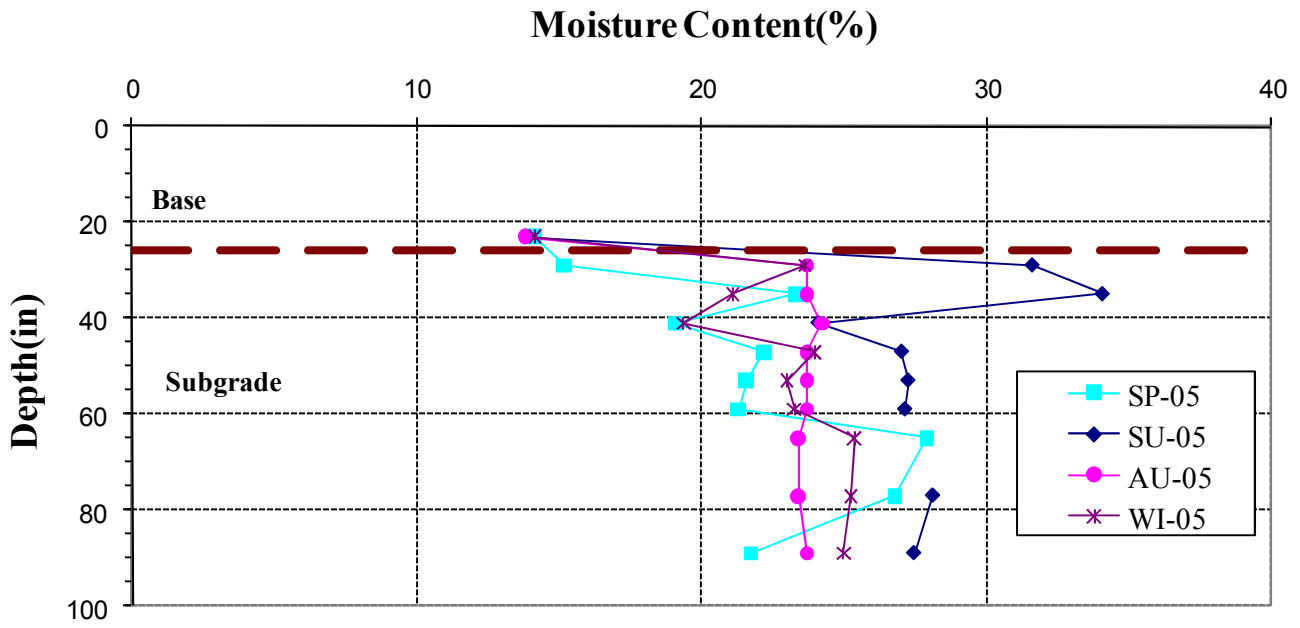


Figure 5.4 Seasonal Moisture Content for 2005 (390904)

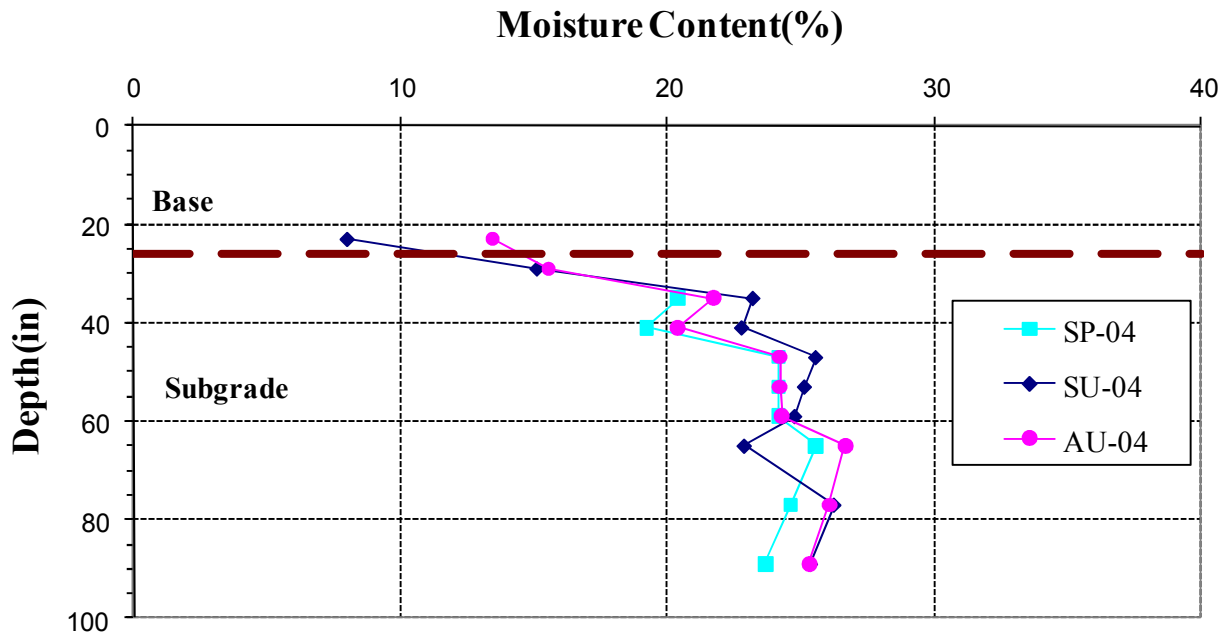


Figure 5.5 Seasonal Moisture Content for 2004 (390904)

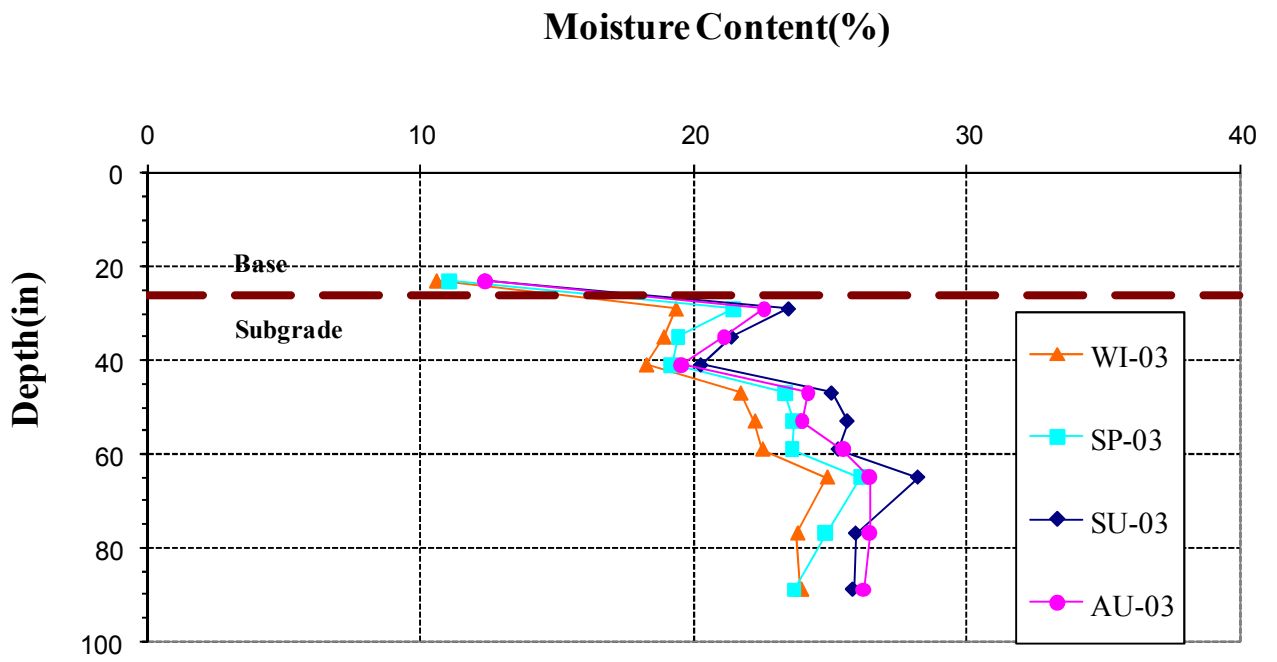


Figure 5.6 Seasonal Moisture Content for 2003 (390904)

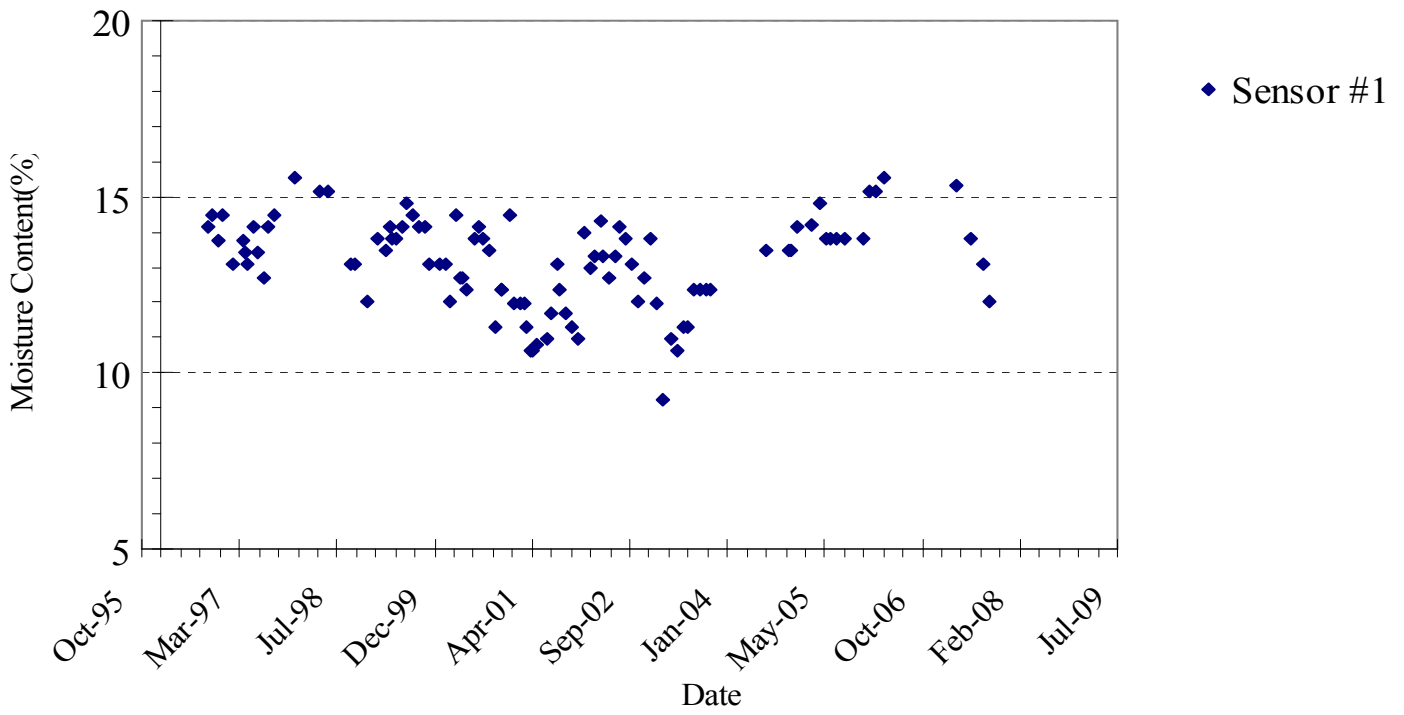


Figure 5.7 Moisture Content (390904) Topmost TDR 1996-2007

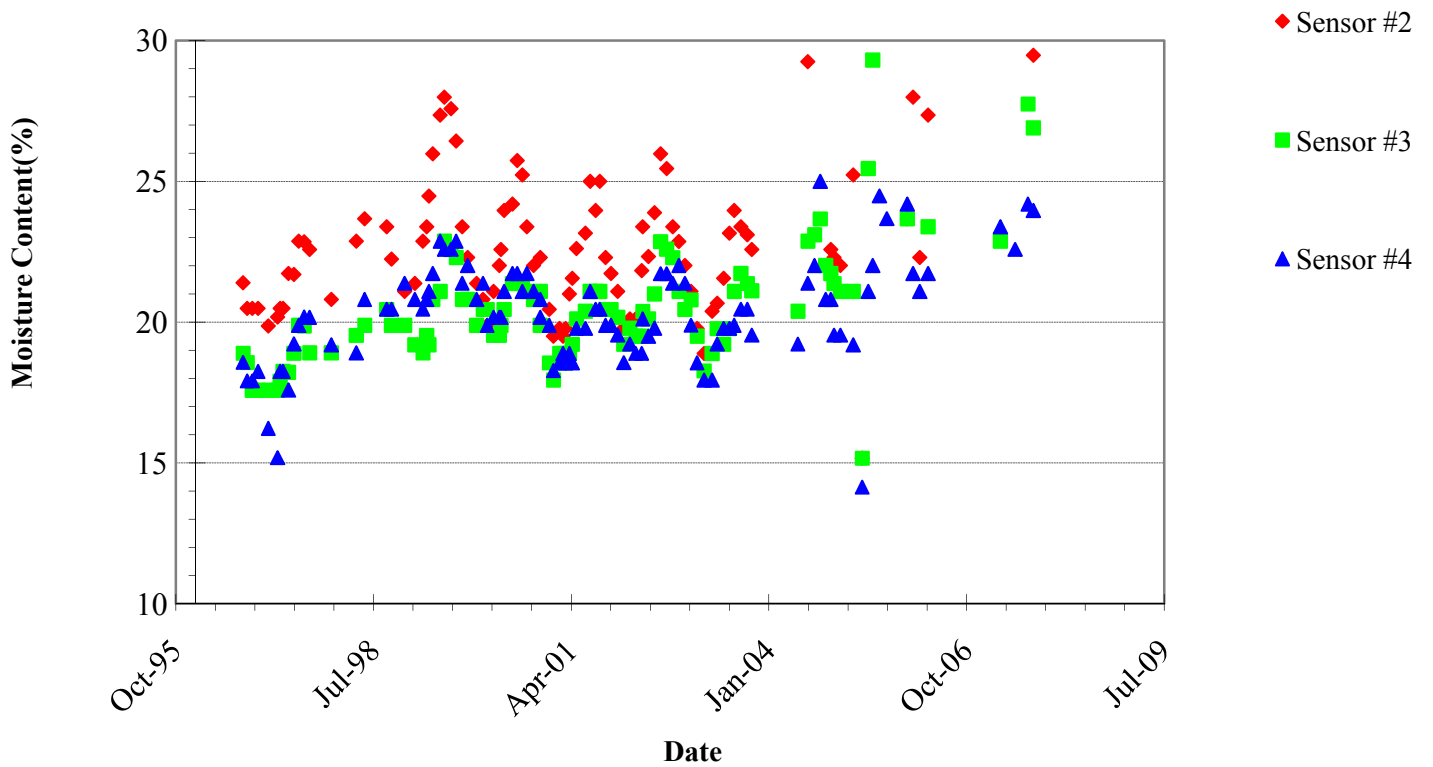


Figure 5.8 Moisture Content (390904) Top of Subgrade 1996-2007

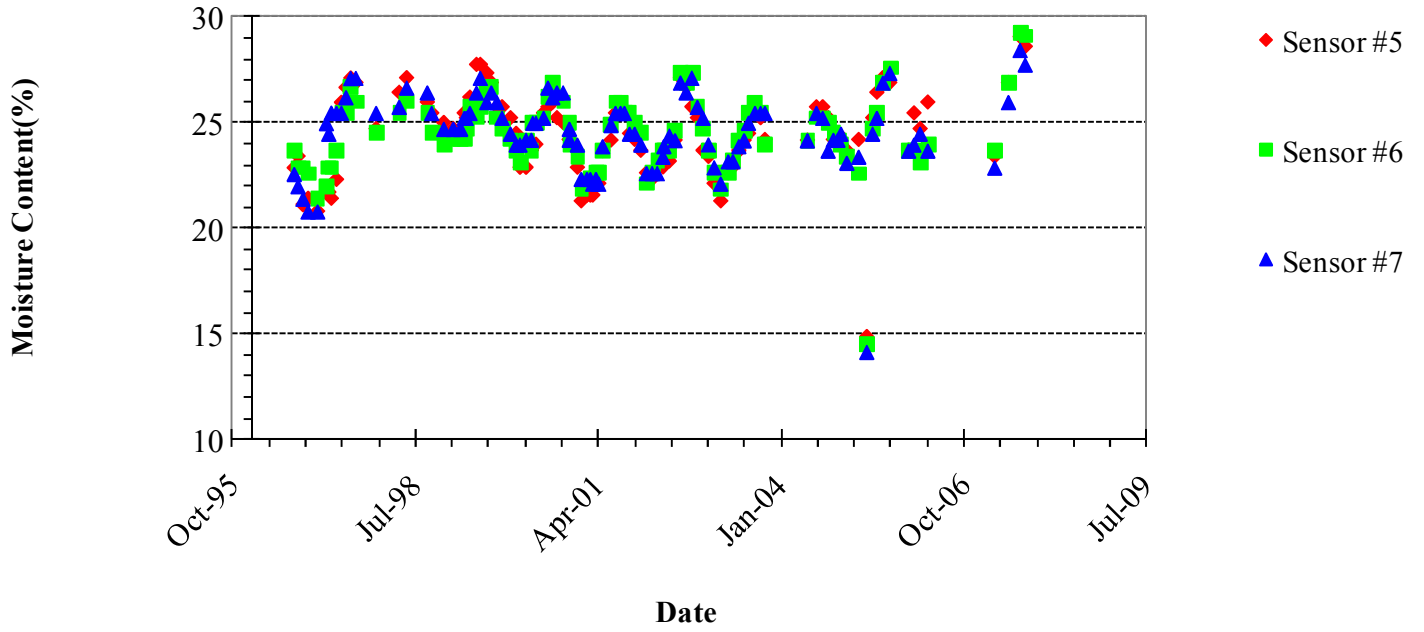


Figure 5.9 Moisture Content Middle of Subgrade 1996-2007 (390904)

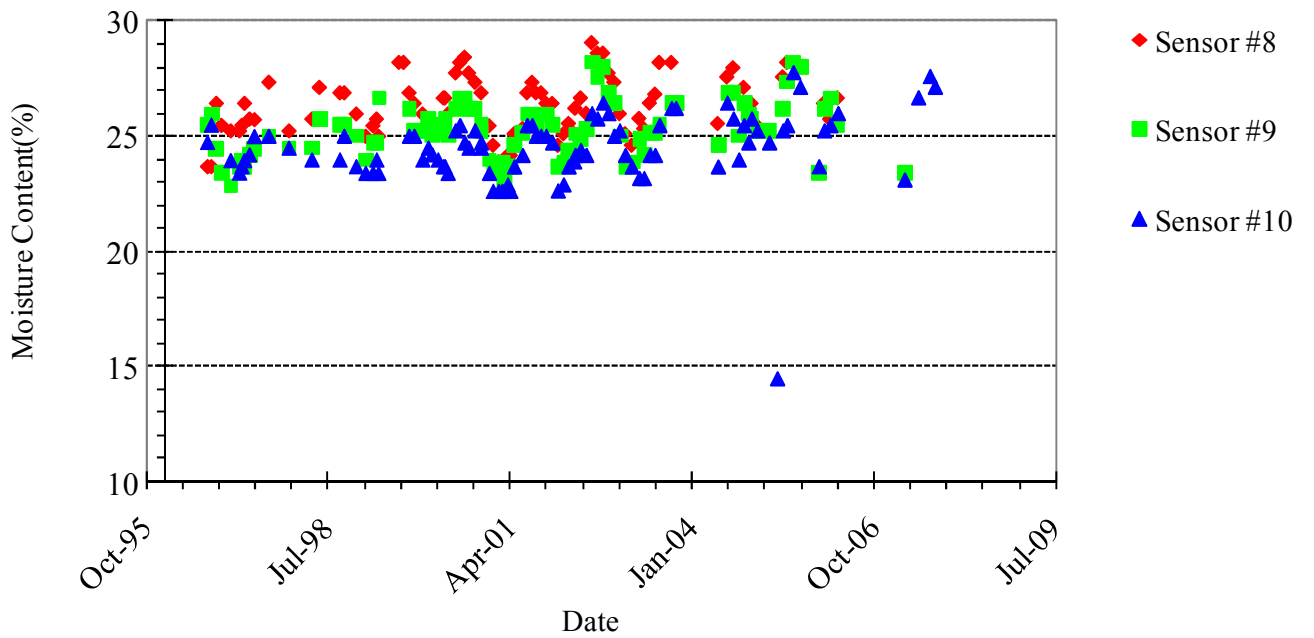


Figure 5.10 Moisture Content Bottom of Subgrade 1996-2007 (390904)

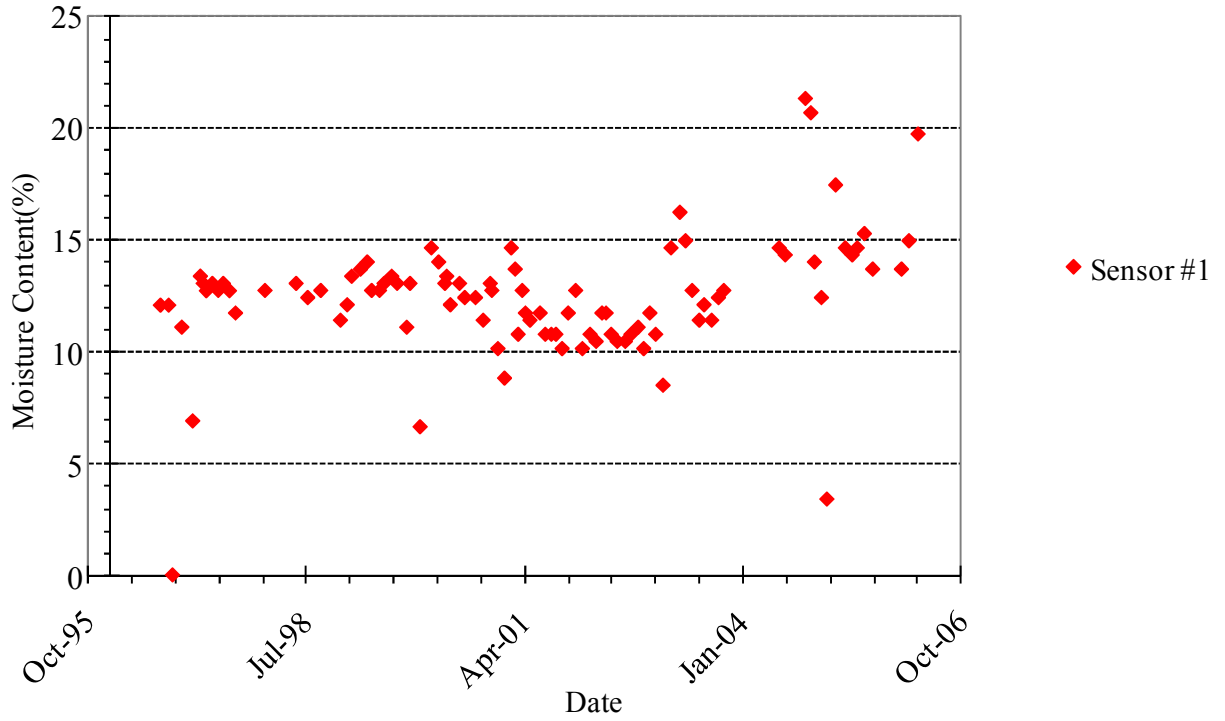


Figure 5.11 Moisture Content at TDR in Base 1996-2006 (390263)

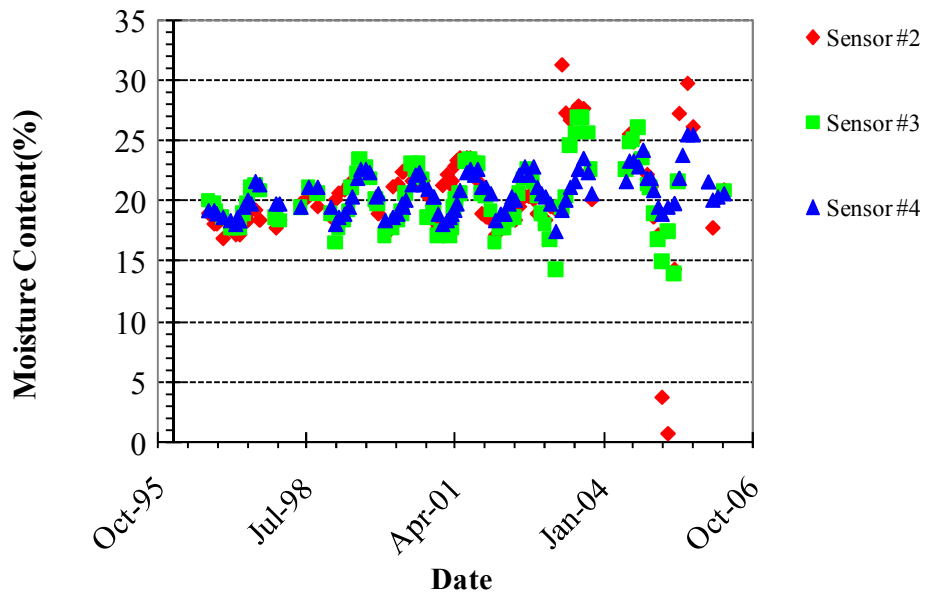


Figure 5.12 Moisture Content at Top of Subgrade 1996-2006 (390263)

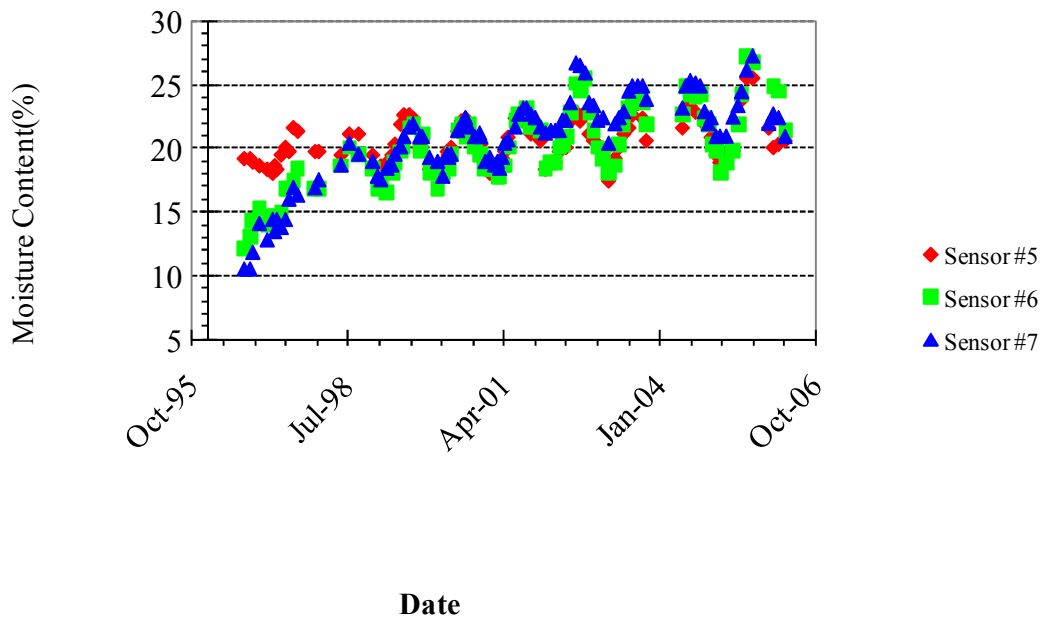


Figure 5.13 Moisture Content Middle of Subgrade 1996-2006 (390263)

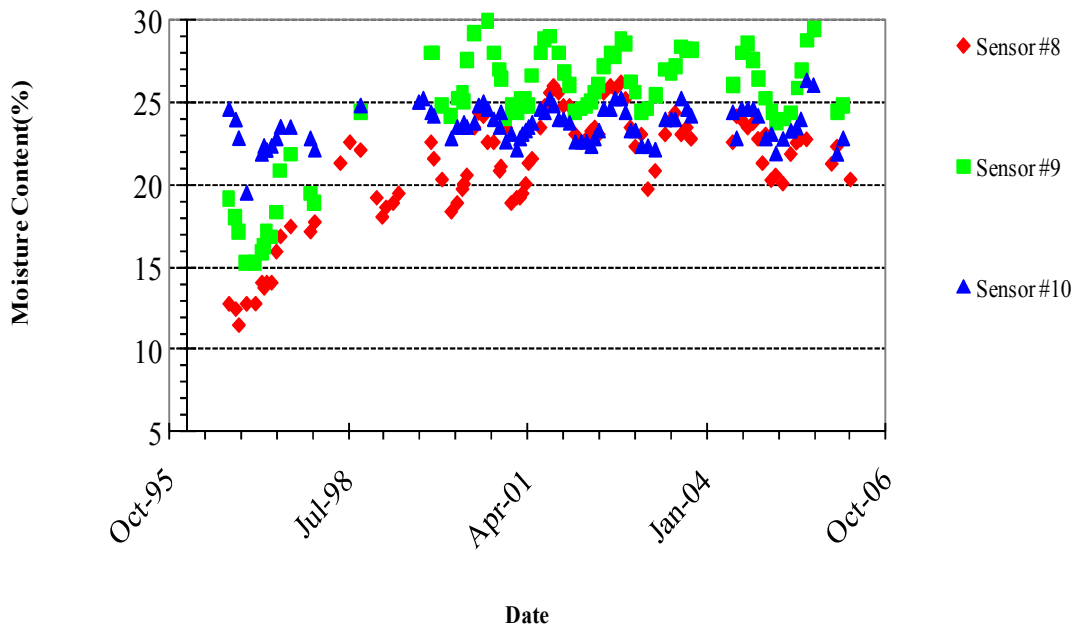


Figure 5.14 Moisture Content Bottom of Subgrade 1996-2006 (390263)

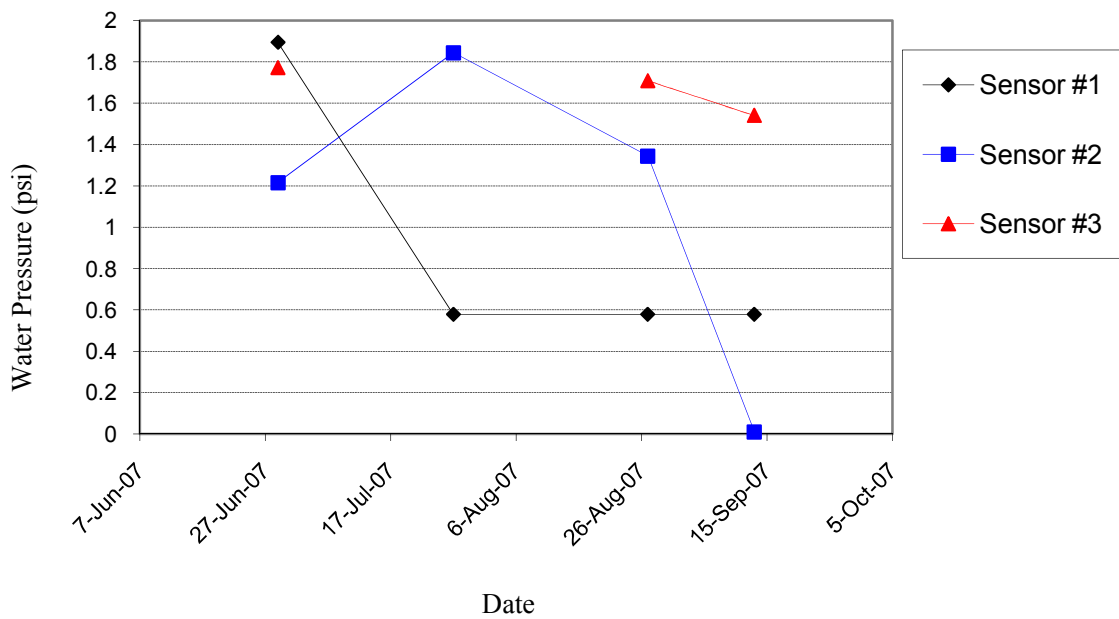


Figure 5.15 Pore Water Pressure at Section 390904

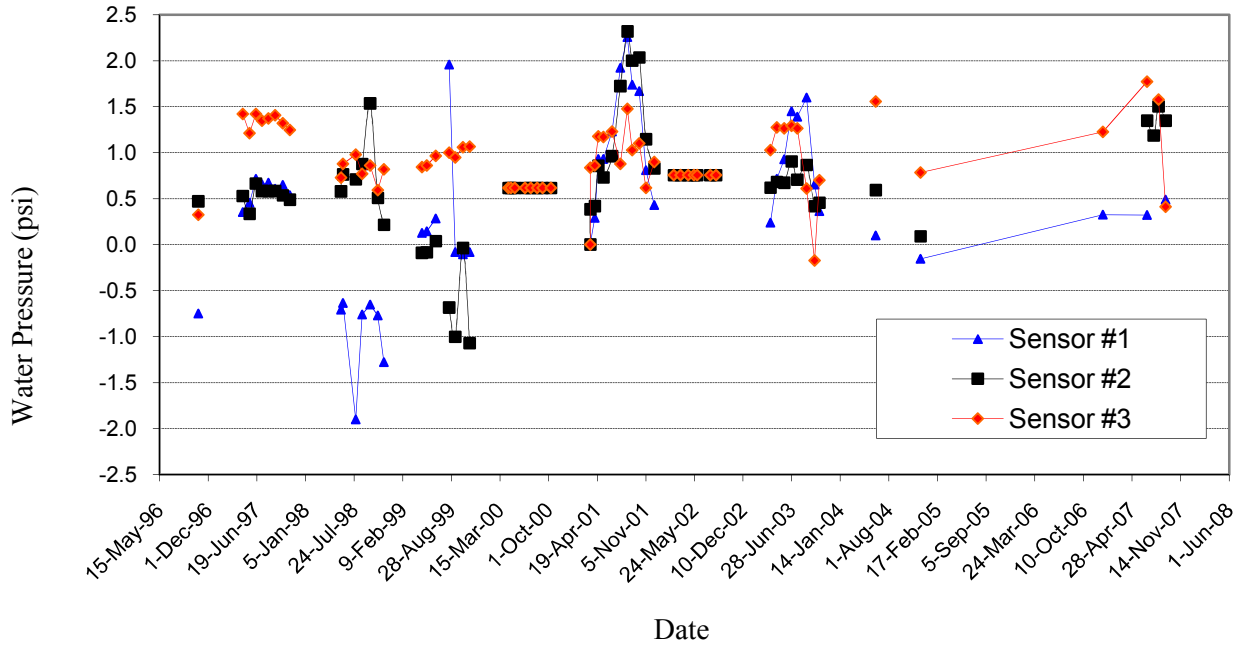


Figure 5.16 Pore Water Pressure at Section 390211

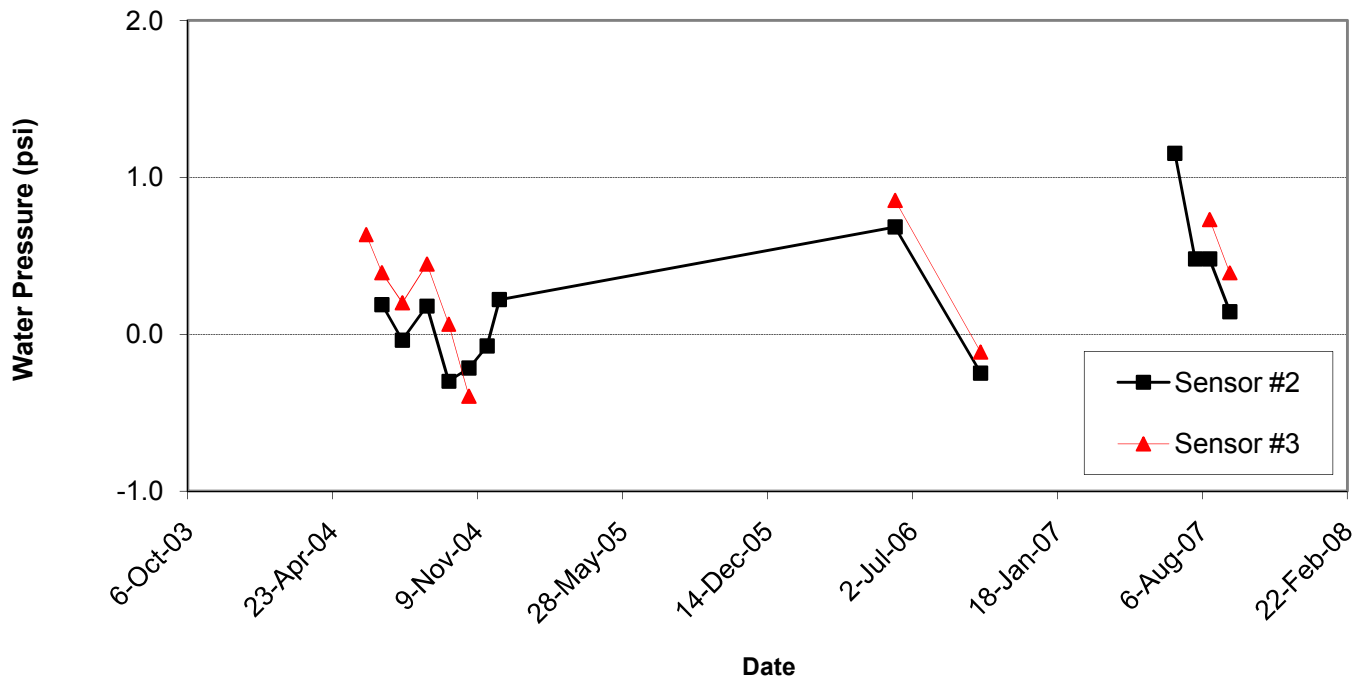


Figure 5.17 Pore Water Pressure at Section 390160

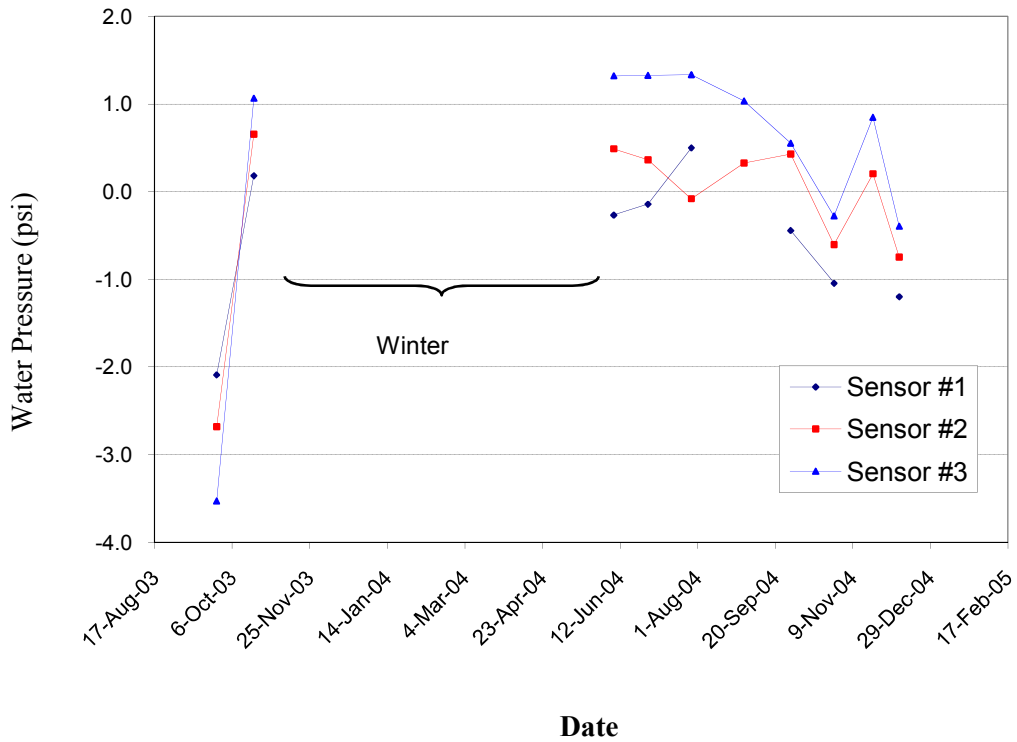


Figure 5.18 Pore Water Pressure at Section 390901

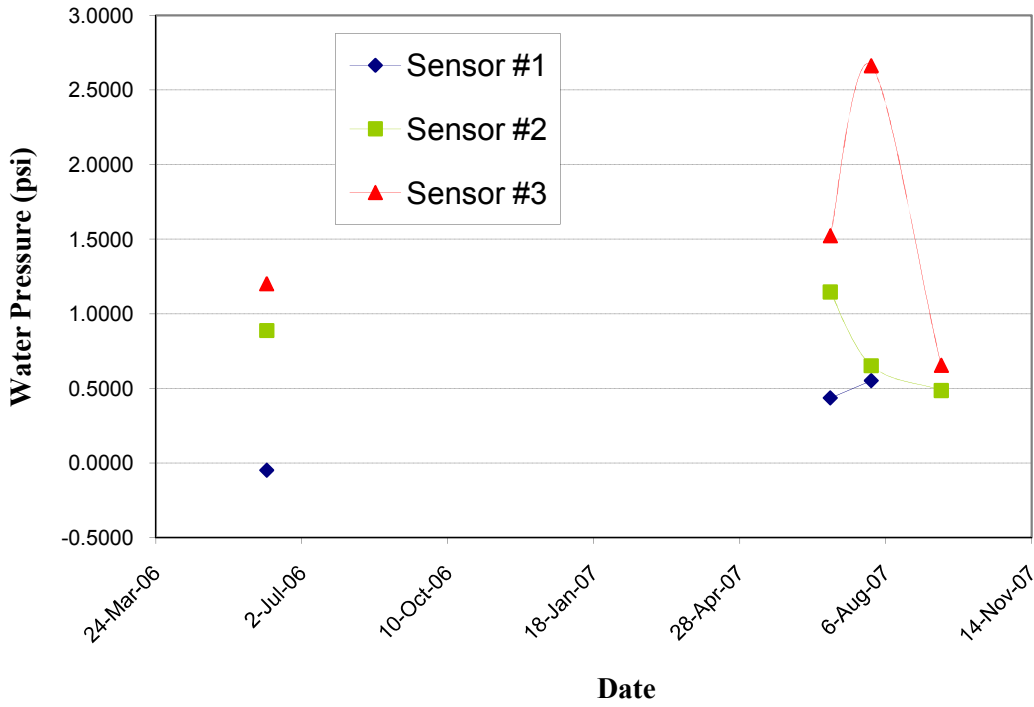


Figure 5.19 Pore Water Pressure at Section 390106

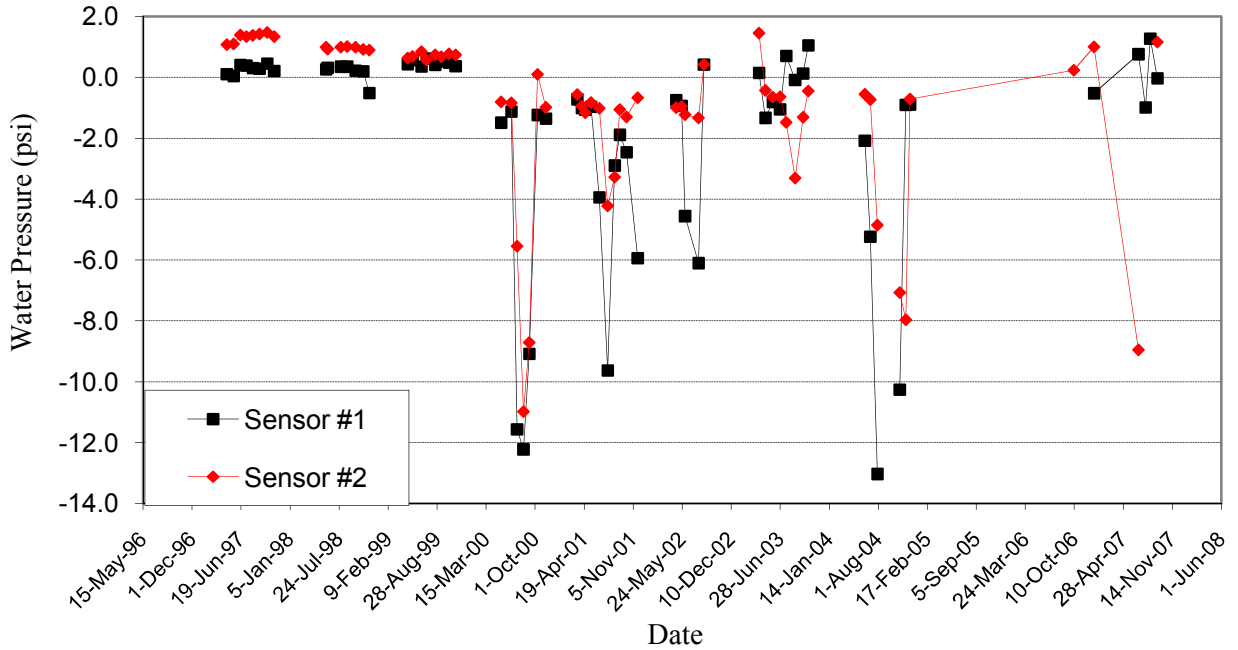


Figure 5.20 Pore Water Pressure at Instrumented Weather Station

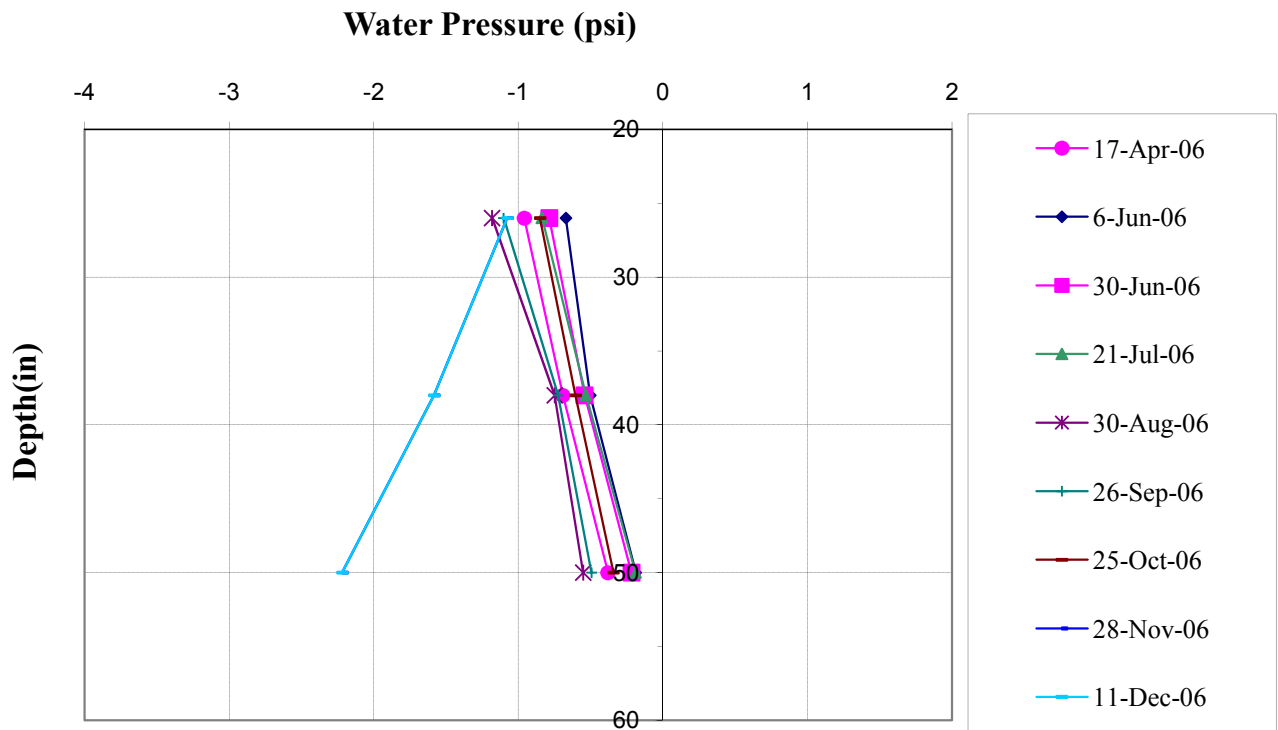


Figure 5.21 Pore Water Pressure at WAY 30 Station 1

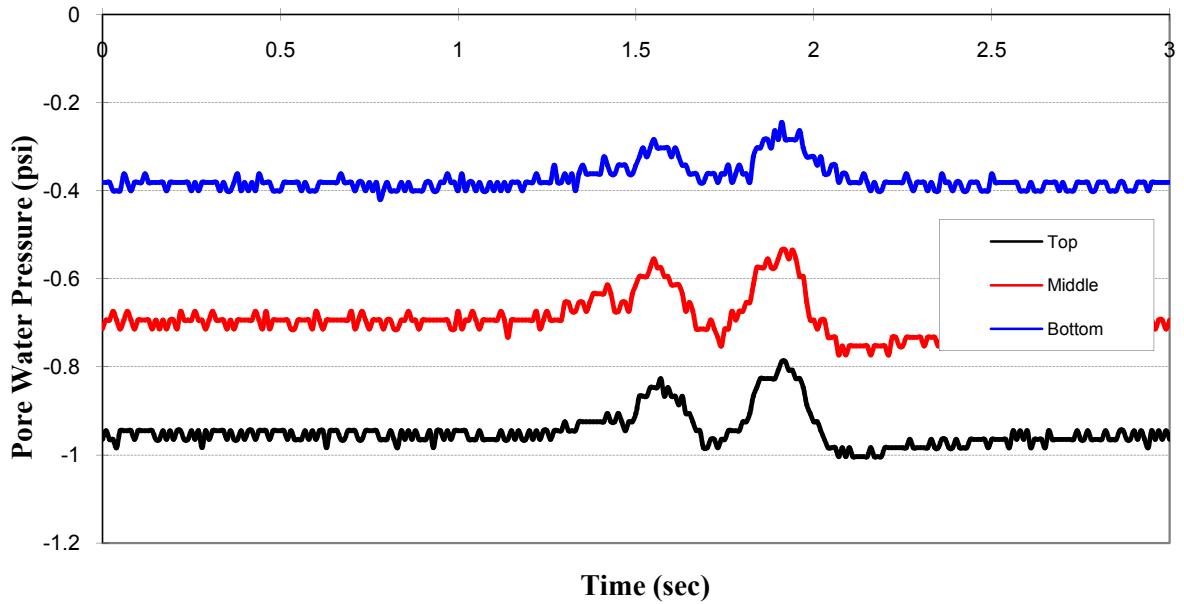


Figure 5.22 Dynamic Pore Pressure Response at WAY 30 Station 1 (April 06)

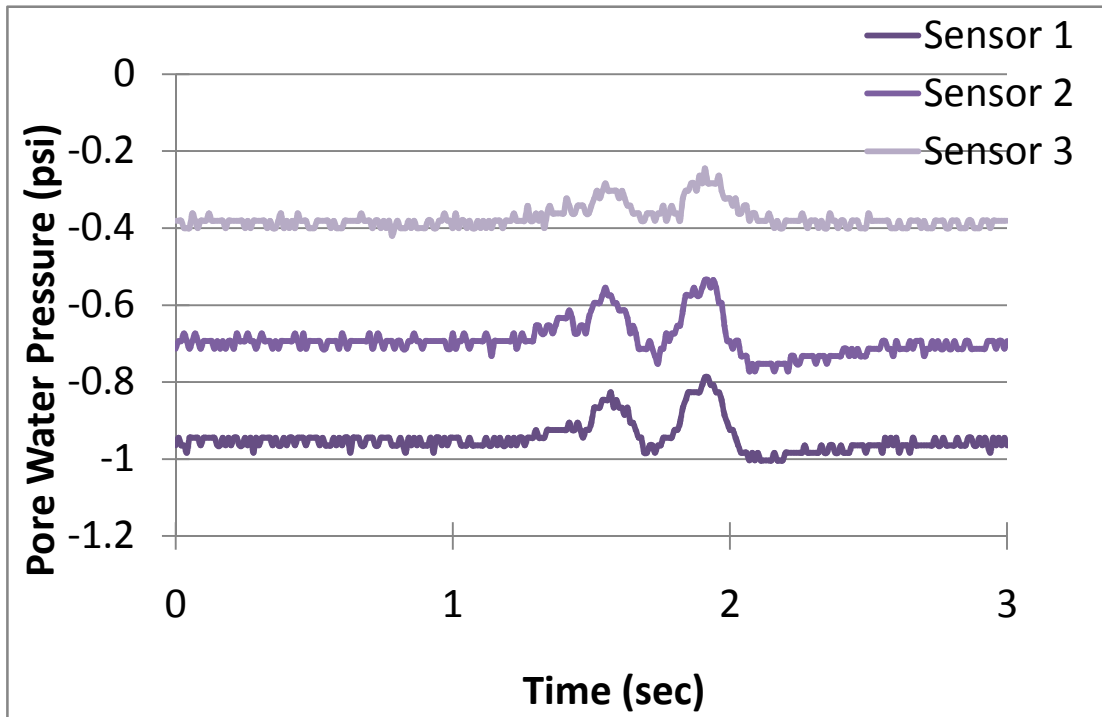


Figure 5.23 Dynamic Pore Pressure Response at WAY 30 Station 2 (April 06)

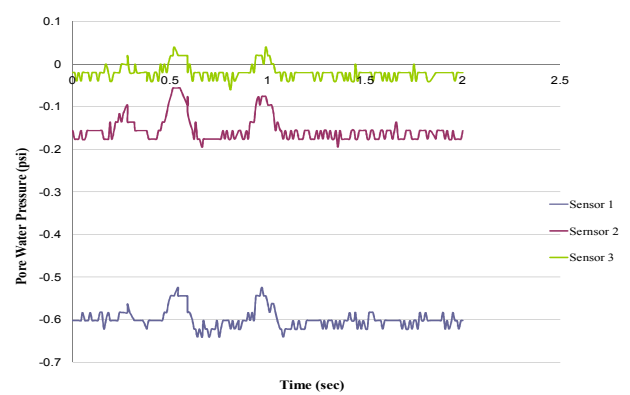


Figure 5.24 Dynamic Pore Pressure Response at WAY 30 Station 4 (April 06)

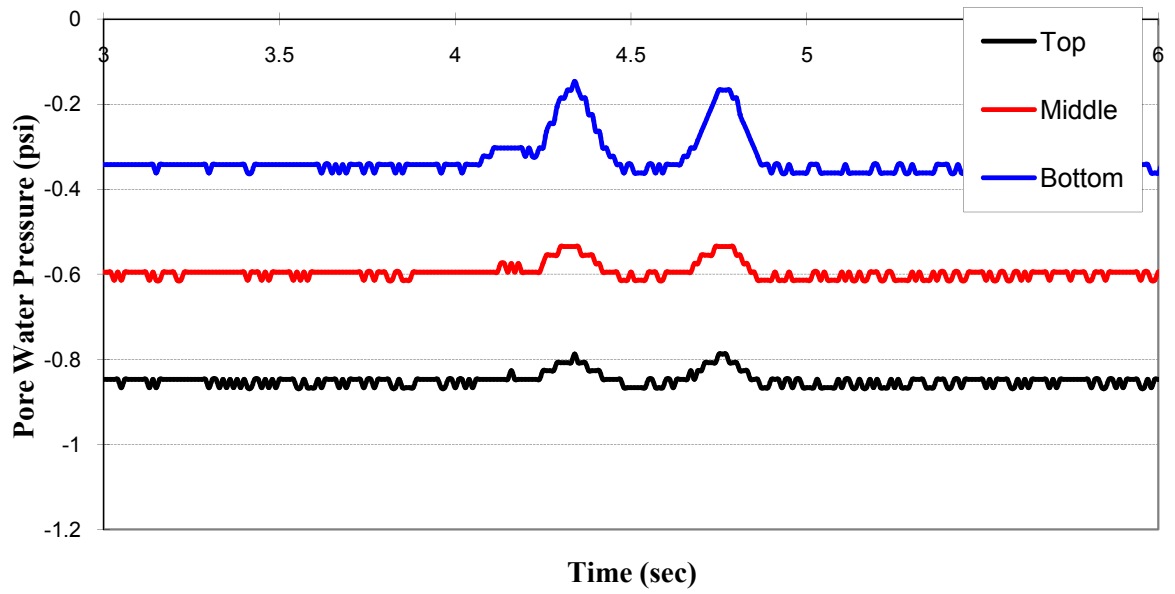


Figure 5.25 Dynamic Pore Pressure Response at WAY 30 Station 1 (October 06)

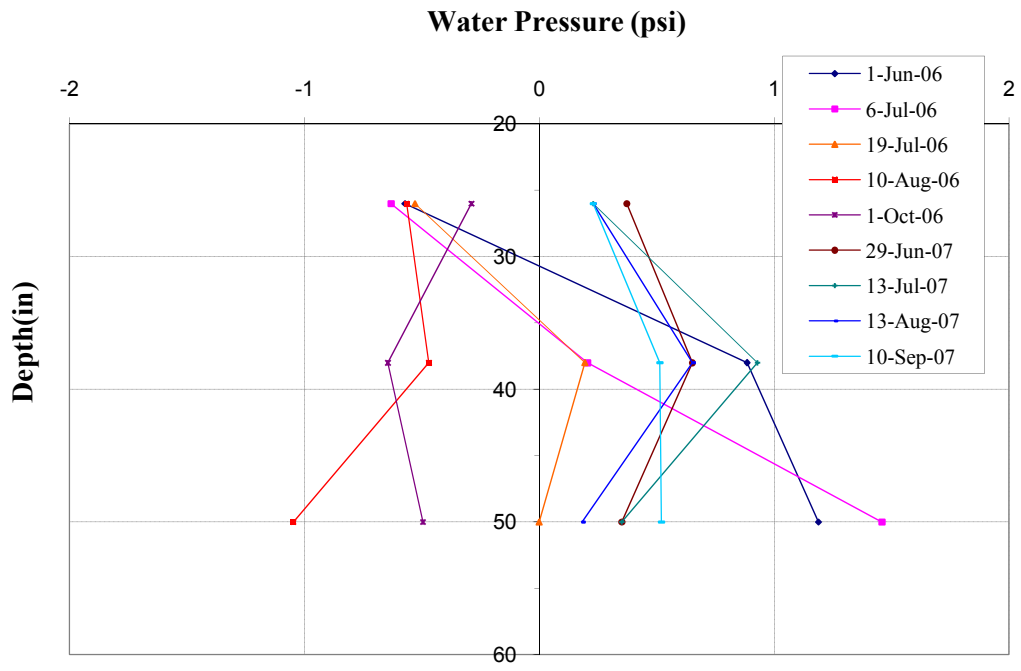


Figure 5.26 Pore Water Pressure at MAD 70 Station 1

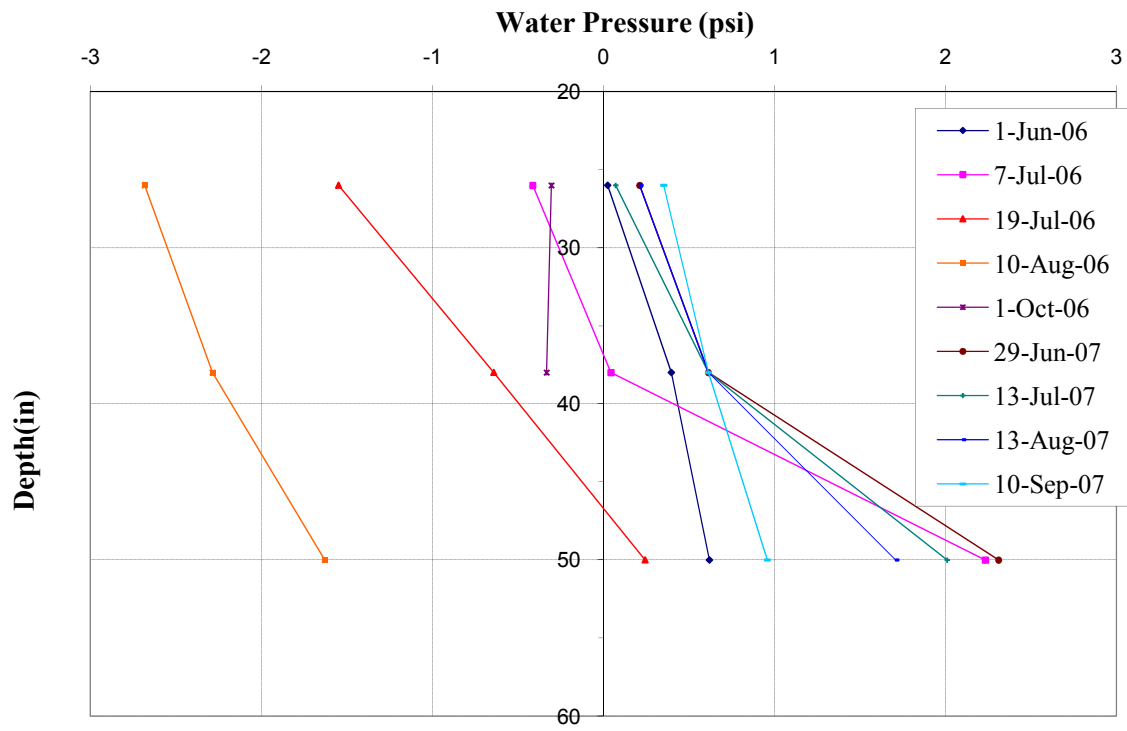


Figure 5.27 Pore Water Pressure at MAD 70 Station 2

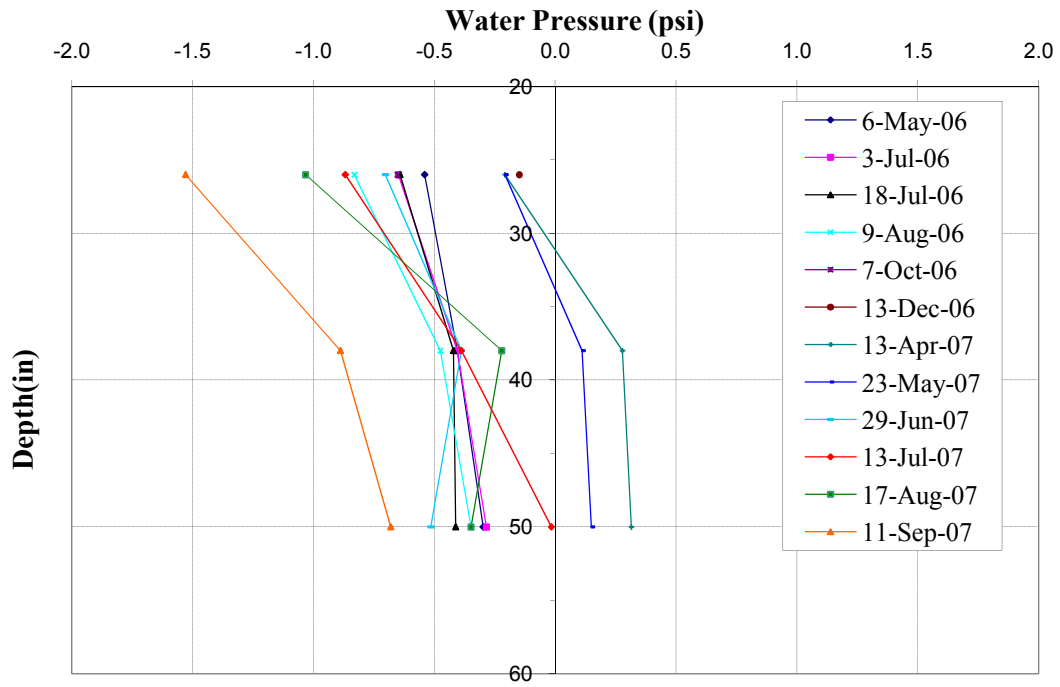


Figure 5.28 Pore Water Pressure at ROS 207

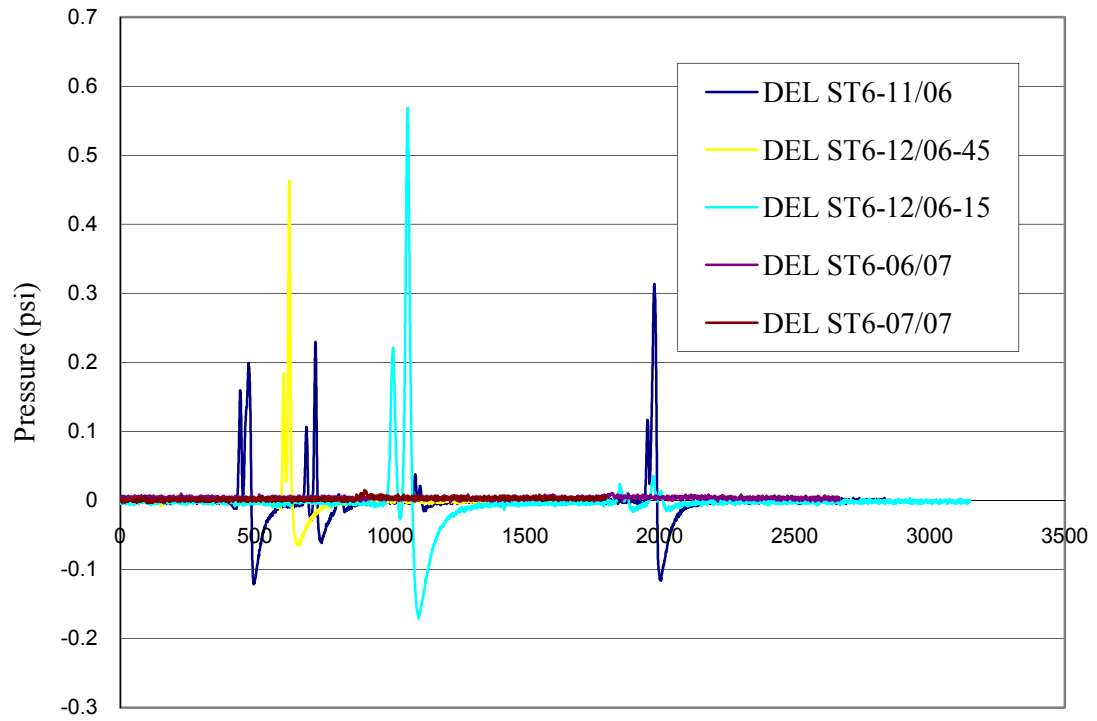


Figure 5.29 Dynamic Pore Water Pressure at Section Line Rd Station 6.

6 ADDITIONAL LABORATORY RESILIENT MODULUS TESTING

Laboratory tests were conducted on samples of the soils collected from the tensiometer installation locations at the WAY30, and MAD70 sites described in Section 4. As was typical of previous laboratory resilient modulus testing programs, Standard Proctor compaction, particle size analysis, Atterberg Limits, unconfined compressive strength and specific gravity tests were performed. Table 6.1 lists when and where the samples were collected and their respective soil types.

Soil Type	Location	Sample Name	Date Collected
A-4	WAY 30 Station 1	W30ST1	SUMMER 05
A-4	MAD 70	MAD	SUMMER 05
A-4	WAY 30 Station 2	W30ST2	SPRING 06

Table 6.1 Sample Description and Location

Using the characterization protocol of earlier laboratory programs, all the samples were identified by location, moisture condition (dry, optimum or wet of optimum) and Sample #. For example: W30ST1WETS1, identified a sample from WAY 30 Station 1, compacted wet of optimum, sample #1.

6.1 Classification Tests

All tests were performed in accordance with the appropriate industry standards.

Soil Type		Sample Name	Liquid Limit	Plastic Limit	Plasticity Index	% Passing #200	% of sand	% of silt	% of clay	G _s
AASHTO	USCS									
A-4	ML	W30ST1	25	23	2	61	20	54	7	2.75
	CL	MAD	26	17	9	62	29	48	15	2.76
	CL-ML	W30ST2	26	20	6	59	24	51	8	2.74

Table 6.2 Classification and Engineering Properties

Table 6.3 presents the values for optimum moisture content and maximum dry density for each of the three soils.

Soil Type	Sample Name	Optimum Moisture Content (%)	Maximum Dry Density (kg/m ³)
A-4	W30ST1	14	1929
	MAD	13	1941
	W30ST2	14.5	1918

Table 6.3 Optimum Moisture Content and Maximum Dry Density

6.2 Unconfined Compression Tests

Specimens were tested 24 hours after compaction to allow for uniform moisture content throughout the specimen. The UCS tests were performed on each soil sample at three different moisture contents: 2% dry of optimum (DRY), at optimum (OMC) and 2% wet of optimum (WET) (Table 6.4).

Soil Type	Sample Location	OMC (%)	Max. Dry Density (g/cm ³)	Sample Number	Sample Moisture Content (%)	Sample Dry Density (g/cm ³)	q _u (psi)	q _u (kPa)
A-4	WAY 30 Station 1	14	1.928	DRY S3	11.27	1.91	103.8	715.74
				OMCS1	13.7	1.9	72.6	500.56
				WET S3	15.88	1.86	73.7	508.14
A-4	MAD70	13	1.941	DRY S3	10.42	1.88	90	620.52
				OMCS2	12.29	1.94	77.64	535.30
				WET S6	15.37	1.88	27.15	187.19
A-4	WAY30 Station 2	14.5	1.918	DRY S3	12.46	1.92	62.29	429.47
				OMCS1	14.35	1.89	43.9	302.68
				WET S2	16.29	1.81	27.23	187.74

Table 6.4 Unconfined Compressive Strength Test Results

6.3 Resilient Modulus Tests

The resilient modulus was determined in accordance with AASHTO T294-94 (Resilient Modulus of Unbound Granular Materials and Subgrade Soils- SHRP Protocol P46) testing procedure. At the beginning of the test, the sample was subjected to a preconditioning stage (1000 load cycles) followed by five steps (100 cycles each) with a confining pressure of 41, 21 and 0 kPa (6, 3 and 0 psi) for a total of 2500 cycles. As specified in the standard, the response to each load cycle was recorded. A plot of M_R vs. deviator stress for each confining pressure was generated for each test. As illustration of the data, test results for WAY 30 Station 1 OMC S2 are presented in figure 6.4. Figures 6.5 through 6.13 show typical M_R test results for WAY30 Station 1, MAD70 and WAY30 Station 2.

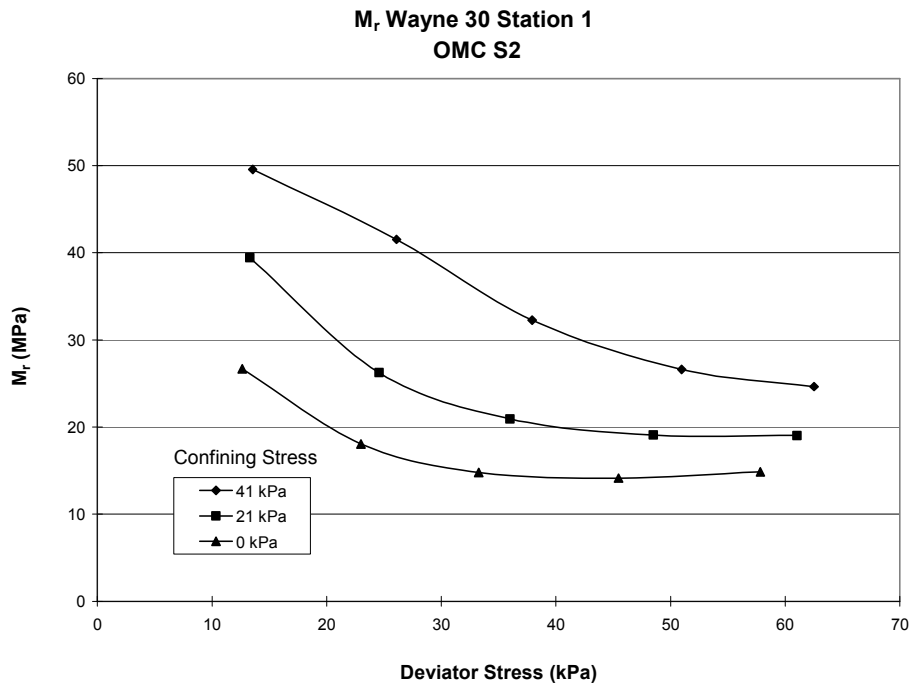


Figure 6.4 M_R test results for W30ST1OMCS2

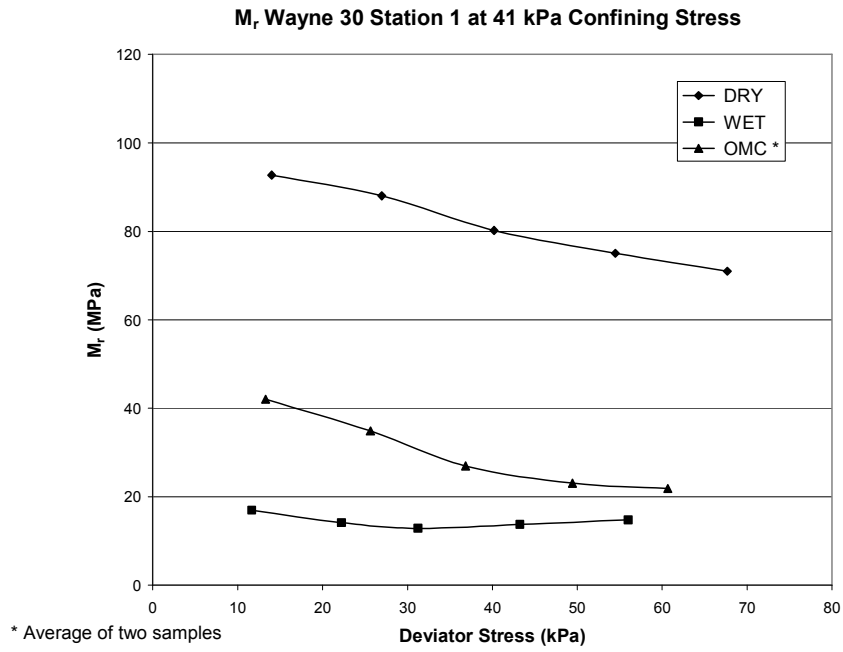


Figure 6.5 M_R test results for WAY 30 Station 1 at 41 kPa Confining Stress

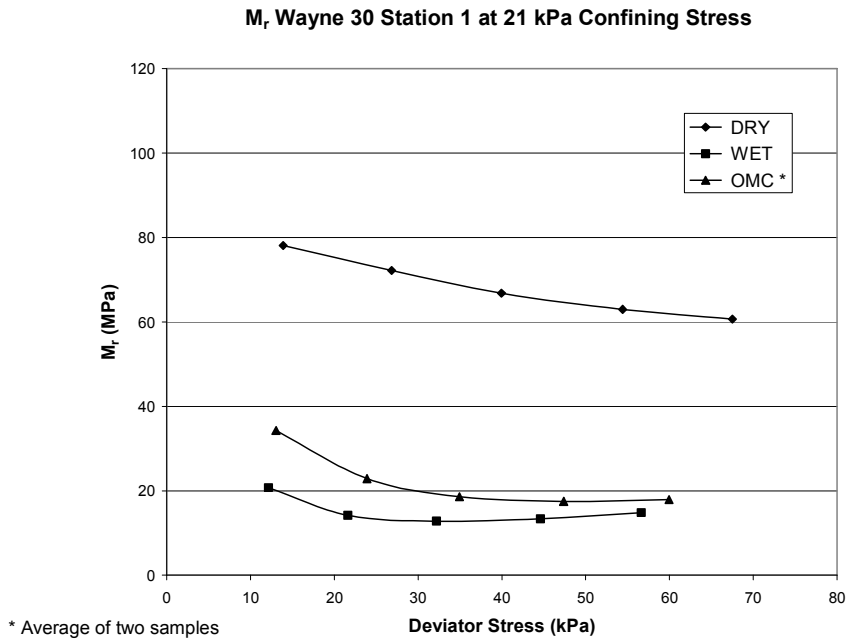


Figure 6.6 M_R test results for WAY 30 Station 1 at 21 kPa Confining Stress

M_r Wayne 30 Station 1 at 0 kPa Confining Stress

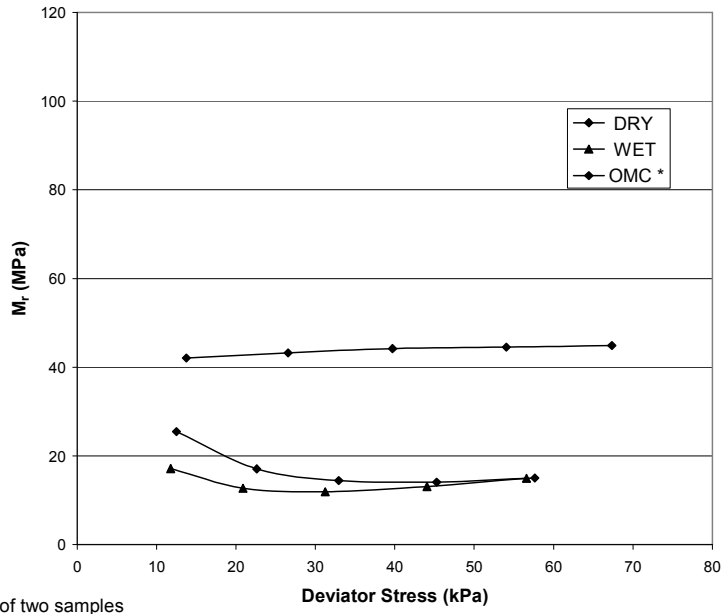


Figure 6.7 M_R test results for WAY 30 Station 1 at 0 kPa Confining Stress

M_r Madison County at 21 Confining Stress

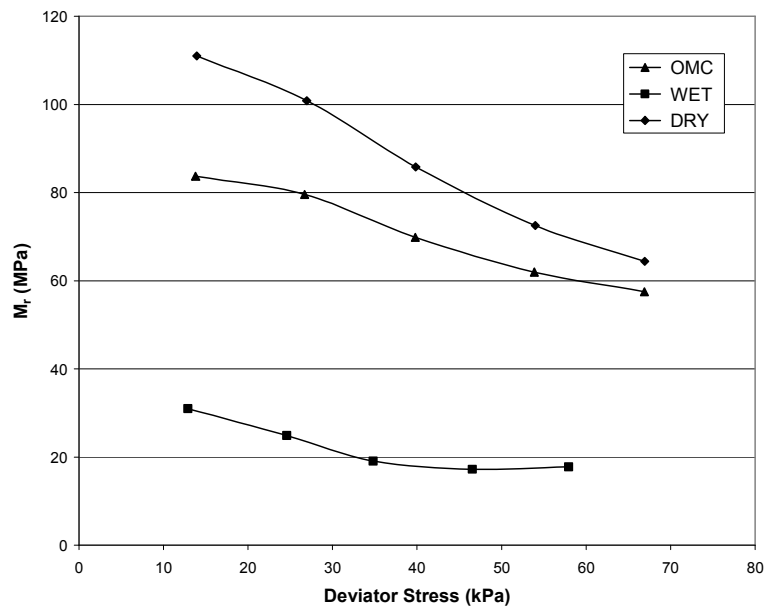


Figure 6.8 M_R test results for MAD 70 at 41 kPa Confining Stress

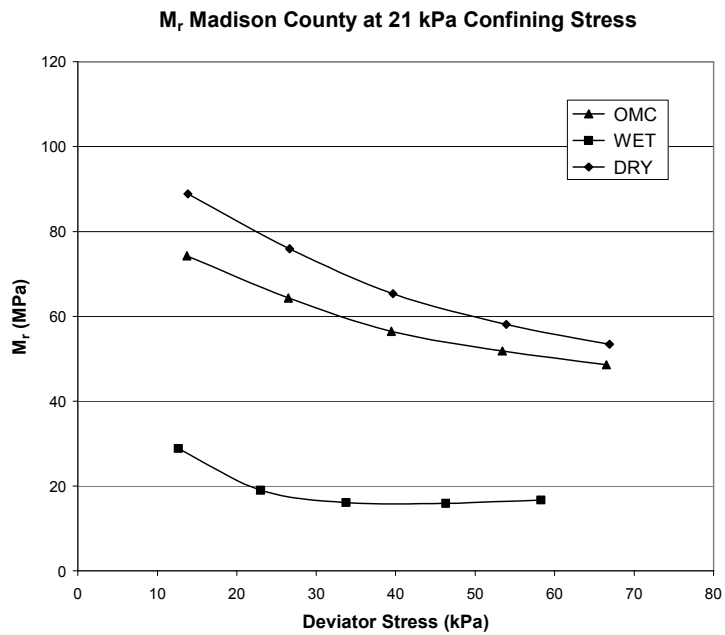


Figure 6.9 M_R test results for MAD 70 at 21 kPa Confining Stress

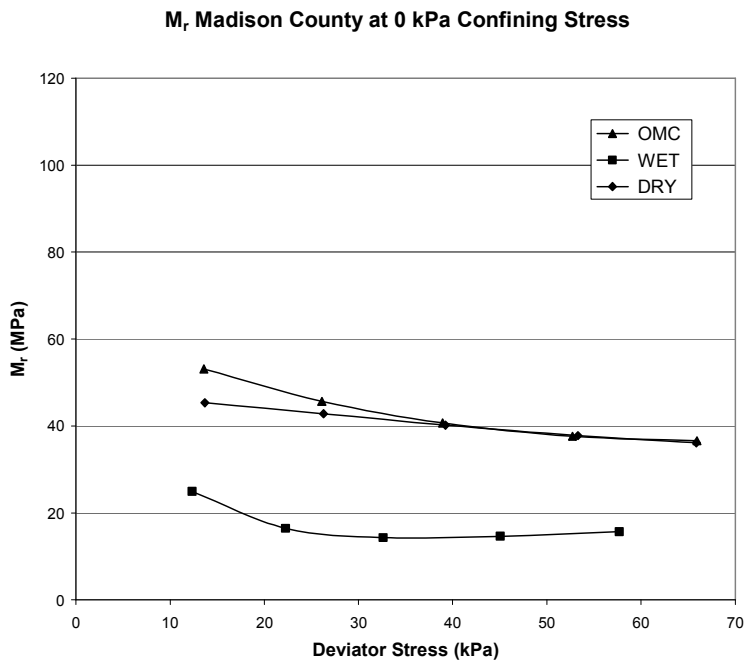


Figure 6.10 M_R test results for MAD 70 at 0 kPa Confining Stress

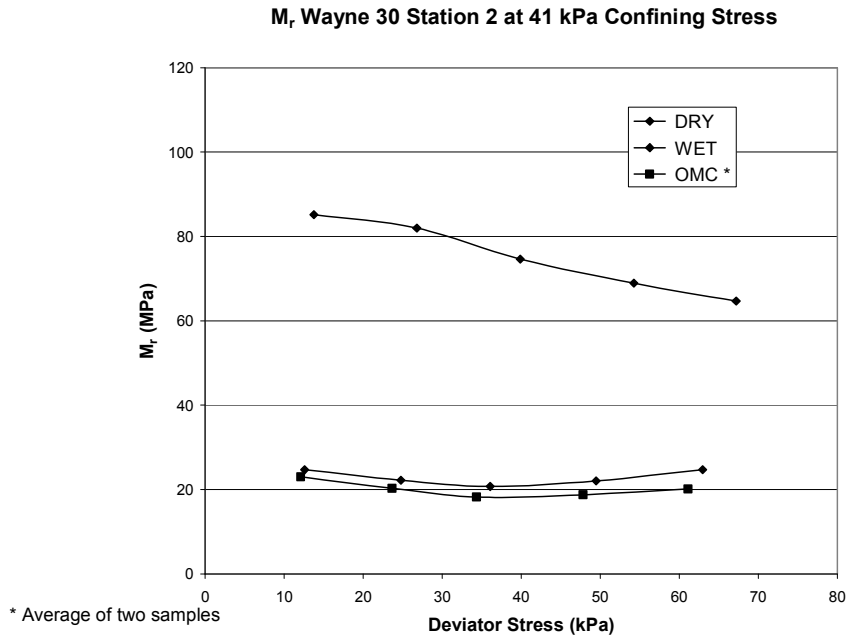


Figure 6.11 M_R test results for WAY 30 Station 2 at 41 kPa Confining Stress

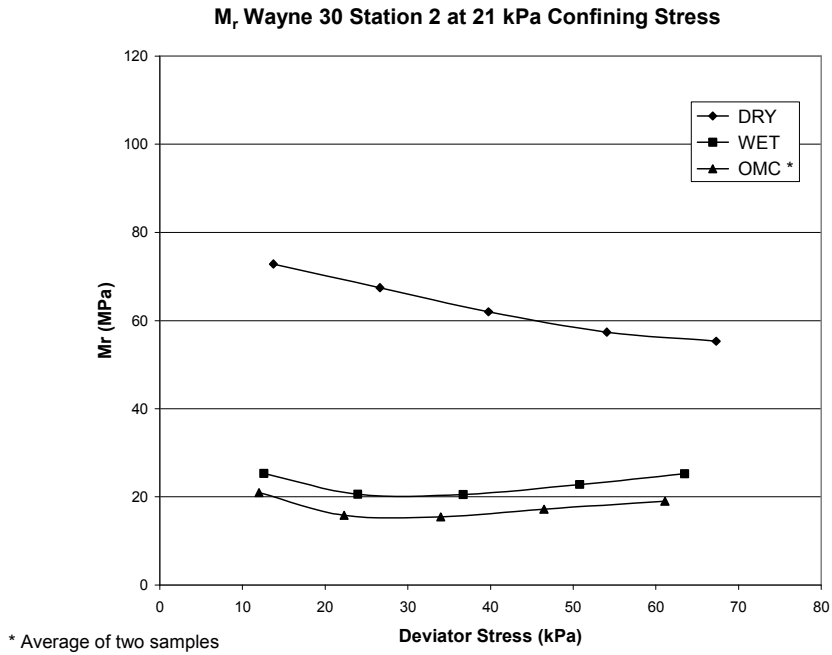


Figure 6.12 M_R test results for WAY 30 Station 2 at 21 kPa Confining Stress

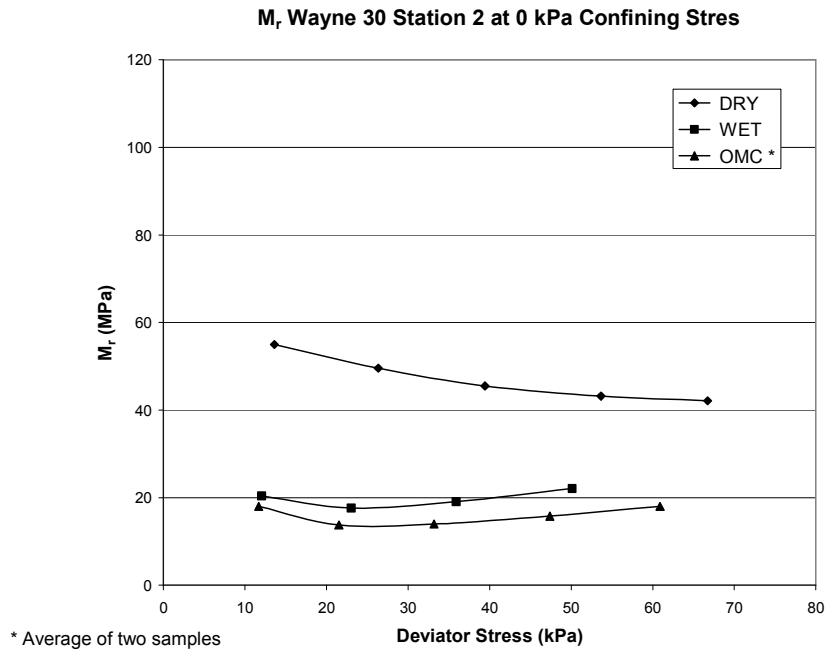


Figure 6.13 M_R test results for WAY 30 Station 2 at 0 kPa Confining Stress

As shown in Figures 6.8 through 6.13, M_R increased with an increase in confining stress. At constant confining stress, M_R gradually decreased with increasing deviator stress. This trend was observed and has been reported by other researchers (e.g. Seed, et al. (1962), Fredlund, et al. (1977), Drumm, et al. (1990), Li and Selig (1994), Pezo and Hudson (1994), Lee et al. (1995), Mohammad, et al. (1999)) as well as being observed in the earlier OSU tests and described in our previous project reports.

The modulus generally decreased with increasing moisture content; however for WAY 30 Station 2 the curves, the measured values for M_R at OMC and for M_R at WET conditions were similar at zero confining stress. The measured modulus at the design optimum condition was lower than for the wet of optimum condition at 0 and 21 kPa confining stresses, highlighting the sensitivity of the modulus to slight variations in moisture content and density. Actual sample moisture contents and dry densities are shown in Table 6.5.

Sample Location	Sample ID	w target (%)	Max. Dry Density target (g/cm ³)	w actual (%)	Dry Density (g/cm ³)
W30ST1	DRY S2	12	1.89	12.64	1.92
	OMC S2	14	1.928	14.93	1.86
	OMC S3	14	1.928	14.92	1.9
	WET S3	16	1.877	16.61	1.82
MAD	DRY S2	11	1.886	11.94	1.92
	OMC S1	13	1.941	12.86	1.93
	WET S1	15	1.915	14.82	1.89
W30ST2	DRY S1	12.5	1.882	13.01	1.89
	OMC S1	14.5	1.918	14.72	1.88
	OMC S2	14.5	1.918	15.21	1.83
	WET S1	16.5	1.82	15.51	1.82

Table 6.5 Design and Actual Soil Sample Moisture Contents and Dry Densities

6.4 Summary

Additional resilient modulus tests were performed on soil samples retrieved from three locations where field tensiometers were installed (Sections 4 and 5). General trends similar to those observed during earlier testing were observed.

7 RESILIENT MODULUS NEURAL NETWORK MODELS

The artificial neural networks developed in this research program were created using six principal parameters. The six values were: confining stress (kPa); deviator stress (kPa); unconfined compression stress (kPa); plasticity index, liquid limit, and the difference between actual sample water content (w) and the optimum moisture content (OMC). These parameters were identified in the extensive laboratory testing program (presented in detail in our previous reports) as having the most significant influence on the value of the resilient modulus. The program was trained until the neural networks were able to reproduce the resilient modulus vs. deviator stress laboratory curve and predict resilient modulus values within a small error (high correlation coefficient) for all three soil types (A-4, A-6 and A-7-6). Examples of comparisons between measured data and predicted values for the Resilient Modulus are presented in Figures 7.1 (A-4), 7.2 (A-6) and 7.3 (A-7-6) for the three soil types examined.

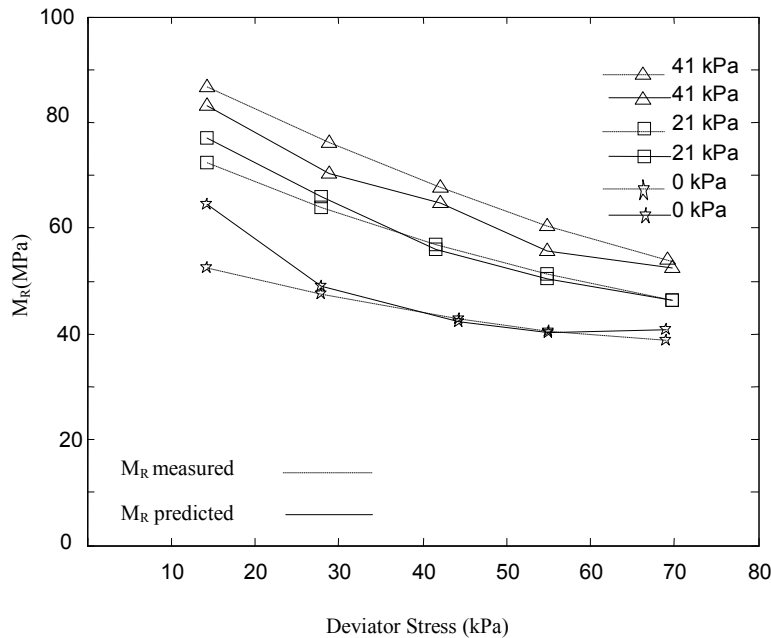


Figure 7.1 M_R vs. Deviator Stress, A-6 Soil

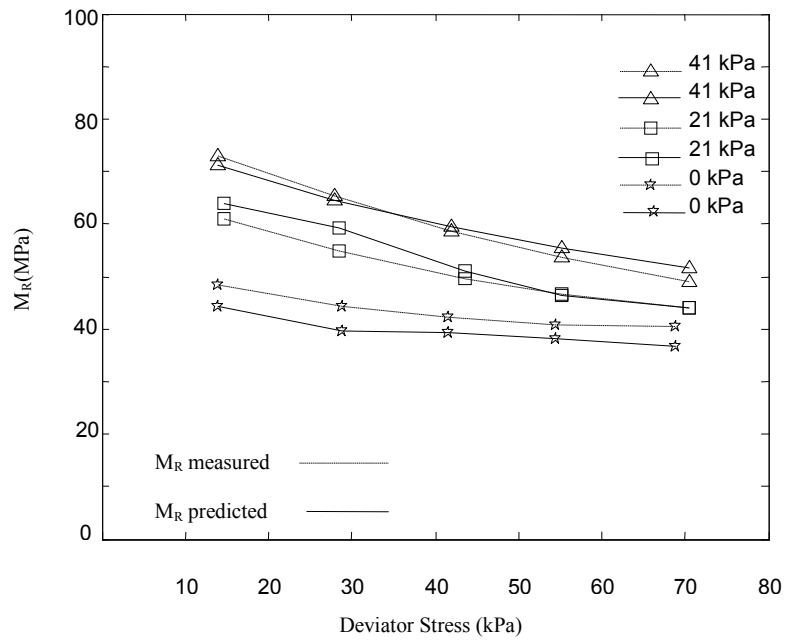


Figure 7.2 M_R vs. Deviator Stress, A-4 Soil

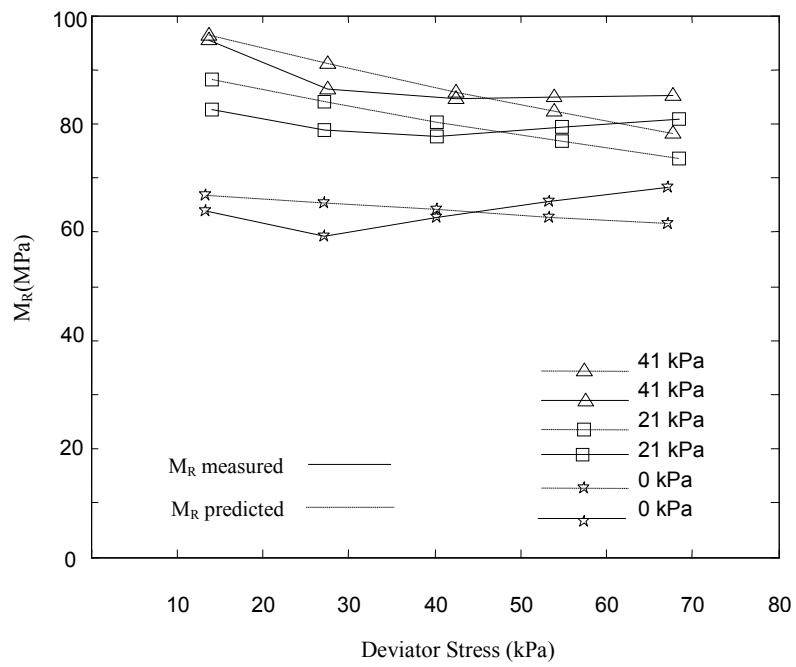


Figure 7.3 M_R vs. Deviator Stress, A-7-6 Soil

Even the predictions of the A-7-6 soil moduli show quite good correlation with the observations in spite the fact that the A-7-6 data set was much smaller than were the A-4 and A-6 data files.

The present study improves on the correlations between the results of commonly used laboratory tests and the resilient modulus. Given that neural networks do identify patterns and associate input values with output target values, it can be used to estimate M_R for samples that were not included in the training process. One of the most important advantages of neural networks is that they recognized the nonlinear behavior of M_R with respect to its inputs and can without difficulty accommodate new data additions. Since only the Ohio soil samples were used to train the network, it is useful to evaluate the performance of the neural network model with soils that were not used in the training process. In the present study, tests conducted at the University of Mississippi and at Purdue University were evaluated.

As seen in Figure 7.4, the network is capable of successfully predicting the resilient modulus of Mississippi study soils accurately, with a correlation coefficient of 0.963.

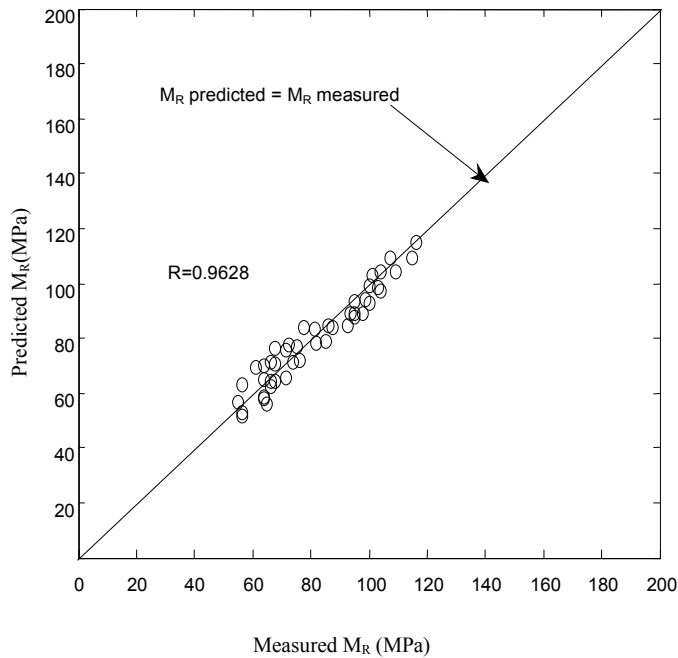


Figure 7.4 Predicted vs. Measured M_R University of Mississippi Test Soils

Figure 7.5 shows the predictions for the Purdue study soils were not as accurately made. This inability to accurately predict the behavior of both the Mississippi and Purdue soils equally well points to the fact that M_R is very sensitive to the differences in testing procedures and test equipment (Mohammad et al. (1994), Durham et al. (2003)). The Ohio and Mississippi soils were tested following the current T294-94 (SHRP Protocol P46) testing procedures, but in the case of the Purdue soils, the M_R laboratory tests were performed using an earlier (AASHTO T274-82) procedure and a special compaction method design for the particular project.

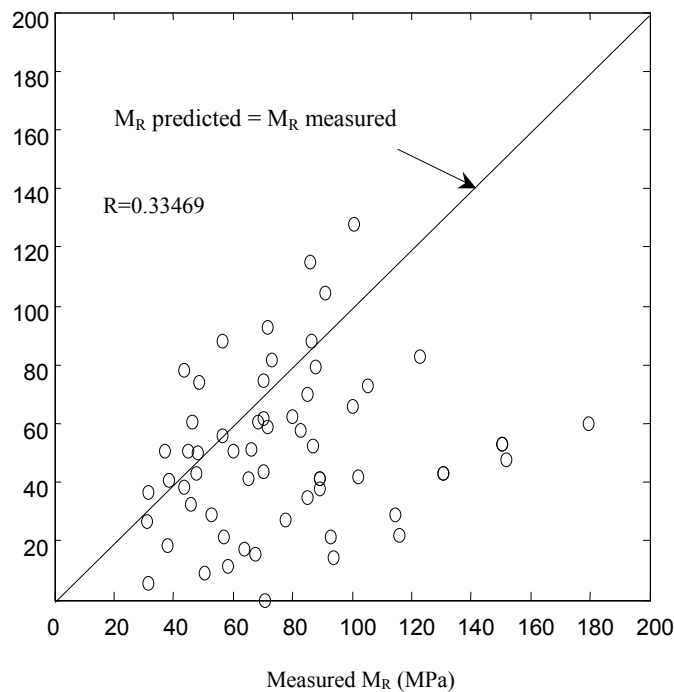


Figure 7.5 Predicted vs. Measured M_R Purdue Test Soils

Clearly, consistent testing procedures and preparation are required for a reliable model of modulus behavior to be useful. The Neural Network method developed in this study is capable of predicting with high precision an appropriate value for the Resilient Modulus for different cohesive soils provided the soils are tested according to current standards.

8 RESILIENT MODULUS PREDICTION MODEL

8.1 Introduction

The goal of this study was to develop an interface package to be used for resilient modulus (M_R) prediction. In this section a numerical program developed according to the algorithms described in Section 4 is presented. Since some required input parameters may not be directly measured but can be calculated from other parameters, we designed a model capable of assisting the user in the development of the input data set required to execute the model. Figure 8.1. shows the input screen of the M_R prediction model.

8.2 Input Command Controls for Data Entry

The topmost three input boxes (percent passing the #200 sieve ($P_{\#200}$), liquid limit (LL), plasticity index (PI)) are used to determine soil type. Alternatively, if these three inputs are unknown, soil type (A-4, A-6 or A-7-6) can be specified. The next two lower boxes accept data (Maximum Dry Density and % Optimum Moisture Content) from the Standard Proctor test. The next four boxes are application specific soil values (percent compaction, percent moisture content, soil unit weight, dry unit weight) that typically would be either measured or specified. Since not all these inputs are independent, the program is designed to calculate those values not specified, provided enough information to do so has been entered. Data from a specific gravity test should be entered if the test has been performed. However, since a direct measure of this parameter is typically made less commonly than the other inputs, the program will calculate the specific gravity (G_s), based on the other input values entered.

The range of values measured for each input parameter in the database during the extensive laboratory detailed in our 1998 and 2004 studies is given to the left of the corresponding input box. The reader should refer to those earlier reports and section 3 of this report for a list of materials studied and tests performed. Although a value outside the data range specified can be entered, the color of the input box will change to alert the user. The final inputs are the unconfined compressive strength, the design confining and deviator stresses. When all these inputs have been provided, a calculation of resilient modulus is made.

8.3 Additional Features and Functions

If the $P_{\#200}$, LL, and PI, data are provided, they can also be used to estimate the CBR based upon either ODOT or ME-PDG guidelines. The CBR results display in window screens as shown in Figures 8.2, 8.3 and 8.4. Figure 8.5 displays an estimate of

the graph used to determine the optimum moisture content and maximum density using a one point Proctor test. Figure 8.6 shows the page where the one point Proctor information is entered.

As stated previously, several neural networks were developed specifically to calculate the unconfined compressive strength from classification and compaction moisture and density tests. To predict a design value for the unconfined compression from the other inputs, the user should click on the “Estimate” button located beneath the q_u input box. A range of values for q_u will be returned. With all input information either entered or calculated, values for M_R will be calculated when the “Predict Soil M_R ” button is clicked. If any of the inputs were given as a range of values, a range of moduli consistent with the observed terms recorded in the database will be returned.

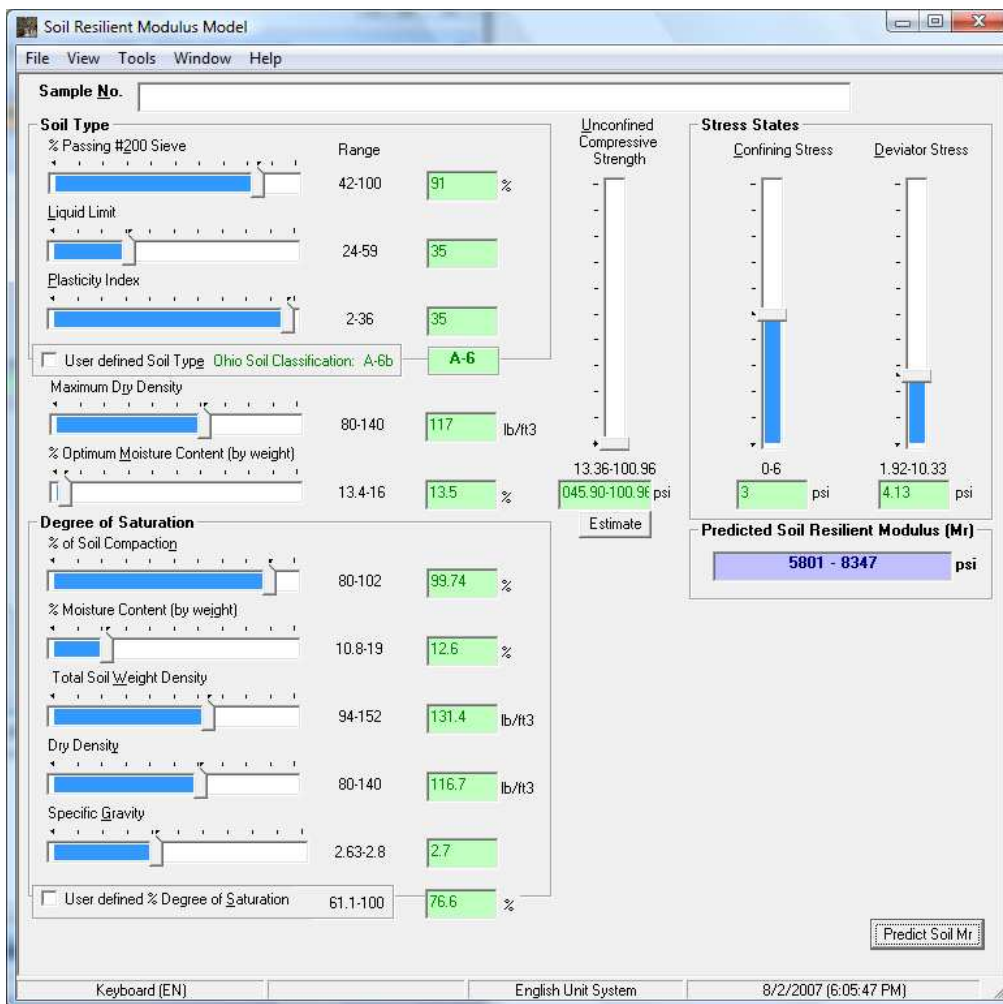


Figure 8.1 The main window screen for M_R prediction

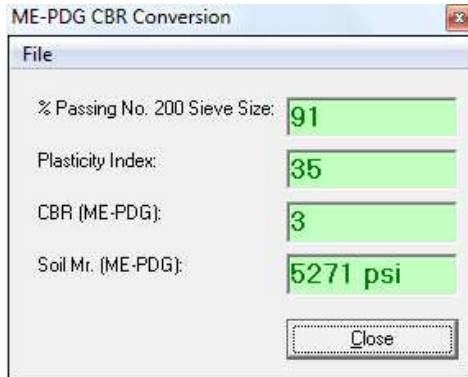


Figure 8.2 Window screen for CBR and M_R prediction according to the ME-PDG model

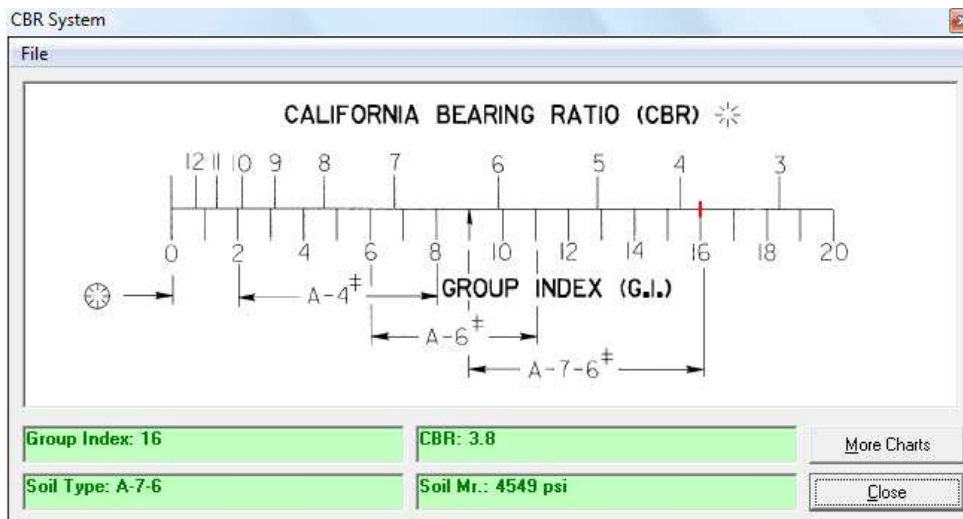


Figure 8.3 Window screen for CBR and M_R prediction according to ODOT [ODOT, 1999]

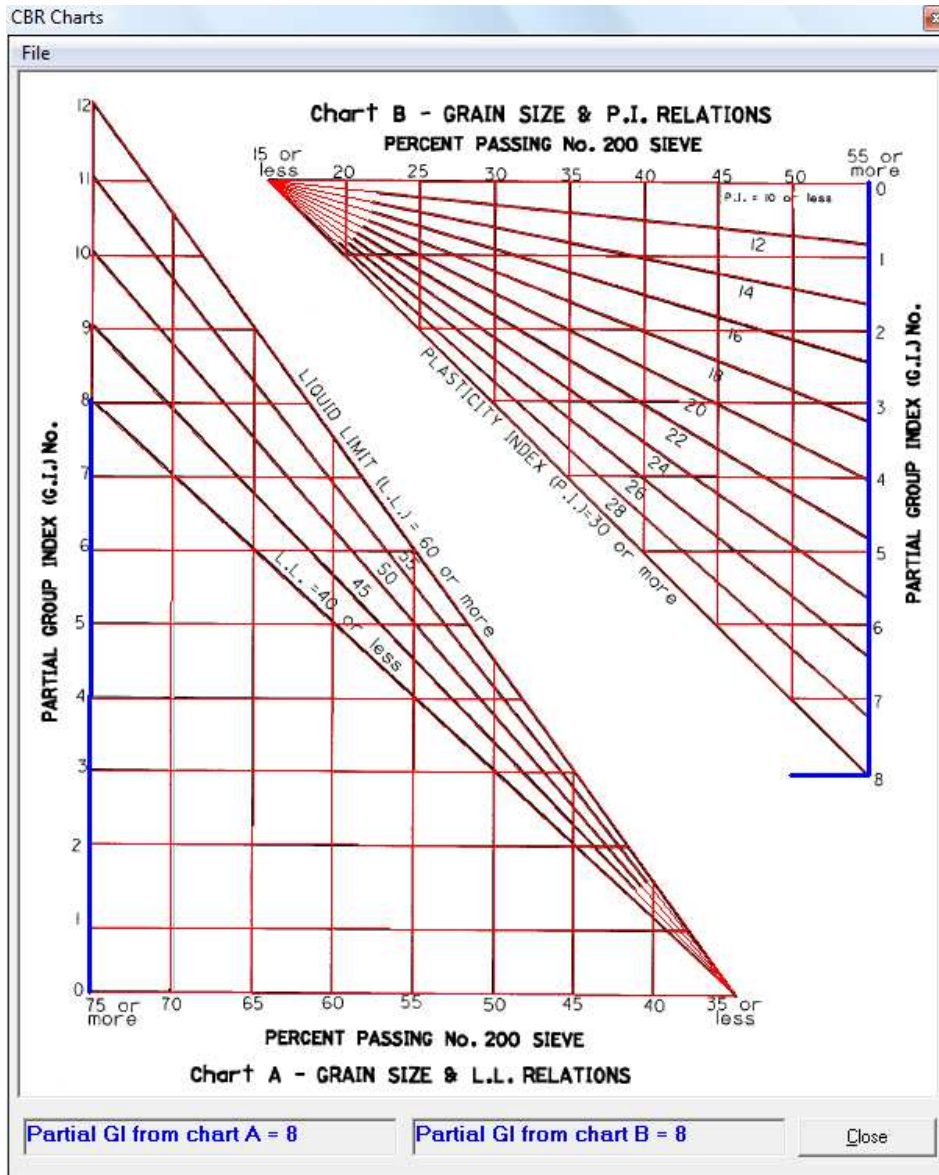
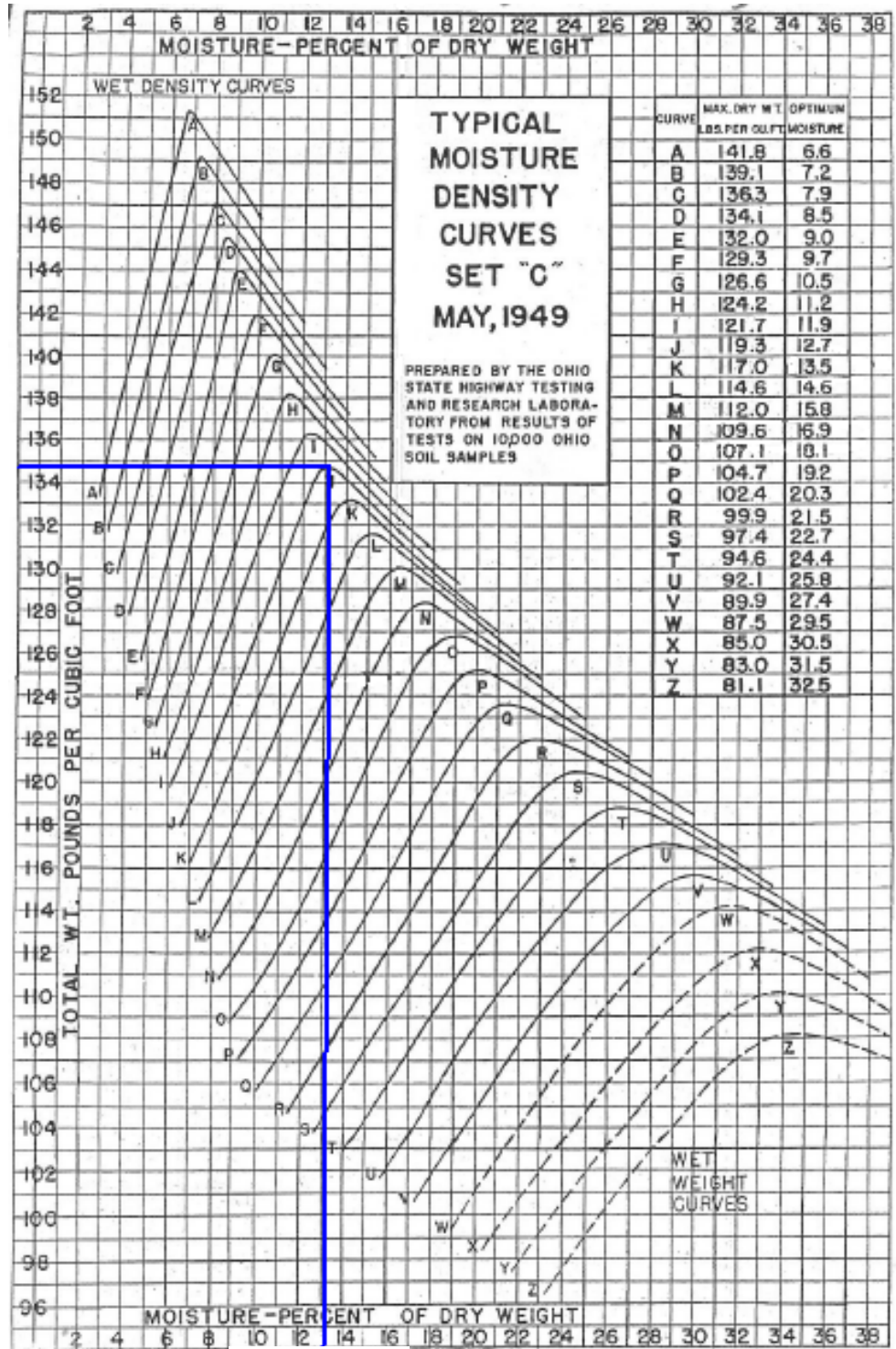


Figure 8.4 Charts to determine Group Index for Ohio soils from a CBR

134.7 lb/ft³



13.1%

Figure 8.5 Ohio Typical Soil Moisture vs. Density Family Curves [ODOT, 2002]

Optimum Moisture Content Estimation

File Unit System

Ohio Typical Moisture Density Curve

Total wet soil weight (lb/ft ³)	131.4
Moisture % of soil dry weight	12.6
% Materials retained on 3/4" sieve (by weight)	2
Maximum soil dry density (lb/ft ³)	117
<input type="checkbox"/> User defined maximum dry soil density provided	
Moisture density curve no.	K
<input type="checkbox"/> User defined moisture density curve no. provided	

Show Graphic

When Coarse Aggregates (equal to or greater than) >= 10%

Specific gravity of materials retained on 3/4" sieve	
Corrected Maximum soil dry density (lb/ft ³)	117
Corrected moisture density curve no.	K

More Graphic

Optimum Moisture Content

Final estimated % optimum moisture content	13.5
--	------

Apply Close

Figure 8.6 Optimum moisture content using one point proctor testing

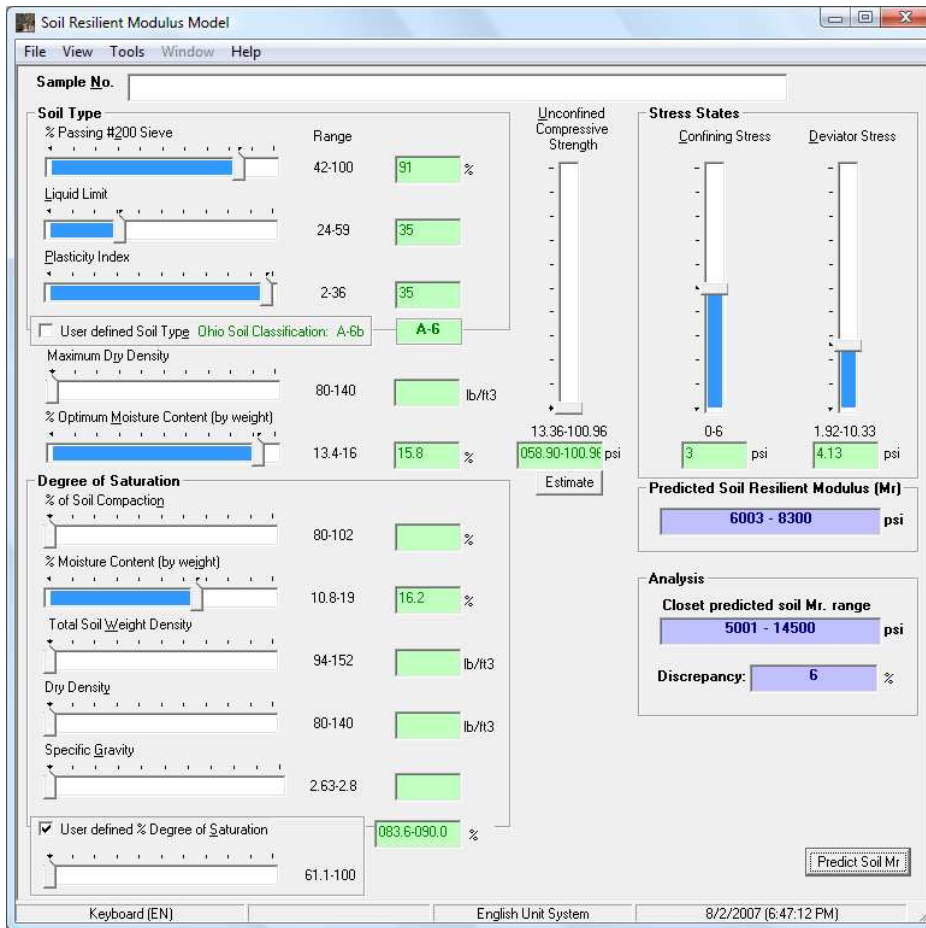


Figure 8.7 The main window screen with a predicted M_R range

8.4 Summary

Three distinct research programs were performed and discussed in this report. Monitoring of the environmental instrumentation for the pavements at the DEL 23 LTPP research site begun in 1995 was completed. Measurement of volumetric water content (TDR) continued throughout the study period but temperature and frost depth data could only rarely be collected due to repeated failures of the sensors and/or collection systems.

A research program to monitor the location of the groundwater under highway pavements that began with three locations under the LTPP pavements and was extended to additional sections at the DEL 23 site and at other locations across the state was completed. The measurements taken over the duration of the project clearly showed that the soil under the pavement sections studied became saturated as the water tables rose. In most locations saturated conditions up to the base layer (none of the instruments were installed in the base so the maximum height of the water table could not be determined by direct measurement) within a year of construction. It is reasonable to conclude that saturated conditions typically exist for much of the life of the pavement.

In the third activity a model for predicting the resilient modulus from static soil properties was developed for compacted cohesive subgrade soils typical of those found in Ohio. A laboratory program designed to develop a database sufficient to establish relationships between dynamic soil behavior and static properties was conducted.

The development of the mathematical model is based on the implementation of artificial neural networks (ANNs). One advantage to using ANN algorithms for regression analysis is that they are flexible and based on mathematical applications without strict statistical boundaries. Once required input parameters and targeted parameters are determined and proper ANN algorithms are set, the algorithms are capable of handling complex problems. The ANNs developed in this study were incorporated with multilayer back-propagation (supervised learning) algorithms. Further exploration using different ANN algorithms with improved overall prediction and a better fit to the nature of the problems should be encouraged.

The database could be strengthened with additional test results. Although nearly 800 M_R tests were performed, there are only about 80 soil samples in the database for predicting q_u . In addition, even though our field data show that saturated conditions can be expected in most pavement systems in Ohio, the number of tests performed on saturated samples is not sufficient to provide seasonal M_R values for the ME-PDG model as required. The development of ANNs for soil property prediction with expediting algorithms capable of handling small data sets should be explored. Another possible approach would be to use artificial neural network algorithms to determine the 3 regression coefficients (k_1 , k_2 , and k_3) required in the input Level 1 of the ME-PDG model for M_R prediction. The same ANN concept can be applied to aggregated or coarse-grained soils which are key materials for the base layers of pavement structure.

9 IMPLEMENTATION

Subsurface soil data collected at the DEL23 site over the duration of the current project, combined with the data from our two previous projects, have provided the environmental background information for researchers studying pavement performance at the Ohio LTPP site. Over the duration of the projects, much of the thermal and resistivity instrumentation failed but the devices recording the changing groundwater conditions continued to provide useful information for the full duration of the projects. The pore pressure instrumentation installed at the DEL23 and other sites across Ohio documented a significant rise in groundwater levels over time under virtually all monitored highway sections. Recognition that high water levels are typical under pavement sections throughout the state should impact the design of new and repaired pavements across Ohio. The method presented should replace current procedures for most A-4, A-6 and A-7-6 soils.

The numerical method presented in this report will calculate the resilient modulus of cohesive soils for use in pavement design based on the results of nearly 1000 laboratory dynamic resilient modulus tests. Because the data base behind the numerical methods employed in the model is so extensive, comparison of predicted moduli with laboratory measured values is very good even when only classification test results and static soil properties are used as inputs. Provided current ASTM standard procedures are followed, good agreement between measured and predicted moduli was maintained even for tests conducted by other agencies on soils with different geologic origin and from other parts of the country.

10 REFERENCES

AASHTO Guide for Design of Pavement Structures, 1993, American Association of State Highway and Transportation Officials, Washington, D.C.

AASHTO Guide for Design of Pavement Structures, 1998, American Association of State Highway and Transportation Officials, Washington, D.C.

AASHTO T88-00, "Particle Size Analysis of Soils," American Association of State Highway and Transportation Officials, Washington, D.C., 2004.

AASHTO T89-02, "Determining the Liquid Limit of Soils," American Association of State Highway and Transportation Officials, Washington, D.C., 2004.

AASHTO T90-00, "Determining the Plastic Limit and Plasticity Index of Soils," American Association of State Highway and Transportation Officials, Washington, D.C., 2004.

AASHTO T99-01, "The Moisture-Density Relations of Soils Using a 5.5 lb [2.5 kg] Rammer and a 12-in. [305 mm] Drop," American Association of State Highway and Transportation Officials, Washington, D.C., 2004.

AASHTO T100-03, "Specific Gravity of Soils," American Association of State Highway and Transportation Officials, Washington, D.C., 2004.

AASHTO T208-96, "Unconfined Compressive Strength of Cohesive Soil," American Association of State Highway and Transportation Officials, Washington, D.C., 2004.

AASHTO M 145-91, Classification of soils and Soil-Aggregate Mixtures for Highway Construction Purposes," American Association of State Highway and Transportation Officials, Washington, D.C., 2004.

AASHTO T274-82, "Standard Method of Test for Resilient Modulus of Subgrade Soils," American Association of State Highway and Transportation Officials, Washington, D.C., 1984.

AASHTO T292-91, "Standard Method of Test for Resilient Modulus of Subgrade Soils and Untreated Base/Subbase Materials," American Association of State Highway and Transportation Officials, Washington, D.C., 1994.

AASHTO T294-94 “Standard Method of Test for Resilient Modulus of Subgrade Soils and Untreated Base/Subbase Materials – SHRP Protocol P46,” American Association of State Highway and Transportation Officials, Washington, D. C., 1995.

AASHTO T307-99 “Standard Method of Test for Resilient Modulus of Subgrade Soils and Untreated Base/Subbase Materials,” American Association of State Highway and Transportation Officials, Washington, D. C., 2000.

ASTM D2487-98, “Standard Classification of Soils for Engineering Purpose (Unified Soil Classification System),” Annual Book of ASTM Standards, Vol. 04.08, 2000.

Ali, Osman. [2005] “*Evaluation of the Mechanistic Empirical Pavement Design Guide*,” (NCHRP 1-37A), report no. IRC-RR-216/UR 3002.1, research report 216, Urban infrastructure program, September 2005 National Research Council Canada, September, 1. . last retrieved on 9-12-2007, from [Hhttp://irc.nrc-cnrc.gc.ca/pubs/rr/rr216/rr216.pdf](http://irc.nrc-cnrc.gc.ca/pubs/rr/rr216/rr216.pdf)H.

Amber, Yau and H. L. Von Quintus. [2002] “*Study of LTPP Laboratory Resilient Modulus Test Data and Response Characteristics*,” Final Report, October 2002 (FHWA-RD-02-051), USDOT, FHWA, October.

ARA, Inc., Eres Consultants Division. [2004] “*Guide for Mechanistic-Empirical Design of New and Rehabilitated Pavement Structures*,” prepared for National Cooperative Highway Research Program Transportation Research Board National Research Council under NCHRP project 1-37A. last retrieved on 9-12-2007, from [Hhttp://www.trb.org/mepdg/guide.htm](http://www.trb.org/mepdg/guide.htm)H.

Baczyński D. and M. Parol. [2004] “Modern Electric Power Systems: structure on quality of short-term electric energy consumption forecast,” *IEE Proc.-Gener. Transm. Distrib., Vol. 151, No. 2, March*, [Hhttp://ieeexplore.ieee.org/iel5/2195/28621/01281029.pdf?arnumber=1281029](http://ieeexplore.ieee.org/iel5/2195/28621/01281029.pdf?arnumber=1281029)H.

Bayrak, Mustafa Birkan, Alper Guclu, and Halil Ceylan. [2005] “Rapid Pavement Backcalculation Technique for Evaluating Flexible Pavement Systems,” *Proceedings of the August 2005 Mid-Continent Transportation Research Symposium*, Ames, IA.

Brendenh, S. J. and M.F.C. van de Ven. [2004] “Application of Artificial Neural Networks in the Back-Calculation of Flexible Pavement Layer Moduli from Deflection Measurements,” (unpublished edition) *Proceedings of the 8th Conference on Asphalt Pavements for Southern Africa (CAPSA’04)* 12-16 September, Sun City, South Africa ISBN: 1-920-01718-6.

Brown S. F. and A.F.L. Hyde, “Significance of Cyclic Confining Stress in Repeated-load Triaxial Testing of Granular Materials”, *Transportation Research Record 537*, National Research Council, Washington, D.C., pp. 49-58, 1975.

Burland, J.B., Ninth Lauritis Bjerrum Memorial Lecture: Small is Beautiful – The stiffness of Soils at Small Strains, *Canadian Geotechnical Journal*, Vol. 26, pp. 499-516, 1989.

Butalia, T. S., Huang, J., Kim, D. G., and Croft, F., “Effect of Moisture Content and Pore Water Pressure Buildup on Resilient Modulus of Cohesive Soils,” *Resilient Modulus Testing for Pavement Components*, ASTM STP 1437, G. N. Durham, W. A. Marr, and W. L. De Croff, Eds., ASTM International, West Conshohocken, PA, 2003.

Burczyk, James M., Ksaibati, Khaled., Anderson-Sprecher, Richard., “Factors Influencing Determination of a Subgrade Resilient Modulus Value,” in *Transportation Research Record 1462*, TRB, National Research Council, Washington, D.C. 1994, pp. 72-79.

California Department Of Transportation. [1990] “*Trenching And Shoring Manual*” Jan-1990, Revision 11 on 12-1996, DeRosia, T. E., G. W. Thomson, J. J. Abercrombie, and R. A. Stott (Eds.), Division of structure construction, Office of Structure Construction, North Highlands, CA. last retrieved on 9-12-2007, from <http://www.dot.ca.gov/hq/esc/construction/Manuals/OSCCCompleteManuals/TrenchingandShoringManualRev12.pdf>

Carmichael, R. F. III and Stuart, E. [1985] “Predicting Resilient Modulus: A Study to Determine the Mechanical Properties of Subgrade Soils,” *Transportation Research Record*, No 1043, Transportation Research Board, National Research Council, pp. 145-148.

Chapel, Thomas. [2002] “*A Contractor's Guide To Geotechnical Engineering: Knowing How To Decipher A Soils Report And Make Sure That It Reflects Field Conditions Will Save Everyone Time And Money*,” - Brief Article, May 2002.

Choate, Pat and Walter, Susan. [1981] “*America in Ruins: Beyond the Public Works Pork Barrel*” Council of State PLANNing Agencies, Washington, D. C.

Chopra, Paras. [2007] No title, source codes for a neural network model to solve the “exclusive or” (XOR) conditions, [HDelhi College of Engineering](http://www.delhi-college-of-engineering.edu/)H, New Delhi, INDIA.

Cromwell, Brian A. [1989] “*Capital Subsidies and the Infrastructure Crisis: Evidence from the Local Mass-Transit Industry*” National Council of Public Works Improvement. Q. 2. last retrieved on 9-12-2007, from <http://www.clevelandfed.org/research/review/1989/89-q2-cromwell.pdf>

Dai, S, and Zollars, J., “Resilient Modulus of Minnesota Road Research Project Subgrade Soil,” in Transportation Research Record No 1786, Transportation Research Board, National Research Council, 2002, pp. 20-28.

Davich, P. J. Labuz, B. Guzina and A. Drescher. [2004]. “*Small Strain And Resilient Modulus Testing Of Granular Soils*” University of Minnesota, Minneapolis, Minnesota, Final Report 2004-39 for Minnesota Department of Transportation, Research Services Section, St. Paul, Minnesota, August 2004. last retrieved on 9-12-2007, from <http://www.lrrb.org/pdf/200439.pdf>

Departments of the Army and the Air Force. [1994] “Design for Roads, Streets, and Open Storage Areas, Elastic Layered Method” Army TM 5-822-13/Air Force AFJMAN 32-1018, October 1994.

Durham, Gary., Marr, Allen., and DeGroff, Willard., “Resilient Modulus Testing for Pavement Components,” ASTM Stock Number:STP1437, ASTM International, 2003.

Drumm, E. C., Boateng-Poku, Y. and Pierce, T. J., “Estimation of Subgrade Resilient Modulus from Standard Tests,” Journal of Geotechnical Engineering, ASCE, Vol. 116, No. 5, May, 1990, pp. 774-789.

Drumm E.C., J.S. Reeves, M.R. Madgett, and W.D. Trolinger, “Subgrade Resilient Modulus Correction for Saturation Effects”, *Journal of Geotechnical and Geoenvironmental Engineering*, Vol.123, Issue 7, pp. 663-670, 1997.

Elliot, R. P. [1992] “Selection of Subgrade Modulus for AASHTO Flexible Pavement Design,” *Transportation Research Record*, No. 1354, TRB, National Research Council, Washington, D. C.

Farrar, M J and J P Turner. [1991] “*Resilient Modulus Of Wyoming Subgrade Soils*,” Mountain Plains Consortium Report No 91-1, The University Of Wyoming, Laramie, WY.

Fausset, Laurene V., Fundamentals of Neural Networks: architectures, algorithms, and applications, Florida Institute of Technology, Prentice Hall, Englewood Cliffs, NJ 07632, 1994.

FHWA. [2006] "Lead States Group and Mission," an online web page, Federal Highway Administration. last retrieved on 9-12-2007, from <http://www.fhwa.dot.gov/pavement/dgit/leadstates/index.cfm>, last updated on 07-26-06.

Fredlund, D.G., A. T. Bergan and P.K. Wong, "Relation between Resilient Modulus and Stress Conditions for Cohesive Subgrade Soils". *Transportation Research Record 642*, TRB, National Research Council, Washington, D.C., pp. 73-81, 1977

Fredlund, D. G., Bergan, A. T., and Wong, P. K., "Relation between Resilient Modulus and Stress Research Conditions for Cohesive Subgrade Soils," Transportation Record No 642 Transportation Research Board, National Research Council, Washington, D.C.1977, pp. 73-81.

Fredlund, D. G. and A. Xing. [1994] "Equations for the Soil-Water Characteristic Curve," *Canadian Geotechnical Journal*, Vol. 31, No. 4 pp. 521-532.

Frost, Matthew W., Fleming, Paul R., and Rogers, Christopher D. F., "Cyclic Triaxial Tests on Clay Subgrades for Analytical Pavement Design," *Journal of Transportation Engineering*, ASCE, Vol. 130, No. 3, May 1, 2004, pp. 378-386.

George, K. P., "*Prediction of Resilient Modulus from Soil Index Properties*," Department of Civil Engineering The University of Mississippi, 2004

George, K.P. [2004] "*Prediction Of Resilient Modulus From Soil Index Properties*," Final Report, The Mississippi Department Of Transportation, U.S Department Of Transportation, Federal Highway Administration, Department Of Civil Engineering, The University Of Mississippi, November 2004. last retrieved on 9-12-2007, from [Hhttp://www.mdot.state.ms.us/research/pdf/ResMod.pdf](http://www.mdot.state.ms.us/research/pdf/ResMod.pdf)H.

Green, J. L. and Jim W. Hall. [1975] "*Nondestructive Vibratory Testing Of Airport Pavements*," Report No. FAA-RD -73-205, Volume I, September 1975, NTIS, Washington, D. C.

Groeger J. L., G. R. Rada, and A.Lopez. [2003] "AASHTO T307 Background and Discussion," in Durham G. N., W. A. Marr, W. L. Degrof. (Eds.), *Resilient Modulus*

Testing for Pavement Components, page 16–30, Jan-03., ASTM International Standards Worldwide STP1437, West Conshohocken, PA.

Guan, Yun., Drumm, Eric C., and Jackson, N. Mike., “ Weighting Factor for Seasonal Subgrade Resilient Modulus,” in *Transportation Research Record 1619*, TRB, National Research Council, Washington, D.C., 1998, pp. 94-101.

Hall, Kevin D., and Thompson, Marshall R., “Soil-Property-Based Subgrade Resilient Modulus Estimation for Flexible Pavement Design,” *Transportation Record No 1449* Transportation Research Board, National Research Council, Washington, D.C.1994, pp. 30-38.

Harrigan, Edward T. [2004] “*Laboratory Determination Of Resilient Modulus For Flexible Pavement Design*,” *Research Results Digest*, National Cooperative Highway Research Program, January, No 285. last retrieved on 9-12-2007, from [Hhttp://onlinepubs.trb.org/onlinepubs/nchrp/nchrp_rrd_285.pdf](http://onlinepubs.trb.org/onlinepubs/nchrp/nchrp_rrd_285.pdf)H.

Hashash, Youssef M. A., Jamshid Ghaboussi, Qingwei Fu, and Camilo Marulanda. [2006] “Constitutive soil behavior representation via artificial neural networks: A shift from soil models to soil behavior data,” in *Proceedings of GeoCongress*, ASCE, Don J. DeGroot, Jason T. DeJong, J. David Frost, Laurie G. Baise- editor, February 26–March 1, Atlanta, GA.

Haykin, Simon. [1994] “*Neural Networks*,” Macmillan College Publishing Company, New York NY

Heukelom, W., and Klomp, A.J.G. [1962] “Dynamic Testing As A Means Of Controlling Pavement During And After Construction,” *Proceedings of the 1st international conference on the structural design of asphalt pavement*, University of Michigan, ANN Arbor, MI.

Heydinger, Andrew G. [2003] “*Monitoring Seasonal Instrumentation and Modeling Climatic Effects on Pavements at the Ohio/SHRP Test Road*,” Report no. FHWA/OH-2003/01, Department of Civil Engineering, The University of Toledo, in cooperation with ODOT, U. S. ODOT, and FHWA.

Hoffman, Gary. [2002] “Benefiting from LTPP – A State’s Perspective,” *Public Roads* May/June Vol. 65. No. 6. last retrieved on 9-12-2007, from [Hhttp://www.tfrc.gov/pubrds/02may/09.htm](http://www.tfrc.gov/pubrds/02may/09.htm)H.

Huang, J. [2001] “*Degradation of Resilient Modulus of Saturated Clay Due to Pore Water Pressure Buildup under Cyclic Loading*,” Master Thesis, Department of Civil and Environmental Engineering and Geodetic Science, The Ohio State University, Columbus, OH.

Kaw, Autar K.. [2002] “*Introduction to MATRIX ALGEBRA*,” University of South Florida, Tampa, FL. last retrieved on 9-12-2007, from <http://numericalmethods.eng.usf.edu/matrixalgebrabook/downloadma/matrixalgebra.pdf>.

Khasawneh, Mohammad Ali., 2005, *Laboratory Characterization of Cohesive Subgrade Materials*, Thesis, Department of Civil Engineering The University of Akron, 2005.

Kim, Daehyeon and Jong Ryeol Kim. [2007] “Resilient behavior of compacted subgrade soils under the repeated triaxial test,” *Construction and Building Materials*, Vol. 21, July Issue 7, pp. 1470-1479.

Kim, Dong-Gyou. [1999] “*Engineering Properties Affecting the Resilient Modulus Of Fine-Grained Soils As Subgrade*,” Master Thesis, The Ohio State University, Columbus, OH.

Kim, Dong-Gyou. [2004] “*Development Of A Constitutive Model For Resilient Modulus Of Cohesive Soils*,” Dissertation, The Ohio State University, Columbus, OH.

Kohonen, Teuvo. [1995] “*Self-organizing maps*,” Berlin; Heidelberg; New-York: Springer. Lee, W., Bohra, N. C., Altschaeffl, A. G., and White, T. D., “Subgrade Resilient Modulus for Pavement Design and Evaluation,” Joint Highway Research Project Engineering Experiment Station Purdue University, 1993.

Lee, W. J., Bohra, N. C., Altschaeffl, A. G., and White, T. D., “Resilient Modulus of Cohesive Soils and the Effect of Freeze-Thaw,” *Canadian Geotechnical Journal*, Vol. 32, 1995, pp. 559-568.

Lee, Yong-Woong, “An Evaluation of the Engineering Properties Affecting the Resilient Modulus of Ohio Subgrade Soils,” Thesis, The Ohio State University, 2002.

Li, D. and Selig, E. T., “Resilient Modulus for Fine-grained Subgrade Soil,” *Journal of Geotechnical Engineering*, ASCE, Vol. 120, No. 6, 1994, pp. 939-957.

Li, J., and Qubain, B. S., “Resilient Modulus Variations with Water Content,” *Resilient Modulus Testing for Pavement Components*, ASTM STP 1437, G. N. Durham, W. A.

Marr, and W. L. De Groff, ASTM International, West Conshohocken, PA, 2003, pp. 59-69.

LTPP. [2007] "Resilient Modulus Testing and Startup Procedures: A LTPP product line," an online web page, *Long-Term Pavement Performance Program*, FHWA, Federal Highway Administration, US DOT. last retrieved 9-12-2007, <http://www.fhrc.gov/pavement/ltp/ppt/rm1.ppt>.

Masada, T. and Sargand, S. M., 2002, "Laboratory Characterization of Materials and Data Management for Ohio-SHRP Projects (U.S. 23)," Job No. 14695(0), Final Report, for Ohio Department of Transportation and Federal Highway Administration, Ohio University, Athens, Ohio.

McCulloch, Warren S. and Walter Pitts. [1943] "A Logical Calculus Of The Ideas Immanent In Nervous Activity," *Bulletin of Mathematical Biophysics*, 5: pp. 115 - 133.

McCullough, B. D. and H. D. Vinod. [2004] "Verifying the Solution from a Nonlinear Solver: A Case Study: Reply," *The American Economic Review*, Vol. 94, No. 1. Mar., pp. 400-403. last retrieved on 9-12-2007, from <http://links.jstor.org/sici?sici=0002-8282%28200403%2994%3A1%3C400%3AVTTSFAN%3E2.0.CO%3B2-C>

Meier R. W. and Rix G. J. [1994] "Backcalculation of Flexible Pavement Moduli Using Artificial Neural Networks," *Transportation Research Record* No. 1448 Transportation Research Board. Washington D. C.

Meier, R. W. and Rix G. J. [1995] "Backcalculation of Flexible Pavement Moduli From Dynamic Deflection Basins Using Artificial Neural Networks," *Transportation Research Record*, No. 1473 Transportation Research Board, Washington, D. C.

Minsky, Marvin and S. Papert. [1969] "*Perceptrons*," MIT Press, Cambridge, MA.

Mohammad L. N., B. Huang, A J. Puppala, and A. Allen. [1999] "Regression Model for Resilient Modulus of Subgrade Soils," *Transportation Research Record*, Volume 1687, TRB of National Academies, National Research Council, Washington, D.C., pp. 47-54.

Mohammad, Louay N., Hani H. Titi, and Ananda Herath. [2000] "*Investigation of the Applicability of Intrusion Technology to Estimate the Resilient Modulus of Subgrade Soil*," Final Report, Louisiana Transportation Research Center, Baton Rouge, LA.

Mohammad, L.N. Puppala, A.J. and Alavilli, P., “Resilient Properties of Laboratory Compacted Subgrade Soils,” *Transportation Research Record 1504*, Transportation Research Board, National Research Council, pp. 87-102, 1996.

Mohammad, L.N., A.J. Puppala, P. Alavilli, “Influence of Testing Procedure and LVDT Location on Resilient Modulus of Soils”, *Transportation Research Record 1462*, National Research Council, Washington, D.C., pp. 91-101, 1994.

Mohammad, L. N., Titi, H. H., and Herath, A., “Evaluation of Resilient Modulus of Subgrade Soil by Cone Penetration Test,” *Transportation Research Record No 1652*, Transportation Research Board, National Research Council, Washington, D.C.1999, pp. 236-245.

Muhanna, A.S., Rahman, M.S., and Lambe, P.C., “Model for Resilient Modulus and Permanent Strain of Subgrade soils,” in *Transportation Research Record 1619*, TRB, National Research Council, Washington, D.C. 1998, pp. 85-93.

Myers, Leslie [2005] “*General Overview of M-E Pavement Design*” in *Materials Inputs for Mechanistic Empirical Pavement Design Workshop*, webcast on March 30 – 31, Rocky Hill, Connecticut. last retrieved on 9-12-2007, from <http://www.ct.gov/dot/cwp/view.asp?a=1617&Q=300236&PM=1>

National Highway Institute, *Analysis of New and Rehabilitated Pavement Performance with Mechanistic-Empirical Design Guide Software*, NHI Course No. 131109 Participant Workbook, June 2007.

National Highway Institute (NHI) Course No. 131064, “Introduction to Mechanistic-Empirical Design of New and Rehabilitated Pavements”, FHWA, April 2002.

NCHRP, “Guide for Mechanistic-Empirical Design of New and Rehabilitated Pavement Structures”, Final Report for NCHRP project 1-37A, 2004.

Neural Network Toolbox User’s Guide. The Mathworks, Inc., August 2005.

ODOT. [1999] “*Pavement Design & Rehabilitation Manual*,” Morse, Aric A. and David W. Miller (Eds.), Ohio Department of Transportation office of materials management, Columbus OH

ODOT. [2002] “*Construction Inspection Manual of Procedures*”: Office of construction Administration State of Ohio Department of Transportation, Columbus, OH

Parker, D. B. [1985] “*Learning-Logic: Casting The Cortex Of Human Brain In Silicon,*” Technical Report TR-47. Center for Computational Research in Economics and Management Science, MIT, Cambridge, MA.

Puppala, Anand J.[2004] “*CE 3143 - Soil Mechanics Laboratory,*” Class handouts, Center For Geotechnical Engineering Research, The University Of Texas At Arlington. last retrieved on 9-12-2007, from <http://geotech.uta.edu/lab/Main/>

Pezo, R and Hudson, W. R. [1994] “Prediction Models of Resilient Modulus for Nongranular Materials,” *Geotechnical Testing Journal*, GTJODJ, Vol. 17, No. 3, pp. 349 - 355

Ping, W. Virgil., and Ge, Ling., “Field Verification of Laboratory Resilient Modulus Measurements on Subgrade Soils,” Transportation Record No 1577. Transportation Research Board, National Research Council, Washington, D.C.1997, pp. 53-61.

Rahim, Ashraf M and K. P. George.[2004] “*Subgrade Soil Index Properties To Estimate Resilient Modulus,*” Paper Presented at 83rd ANNUAL Meeting of Transportation Research Board, Washington D. C.

Rodgers, Gloria. [2006] “*Resilient Modulus Prediction Using Engineering Properties and Neural Networks,*” Master Thesis, The Ohio State University, Columbus, OH.

Rosenblatt, Frank. [1962] “Principles of Neurodynamic; perceptrons and the theory of brain mechanisms.” Spartan Books, Washington D. C.

Rumelhart, D. E., G. E. Hinton, and R. J. Williams. [1986a] “Learning representations by back-propagating errors.” *Nature (London)*, 323, 533-536

Rumelhart, D. E., G. E. Hinton, and R. J. Williams. [1986a] “Learning internal representations by error propagation” In *Parallel Distributed Processing: Explorations in the Microstructure of Cognition* (D. E. Rumelhart and J. L. Mc Clelland, eds.) Vol. 1 Chapter 8, Cambridge, MA: MIT Press

Santha, B. L. [1994] “Resilient Modulus Of Subgrade Soils: Comparison of Two Constitutive Equations,” *Transportation Research Record*, Vol. 1462, TRB, National Research Council, Washington, D.C., pp. 79-90.

Seed, H.B., Chan C.K., and Lee C.E. [1962] “Resilience characteristics of subgrade soils and their relation to fatigue failures in asphalt pavement,” *Proc. First Int. Conf. On Struct. Design of Asphalt Pavements*, University of Michigan, ANN Arbor.

Simonsen E., V. C. Janoo and U. Isacsson, “Resilient Properties of Unbound Road Materials during Seasonal Frost Conditions”, *Journal of Cold Regions Engineering*, Vol. 16, No. 1, pp. 28-50, 2002.

Sukumaran, Beena Vishal, Kyatham, Amip Shah, and Disha Sheth. [2002] “*Suitability Of Using California Bearing Ratio Test To Predict Resilient Modulus*,” presented for the federal aviation administration airport technology transfer conference, Civil and Environmental Engineering, Rowan University.

Tatsuoka, F.S., S. Shibuya, S. Goto, T. Sato, and X.J. Kong, Discussion on the paper by Clayton et al. *Geotechnical Testing Journal*, Vol. 13, No. 1, pp. 63-67, 1990.

Teng, T. Paul. [2002] “*Study Of LTPP Laboratory Resilient Modulus Test Data and Response Characteristics*,” Final Report, Publication No. Fhwa-Rd-02-051, October 2002, U.S. Department of Transportation, Federal Highway Administration, Research, Development, and Technology, Turner-Fairbank Highway Research Center McLean, VA 22101-2296

Thompson, M.R., and Quentin L. Robnett. [1979] “Resilient Properties Of Subgrade Soils,” *Journal of Transportation Engineering*, ASCE, Vol. 105, No. 1, pp. 71-89.

Tutumluer, E. and Meier, R. W. [1996] "An Attempt at Resilient Modulus Modeling Using Artificial Neural Networks," *Transportation Research Record*. Vol. 1540, TRB, National Research Council, Washington, D. C., pp. 1-6.

Von Quintus, H. and B. Killingsworth. [1998] “*Analyses Relating To Pavement Material Characterizations And Their Effects On Pavement Performance*,” Report No. FHWA-RD-97-085, Federal Highway Administration, U.S. Department of Transportation, Washington, D. C.

Wagner, Christopher. [2001] “*FHWA MEPDG Activities: Reliability in the MEPDG Workshop*” presented at the 86th Annual TRB Meeting, on January 21, 2007. last retrieved on 9-12-2007

Wagner, Christopher. [2005] “*Soils and Unbound Materals*” in Materials Inputs for Mechan.istic Empirical Pavement Design Workshop, webcast on March 30 – 31, Rocky

Hill, Connecticut. last retrieved on 9-12-2007, from
<http://www.ct.gov/dot/cwp/view.asp?a=1617&Q=300236&PM=1>

Werbos, P. J. [1974] “*Beyond Regression: Newtools For Prediction And Analysis In The Behavioral Science*,” PhD. Dissertatoin, Harvard University, Cambridge, MA.

Wilson, B.E., Sargand S. M., Hazen G. A., and Green R. [1990] “Multiaxial Testing Of Subgrade,” *Transportation Research Record*, Vol. 1278, TRB. Washington DC: National Research Council, pp. 91–5.

Witczak, M.W., Houston, W.N., Zapata, C.E., Richter, C., Larson, G. and Walsh, K.. [2000] “*Improvement of the Integrated Climatic Model for Moisture Content Predictions*,” Inter-Team Technical Report (Seasonal 4), NCHRP 1-37 A. last retrieved on 9-12-2007, http://www.esica.com/_docs/testimonials_idaho.pdf

Wolfe, William E. and Tarunjit S. Butalia. [2004] “*Seasonal Instrumentation of SHRP Pavements*,” “ Final report, in Cooperation with the Ohio Department of Transportation and the U.S., Department of Transportation, Federal Highway Administration, Department of Civil & Environmental Engineering & Geodetic Science The Ohio State University, Columbus, OH.

11.1 APPENDIX A

RESILIENT MODULUS USERS GUIDE

Soil Resilient Modulus Determination, version: June 22, 2009

This is a program to estimate soil resilient modulus for three different cohesive soils commonly found in Ohio: A-4, A-6, and A-7-6.

Installation

- 1) On the installation package of this program, look for the "Setup.exe" file.
- 2) Double-click on the "Setup.exe" file and follow the installation process.

Introduction

- 1) Go to the directory where you have installed this program
- 2) Double-click on the "Soil Resilient .exe" file to run the program

Data Entry

- 1) Enter the information in the active input boxes.

Sample No.

Here enter any identifying information you want to provide

Soil Type

% Passing #200 Sieve

Liquid Limit

Plasticity Index

The program will determine which soil type the sample represents (Currently A-4, A-6, A-7-6 are the soil types that can be analyzed) Alternatively the user can enter one of the three modeled soil types directly from a pull down menu.

Proctor Test Results

Optimum Moisture Content (%)

Maximum Dry Density

Total Max Density

Values are entered as Unit Weights. Either Maximum Dry Density or Total Max Density is calculated from the other value when the Optimum Moisture Content is known.

Degree of Saturation

% of Compaction

Value of compaction either required or achieved, given as a percentage of Standard Proctor density as obtained in ASTM D698

% Moisture Content

Measured or required in-place soil moisture content

Total Density

Measured or required in-place total unit weight

Dry Density

Measured or required in-place dry unit weight

Specific Gravity

Degree of Saturation will be calculated or can be supplied as input. If supplied, other inputs in this section are disabled

Unconfined Compressive Strength

The soil strength as measured in an unconfined compression test is entered here. Alternatively, the unconfined compressive strength can be estimated from the supplied data using the program database and the neural network algorithms developed for predicting modulus.

Stress States

Confining Stress

Deviator Stress

Enter test specific boundary conditions.

When all input values have been supplied or estimated the resilient modulus can be calculated by pressing bottom right (Estimate Soil Mr) button.

If any required inputs are missing, pressing the Estimate Soil Mr Button will generate a prompt to continue with data entry

You may use the active scrollbars when they are provided if you prefer.

You can select the system of units. Control +E for English units or Control +I for SI units, or from the View tab, select Unit System then select English or International units.

Under the Tools menu and compare it to the model estimate as would be obtained from the use ME-PDG or Ohio CBR for the given input values.

=====Copy screen function

- 1) On any window screen, go to the "File" menu bar and choose the "Copy Current Screen" option (shutter sound will be provoked indicating that the transaction is completed, the current screen will be captured in a clipboard).
- 2) Go to a word processor window or picture editor window and paste the clipboard to your working window.

=====Optimum Moisture Content Estimator

This feature allows users to use one point proctor test to estimate an optimum soil moisture content. Once you develop your optimum moisture content, click on the "APPLY" button to transfer the data to the main screen.

On the "Optimum Moisture Content Estimator" window,

Method 1:

- 1.1) Provide information about the total wet soil weight, moisture % of soil dry weight, and % maximum dry soil density.
- 1.2) If the % maximum dry soil density is greater or equal to 10, specific gravity of material retained on 3/4" sieve is also required to adjust for gravel factors

Method 2

- 2.1) Double-click on the "Show Graphic" button
- 2.2) On the Typical Moisture Density Curve Set "C" window, place your mouse pointer (a cross shape) within a graphic area to get coordinates
- 2.3) Back to the "Optimum Moisture Content Estimator" window, If the % maximum dry soil density is greater or equal to 10, specific gravity of material retained on 3/4" sieve is also required to adjust for gravel factors.

Method 3

- 3.1) Choose the "User defined maximum dry soil density" option,
- 3.2) Provide information on the % maximum dry soil density and the maximum dry soil density
- 3.3) If the % maximum dry soil density is greater or equal to 10, specific gravity of material retained on 3/4" sieve is also required to adjust for gravel factors

Method 4

- 4.1) Choose the "User defined moisture density curve" option,
- 4.2) Provide information on the % maximum dry soil density and the moisture density curve no.
- 4.3) If the % maximum dry soil density is greater or equal to 10, specific gravity of material retained on 3/4" sieve is also required to adjust for gravel factors

Disclaimer:

This computer program was developed by Department of Civil and Environmental Engineering and Geodetic Science, The Ohio State University. This software has been carefully tested on multiple systems at the University but may not work on every computer.

The soil data used to develop this program did not include all possible soils that might be encountered. Therefore the calculated values should not be used for specific purposes without verification by a professional qualified to verify the applicability of such data or information.

The University may not be held liable for any damages, direct or consequential, which may result from the use of this program.